doi: 10.12029/gc20240410003

叶桂琦, 季文兵, 杨忠芳, 余涛, 侯青叶, 钱鹍. 2025. 氧同位素技术在土壤−植被−生态−环境研究中的应用进展与展望[J]. 中国地质, 52(2): 527−573.

Ye Guiqi, Ji Wenbing, Yang Zhongfang, Yu Tao, Hou Qingye, Qian Kun. 2025. Research progress and prospect of oxygen isotope technique in soil−vegetation−ecology−environment studies[J]. Geology in China, 52(2): 527−573(in Chinese with English abstract).

# 氧同位素技术在土壤−植被−生态−环境研究中的应用进展与展望

叶桂琦[1]，季文兵[2]，杨忠芳[1]，余涛[3]，侯青叶[1]，钱鹍[1]

（1. 中国地质大学 (北京) 地球科学与资源学院, 北京 100083; 2. 生态环境部南京环境科学研究所, 江苏 南京 210042; 3. 中国地质大学 (北京) 数理学院, 北京 100083）

**摘要:【研究目的】**氧是组成生命物质的基本元素之一, 自然界的氧循环是生命活动的基本保证。氧同位素技术是一种强有力的示踪手段, 能够有效指示生物地球化学循环过程, 在生态环境研究中得到了广泛应用。**【研究方法】**本文通过查阅大量氧同位素的文献, 综述了氧同位素的分馏机制以及在土壤−植被−生态−环境方面的应用。**【研究结果】**依赖于同位素质量比值偏差大, 氧同位素可以在自然条件下发生较大程度的同位素分馏。氧同位素的应用主要包括三个方面: (1)示踪环境污染物来源; (2)古环境和古气候恢复; (3)追踪食物(动物)的地理来源。**【结论】**在实际应用中, 氧同位素通常会与其他同位素(氢同位素、碳同位素、氮同位素等)共同使用, 从气候、植被发育程度和地理位置等方面多维度示踪。今后氧稳定同位素可与树轮、有孔虫、黄土、盐湖等全球变化领域的代用物模式结合, 发挥更重要的环境生态学研究价值。

**关 键 词:** 氧同位素; 分馏机制; 示踪技术; 古气候; 环境污染物; 土壤; 植被; 生态环境; 地理来源; 环境地质调查工程

**创 新 点:** 本文归纳总结了氧同位素在生态环境方面的应用现状以及前景展望, 以期为未来氧同位素在土壤、植被、生态环境方面的研究提供参考。

**中图分类号:** X321; P593 **文献标志码:** A **文章编号:** 1000−3657(2025)02−0527−47

# Research progress and prospect of oxygen isotope technique in soil−vegetation−ecology−environment studies

YE Guiqi[1], JI Wenbing[2], YANG Zhongfang[1], YU Tao[3], HOU Qingye[1], QIAN Kun[1]

(1. *School of Earth Sciences and Resources, China University of Geosciences, Beijing* 100083*, China*; 2. *Nanjing Institute of Environmental Sciences, Ministry of Ecology and Environment, Nanjing* 210042*, Jiangsu, China*; 3. *School of Science, China University of Geosciences, Beijing* 100083*, China*)

**Abstract:** This paper is the result of environmental geological survey engineering.

**收稿日期:** 2024−04−10; **改回日期:** 2024−06−24

**基金项目:** 广东省地质勘查与城市地质调查项目 (2023-25)、宁夏回族自治区重点研发计划重大(重点)项目“宁夏中北部土壤碳汇源转化因素与碳库保育研究”(2022BBF02036)联合资助。

**作者简介:** 叶桂琦, 女, 2001 年生, 硕士生, 地球化学专业, 主要从事环境地球化学研究; E−mail: yegq77@163.com。

**通信作者:** 季文兵, 男, 1991 年生, 助理研究员, 主要研究方向为地球化学和生态地球化学; E−mail: 13121531228@163.com。

**[Objective]** Oxygen is one of the basic elements that make up living matter, and the oxygen cycle in nature is the basic guarantee for life activities. Oxygen isotope technology is a powerful tracer that can effectively indicate biogeochemical cycling processes and has been widely used in ecological and environmental research. **[Methods]** This paper reviewes the fractionation mechanism of oxygen isotopes and its application in soil−vegetation−ecological environment by reviewing a large number of literatures on oxygen isotopes. **[Results]** Depending on the large isotope mass ratio difference, oxygen isotopes can undergo the greatest degree of isotope fractionation under natural conditions. The application of oxygen isotopes mainly includes three aspects: (1) Tracing the source of environmental pollutants; (2) Paleoenvironment and paleoclimate restoration; (3) Tracing the geographical origin of food (animals). **[Conclusions]** In practice, oxygen isotopes are usually used together with other isotopes (hydrogen, carbon, nitrogen, etc.) to track multi-dimensional climate, vegetation development, and geographical location. In the future, oxygen stable isotopes can be combined with substitute models in the fields of global change, such as tree rings, foraminifera, loess, and salt lakes, and play a more important role in environmental ecology research.

**Key words:** oxygen isotope; mechanism of fractionation; tracer technology; paleoclimate; environmental pollutants; soil; vegetation; ecological environment; geographical origin; environmental geological survey engineering

**Highlights:** This paper summarizes the current status of oxygen isotope application in the ecological environment and its prospect, which will provide reference for future research on oxygen isotopes in soil, vegetation and ecological environment.

**About the first author:** YE Guiqi, female, born in 2001, master candidate, majors in geochemistry, engaged in environmental geochemistry; E−mail: yegq77@163.com.

**About the corresponding author:** JI Wenbing, male, born in 1991, assistant researcher, majors in geochemistry and ecological geochemistry; E−mail:13121531228@163.com.

**Fund support:** Supported by the projects of Guangdong Geological Exploration and Urban Geology (No.2023−25) and "Research on the transformation factors of soil carbon sinks and carbon pool conservation in north−central Ningxia" of the Key R&D Program of Ningxia Hui Autonomous Region (No.2022BBF02036).

## 1 引 言

氧是地球上丰度最大的元素，是水圈、生物圈和岩石圈最常见的组成部分（Cook and Lauer, 1968; Emsley, 2011），其化合物以固、液、气三态出现，一般都比较稳定，故在地球化学应用中有特殊的地位（郑永飞和陈江峰, 2000）。氧有三种稳定同位素，丰度递减顺序为：$^{16}O$(99.762%)、$^{18}O$(0.200%)、$^{17}O$(0.038%)（Tuli, 1985; Bao et al., 2016）。在宇宙中最初出现的顺序是：$^{16}O$ 是 $^{17}O$ 的上一代，而 $^{18}O$ 与 $^{16}O$ 和 $^{17}O$ 无关（Bao et al., 2016）。$^{16}O$ 是恒星中燃烧的氦核聚变的天然产物，是宇宙中第三丰富的核素，仅次于大爆炸后不久产生的 $^{1}H$ 和 $^{4}He$（Clayton, 2003）。$^{17}O$ 由 $^{16}O+^{1}H\rightarrow^{17}F\rightarrow^{17}O$ 过程形成，是次级核素。$^{18}O$ 通过恒星中的 $^{14}N+^{4}He\rightarrow^{18}F\rightarrow^{18}O$ 过程形成。

氧同位素应用于环境的研究开始于 20 世纪 50 年代（Dansgaard,1953），它是一种广泛存在于自然环境水体中的同位素。由于蒸发、凝结、降水、渗透和径流等条件不同，氧同位素值具有不同的特征（Yuntseover et al., 1981）。$^{18}O$ 与 $^{16}O$ 的比值是地球科学中最常见的同位素测量值之一，由于其同位素质量比值偏差大，可以在自然条件下发生较大程度的同位素分馏，因此在追踪生物地球化学循环途径和重建古气候条件等方面被广泛使用（Dansgaard, 1964; Zachos et al., 2001）。

地球上的水循环将固体地球、生物和大气系统联系在一起，是人类认知地球的重要基石（Gedney et al., 2006; Syed et al., 2008）。氧同位素的最早应用之一是水文循环研究，通过地方性和全球尺度数据整合与分析，确定了控制水循环中同位素分布的基本过程（Dansgaard,1964; Kendall et al., 1998）。自 Dansgaard（1953）年发表第一个水同位素观测结果以来，学术界已构建了丰富的理论体系，并积累了大量的实证数据，可用于在一系列尺度上探索水循环过程（Bowen et al., 2019）。大气过程在风暴期间和整个季节循环中引起了降雨同位素比值的自然波动，土壤或地下水的同位素比值可以记录这种变化特征（O'driscoll et al., 2005; Oerter and Bowen, 2017）。蒸发产生一种独特的同位素效应，可以在

氧同位素数据集中检测到,具体表现为大气湿度与水蒸气同位素比值之间呈现特定的协变关系,这种关系可以通过协方差来量化(Worden et al., 2007)。当水在水文循环中移动时,同位素比值能够综合水的历史信息(Jameel et al., 2016)。随后,氧同位素技术的研究范畴迅速扩展,在多个学科领域引发了广泛而深入的研究讨论。

本文在查阅大量文献资料的基础上,总结了目前国内外氧同位素在生态环境方面的应用,包括示踪环境污染物(Gross and Angert, 2015; Larkins et al., 2018; Zhang et al., 2018)、示踪全球水循环(Barkan et al., 2005; Dütsch et al., 2017; Aron et al., 2021)、重建古气候和古环境(李悦等, 2016; Roy et al., 2019)以及追踪地理来源(Kukusamude et al., 2018)等主要领域,并对未来氧同位素的应用提出展望。

## 2　氧同位素分析技术

### 2.1　氧同位素符号和标准

同位素组成采用样品同位素比值 $R_{sa}$ 相对于标准物质同位素比值 $R_{st}$ 的千分差值($\delta$)来表示。氧稳定同位素组成的表达公式为:

$$\delta^{x}\mathrm{O}=\left(\frac{R_{sa}}{R_{st}}-1\right)\times 1000‰ \qquad (1)$$

式中,$x$ 是 17 或 18,$R_{sa}$ 是样品 $^{x}O/^{16}O$ 的比值,$R_{st}$ 是标准 $^{x}O/^{16}O$ 的比值;$\delta^{x}O$ 值代表待测样品中 $^{x}O/^{16}O$ 的比值与标准物质中 $^{x}O/^{16}O$ 的比值的千分偏差。

氧同位素标准有两种:$\delta^{18}O$(SMOW)和 $\delta^{18}O$(PDB)(Hoefs, 1997)。PDB 标准通常只用于研究碳酸盐氧同位素的丰度(Friedman et al., 1977; Coplen et al., 1994)。为统一标准,研究人员采用 VPDB(Vienna Pee Dee Belemnite)来表示碳酸盐的氧同位素丰度,即 $\delta^{18}O_{NBS\text{-}19/VPDB}=-2.2‰$(Gonfiantini, 1984)。氧同位素分析结果通常以标准平均海水(SMOW)为标准,例如水、硅酸盐、磷酸盐、硫酸盐、高温碳酸盐等的氧同位素分析均与 SMOW 有关。SMOW 的"绝对"氧同位素比值为:$^{18}O/^{16}O=(2005.20\pm0.43)\times10^{-6}$,$^{17}O/^{16}O=(373\pm15)\times10^{-6}$(Hayes,1982)。表 1 给出了常用氧同位素标准在两种尺度上的 $\delta^{18}O$ 值。

在与古温度研究有关的碳酸盐样品氧同位素分析中,习惯采用 PDB 标准,它与 VSMOW 标准之间的转换关系(Coplen et al., 1983)为:

**表 1　常用氧同位素标准样的 $\delta^{18}O$ 值(‰)(据 Hoefs, 1997; 郑永飞和陈江峰, 2000)**

**Table 1　$\delta^{18}O$ values of commonly used oxygen isotope standards (after Hoefs, 1997; Zheng Yongfei and Chen Jiangfeng, 2000)**

| 标准 | 母质 | PDB | VSMOW |
|---|---|---|---|
| NBS-18 | 碳酸岩 | −23.00 | (7.20) |
| NBS-19 | 大理岩 | −2.20 | (28.64) |
| NBS-20 | 灰岩 | −4.14 | (26.64) |
| NBS-28 | 石英 | (−20.67) | 9.60 |
| NBS-30 | 黑云母 | (−25.30) | 5.1 |
| GISP | 格陵兰冰盖水 | (−53.99) | −24.75 |
| SLAP | 南极洲水样 | (−83.82) | −55.50 |

注:VSMOW表示海水经蒸馏后加入其他水配制成的δD值非常接近SMOW值的水样(Gonfiantini, 1978);括号内表示计算值。

$$\delta^{18}O_{V\text{-}SMOW}=1.03091\delta^{18}O_{PDB}+30.91 \qquad (2)$$

$$\delta^{18}O_{PDB}=0.97002\delta^{18}O_{V\text{-}SMOW}-29.98 \qquad (3)$$

### 2.2　氧同位素分馏

氧同位素分馏可以分为热力学平衡分馏、动力学非平衡分馏和非质量相关分馏三类,其中,前两项又属于质量相关分馏。

#### 2.2.1 热力学平衡分馏

体系处于同位素平衡状态时,同位素在两种矿物或两种物相间的分馏称为同位素平衡分馏,该过程仅与温度有关(Majoube, 1971; Bender et al, 1994),因此同位素平衡分馏又称为热力学平衡分馏,是同位素地质温度计的理论依据。一般情况下,同位素分馏系数 $\alpha$ 是温度($T$)的函数,表示为:

$$10^{3}\ln\alpha=\mathrm{A}\times\frac{10^{6}}{T^{2}}+\mathrm{B} \qquad (4)$$

式中 A 和 B 为常数,$T$ 为绝对温度,该函数式称为分馏方程(郑永飞和陈江峰, 2000)。

氧同位素地质温度计在地质学领域应用广泛,根据测定对象的不同,可分为外部测温法、内部测温法和单矿物测温法。例如在古温度研究中最为常用的碳酸盐–海水平衡的氧同位素温度计则为外部测温法。Craig(1964)的经验公式:

$$t(^{\circ}\mathrm{C})=16.9-4.2(\delta_{c}-\delta_{w})+0.13(\delta_{c}-\delta_{w})^{2} \qquad (5)$$

式中 $\delta_c$ 和 $\delta_w$ 分别是 25℃ 下 $CaCO_3$ 的磷酸盐法产生的 $CO_2$ 和水平衡产生的 $CO_2$ 的 $\delta^{18}O$ 值。内部测温法可应用于石英与水之间的氧同位素交换:

$$\frac{1}{2}Si^{16}O_2 + H_2{}^{18}O = \frac{1}{2}Si^{18}O_2 + H_2{}^{16}O \quad (6)$$

在热力学平衡条件下 $SiO_2$ 与 $H_2O$ 之间的氧同位素分馏系数可表达为：

$$\alpha SiO_2 - H_2O = \left({}^{18}O/{}^{16}O\right) SiO_2 / \left({}^{18}O/{}^{16}O\right) H_2O \quad (7)$$

单矿物测温法指通过分别测定含羟基矿物中不同结构位置上氧的同位素组成，应用合适的分馏系数确定矿物的形成温度。Delgado et al.(1996)根据 Savin et al.(1988)的氢同位素分馏方程和 Capuano(1992)的氧同位素分馏方程，得到蒙脱石单矿物温度计(0~150℃)：

$$28.3 \times 10^6 / T^2 = 8\delta^{18}O_M - \delta D_M + 71.61 \quad (8)$$

2.2.2 动力学非平衡分馏

动力学非平衡分馏指偏离同位素平衡而与时间有关的分馏，即同位素在物相之间的分配随时间和反应进程而不断变化，依赖于路径、时间与速度(Merlivat et al., 1975,1979)。伴随着蒸发过程、扩散过程、分解反应过程及光合作用过程等等发生的同位素分馏都属于动力学分馏(Cappa et al., 2003)。生物参与的化学过程，一般同位素动力学效应明显。它与蒸发、解离反应、生物介导反应和扩散等不完全和单向过程有关(Hoefs, 1997)。随着蒸发的进行，重同位素在液相富集，盐度对于重同位素富集有抑制作用(李桐和邱国玉, 2018)。Chiba and Sakai(1985)研究得到，反应速率常数与温度和 pH 值有关，pH 值升高，交换速率迅速下降(图 1)。依据此，可以推断溶解的硫酸盐与水之间的同位素交换是在低 pH 下 $H_2SO_4$ 与 $H_2O$ 之间的碰撞以及中等 pH 下 $HSO_4^-$与 $H_2O$ 之间的碰撞进行的。

水岩相互作用是动力学分馏在地质方面的一个重要应用示例。由于近地表环境演化的驱动力，在化学与力学的耦合作用下，水岩系统会发生地下水溶质迁移和地层地质结构变化等，极大地影响了地层结构的稳定性和地下水环境的演化(沈照理等, 2012)。对于不同类型的湖泊来说，水岩相互作用最强烈的是在碳酸盐型湖泊中，最高 pH 值可达 9.0~9.9，湖水会与内源铝硅酸盐发生强烈相互作用，水解使湖水中 pH 和碳酸根离子增加，较高的 pH 和 $HCO_3^-$、$CO_3^{2-}$离子的含量又使得大量钙、镁和部分钠碳酸盐(如镁铝榴石、钠长石、滑石)形成沉淀(Borzenko, 2021)。

2.2.3 非质量相关分馏

对于氧同位素，地球上遵守质量相关定则的物质普遍有 $\delta^{17}O=0.516\delta^{18}O$。地球样品普遍满足质量相关分馏线，但陨石具有显著的氧同位素非质量分馏。Clayton et al.(1973)发现，Allende 碳质球粒陨石中富 Ca、Al 高温包体的氧同位素分析数据点落在斜率为 1 的直线上，显然不符合质量相关定则。Thiemens et al.(1983)通过实验证实了由 $O_2$ 通过放电制得的 $O_3$ 和残余 $O_2$ 会产生与质量无关的分馏(图 2)。对于这种不遵循质量分馏定律或背离质量分馏线的同位素分馏称为非质量相关分馏(熊志方等, 2007)。

氧同位素非质量分馏源自化学效应，包括核自旋、过渡态化学、分子对称性和光化学反应(Thiemens et al., 1983; Criss et al., 2008)。这些影响会导致三重氧同位素($^{17}O/^{16}O$ 和$^{18}O/^{16}O$)之间发生巨大变化，并且在大气化学、行星科学和生物生产力方面有一系列应用，这些应用已得到较好的评价(Blunier et al., 2012)。氧同位素异常($\Delta^{17}O$)常用来衡量氧同位素非质量分馏(O-MIF)的程度(Assonov et al., 2005)，其定义如下：

$$\Delta^{17}O = \delta^{17}O - \lambda \times \delta^{18}O \quad (9)$$

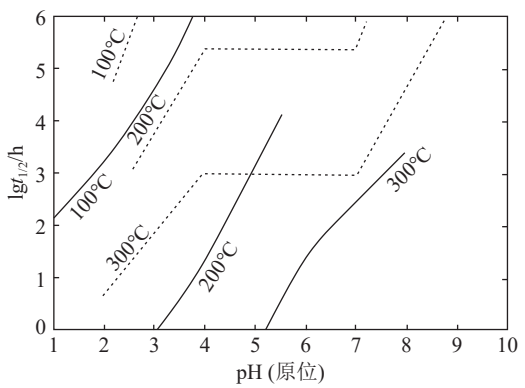


图 1 热液体系中溶解物质之间同位素交换半衰期与 pH 的关系(据 Chiba and Sakai, 1985)

(虚线代表溶解硫酸盐与硫化物之间的硫同位素交换，实线代表溶解硫酸盐与水之间的氧同位素交换)

Fig.1 Relationship between isotope exchange half-life and pH between dissolved substances in hydrothermal systems(after Chiba and Sakai, 1985)

(Dashed line represents sulfur isotope exchange between dissolved sulfate and sulfide, solid line represents oxygen isotope exchange between dissolved sulfate and water)

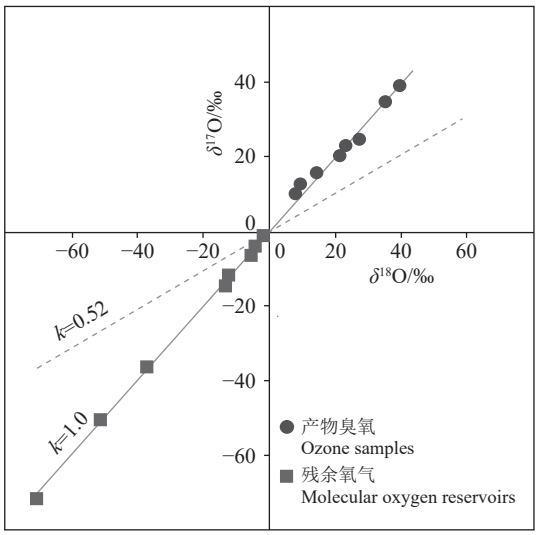


图 2 臭氧形成的同位素分馏(据 Thiemens et al., 1983; Thiemens, 2006)
(虚线是一条穿过原始氧同位素组成的质量分馏线)
Fig.2 Isotopic fractionation of ozone formation(after Thiemens et al., 1983; Thiemens, 2006)
(Dotted line is a mass fractionation line through the original oxygen isotopic composition)

式中分馏斜率 λ 范围在 0.500~0.529 浮动变化(Hoag et al., 2005)。λ 值的选择关系到 $\Delta^{17}$O 的计算结果以及 $\Delta^{17}$O 示踪的准确性,因此选取合适的 λ 值非常重要(曹佳璐等, 2023)。同时为了便于比较不同实验室之间 $\Delta^{17}$O 的测量结果,根据经验结果,常将 λ 值选为 0.516(Boering et al., 2004)。

与氧同位素质量相关分馏(MDF)不同,$O_3$ 在平流层中发生光化学反应会导致$^{18}$O 和$^{17}$O 均匀分配(Luz et al., 1999)。之后,氧气会带着非质量同位素分馏的特征再循环到对流层,形成了大气氧同位素异常,表现为生物圈生产力越高,$\Delta^{17}$O 越偏正(Bender et al., 1994)。Luz et al.(1999)认为$\Delta^{17}$O 可作为全球生物生产力的示踪剂,并且在极低冰芯中用圈闭的 $O_2$ 的氧同位素异常估计了 8.2 万年以来全球不同时期生物圈生产力,与现代相比变化不大。由于硫酸盐很容易保存在地质记录中,$\Delta^{17}$O 还可以与冰芯中硫同位素联合运用,示踪冰芯中硫酸盐、硝酸盐的来源和运移问题。Vostok 冰芯硫酸盐中运用 $\Delta^{17}$O 与 S 同位素(Alexander et al., 2003),证明了冰期时气相氧化路径比液相氧化路径贡献大,并且 S 同位素示踪表明了 Vostok 冰芯硫酸盐是来源于低纬度海洋生物硫在对流层底部(而非平流层)氧化后搬运至南极的结果。由此可见,$\Delta^{17}$O 可以定量确定运移过程中氧化路径的细节信息。

三重氧同位素非质量相关分馏不仅存在于环境臭氧中,也存在于许多含氧的气态分子中,包括 $CO_2$、$H_2O_2$、$N_2O$、CO 和 $O_2$(Lin et al., 2024)。图 3 显示了迄今为止测量到的大气 O–MIF 组分的三重氧同位素组成。$H_2O_2$ 中的 O–MIF 最早是由 Savarino et al.(1999)在雨水中测得的。在加利福尼亚州 La Jolla 收集的雨水中,$H_2O_2$ 显示出相对恒定的 $\Delta^{17}$O 值(1‰~2‰),而由于 $H_2O_2$ 与亚硫酸盐反应或催化分解,$\delta^{18}$O 变化较大(22‰~60‰)(Guo et al., 2022)。同时期,Thiemens 小组开发了测量大气 $N_2O$ 中三重氧同位素的分析方法,与大气中其他含氧分子类似,在 $N_2O$ 中也观察到了 O–MIF 特征($\Delta^{17}$O: 平流层和对流层均约为 1‰)(Cliff et al., 1999),该特征与 $O_3$ 中的氧原子转移有关(Liang et al., 2007)。对于 CO 而言,从各种排放源直接排放的 CO 具有同位素质量依赖性,CO 的 O–MIF 特征源自 CO+OH 反应(Rockmann et al., 1998)以及真空紫外区的 CO 光解。分子氧($O_2$)是现代地球大气中最大的氧气库(约 21%)。通过比较环境空气 $O_2$ 中的三重氧同位素组成与不受平流层过程影响的 $O_2$(通过生物重置其同位素组成),初步研究表明,环境空气 $O_2$ 中的 $\Delta^{17}$O 较小,为负值,同位素特征来自平流层中的 $O_3$–$O_2$–$CO_2$ 光化学循环及其与地球表面光合作用和初级生产力的耦合(Luz et al.,

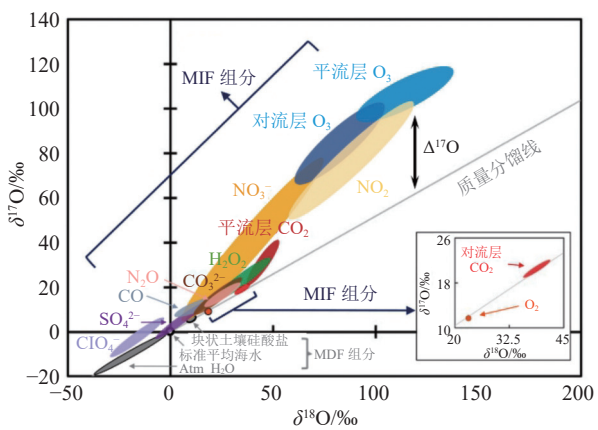


图 3 迄今已测得的大气 MIF 组分的三氧同位素组成(据 Lin et al., 2024)
Fig.3 Triple oxygen isotope compositions of atmospheric MIF component that have been measured to date(after Lin et al., 2024)

1999)。在解释 $O_2$ 微小的 $^{17}O$ 异常时，对 MIF 和 MDF 过程的理论考虑至关重要。

在大气 $CO_2$ 的 O−MIF 研究中，常用 $\Delta^{17}O$ 来估算平流层向对流层输入的 $CO_2$ 通量(Thiemens et al., 2014; Liang et al., 2015)和全球生产力(Liang et al., 2023)，目前多数学者对全球陆地生产力的估算结果约为 120 $Pg\cdot a^{-1}$(Beer et al., 2010; Mahecha et al., 2010; Ryu et al., 2011)。$\Delta^{17}O$ 还可以区分大气 $CO_2$ 不同来源，对于研究全球碳循环和控制碳排放具有重要意义。由表 2 可见，不同来源 $CO_2$ 的 $\Delta^{17}O$ 值存在差异。燃烧所产生的 $CO_2$ 中 $\Delta^{17}O$ 与背景 $CO_2$ 中 $\Delta^{17}O$ 有明显区别，表明了除平流层 $CO_2$ 输入外，燃烧所产生的 $CO_2$ 保留了对流层中 $O_2$ 的氧同位素非质量分馏信号(Hoag et al., 2005)。呼吸产生的 $CO_2$ 中 $\Delta^{17}O$ 值受环境水的限制(曹佳璐等, 2023)，近似为零，可以与燃烧源 $CO_2$ 中 $\Delta^{17}O$ 值明显偏负区分开。

## 3 氧同位素在示踪环境污染物来源方面的应用

同位素是研究元素循环的重要手段，可以示踪元素的来源和迁移转化过程(Tian et al., 2016)。在环境污染物方面，氧同位素可以用来追踪环境中磷生物地球化学行为、解析硝酸盐主要来源以及示踪矿山活动对地下水的污染等。

### 3.1 示踪环境中磷循环

磷作为一种重要的营养元素，在生物体的发育繁殖中起着至关重要的作用(MacDonald et al. , 2011)，但同时磷也是环境污染物之一，过量的磷进入水体中，会引起水体富营养化，影响水质，危害水生生物，甚至造成鱼类大量死亡(Li et al., 2020b)。

**表 2 不同来源 $CO_2$ 的 $\Delta^{17}O$ 值**

**Table 2 $\Delta^{17}O$ values for different sources of $CO_2$**

| $CO_2$来源 | $\Delta^{17}O$值/‰ | 参考文献 |
|---|---|---|
| 天然气燃烧 | −0.34~−0.25（−0.30±0.02） | Horváth et al., 2012（λ=0.522） |
| 丙烷−丁烷燃烧 | −0.38~−0.29（−0.32±0.02） | |
| 汽车尾气 | −0.43~−0.24（−0.32±0.03） | |
| 木屑燃烧 | −0.27~−0.17（−0.21±0.02） | |
| 人类呼吸 | −0.07~0.04（−0.03±0.03） | |
| 稻草燃烧 | 0.05±0.02 | Laskar et al., 2020（λ=0.516） |
| 背景（南海） | 0.335±0.034 | Liang et al., 2017（λ=0.516） |

因此，开展土壤磷循环研究对提高磷肥利用效率和降低磷的生态环境风险具有重要意义。自然界中大多数磷会与氧紧密结合形成正磷酸盐(三代磷酸盐)，P−O 键十分稳定，在自然温度与 pH 条件下，只能通过生物反应打破，非生物的氧同位素分馏可以忽略不计，在沉淀、溶解、解吸等物理过程产生的同位素分馏甚至小于 1‰(Zheng, 2016)。

短时间内，影响生物可利用土壤磷酸盐氧同位素组成($\delta^{18}O_P$)(图 4)的主要机制为(Gross et al., 2015)：(1)如果土壤不同磷库间的 $\delta^{18}O_P$ 值不同，磷酸盐分子可能会发生同位素交换，但这种非生物交换反应不会断裂磷酸盐的 P−O 键(Angert et al., 2012; 赵甜甜等, 2022)；(2)微生物倾向吸收较轻的同位素，因此土壤中残留的磷酸盐会富集重氧同位素；(3)通过生物反应，磷酸盐与水发生氧同位素交换：①细胞外磷酸酶水解有机磷化合物，伴随强烈的动力学效应并产生负的同位素分馏(张弛等, 2018; Tian et al., 2020)；②磷酸盐作为细胞代谢的一部分，与土壤水的同位素平衡中会产生磷酸盐，可用方程式表示：$\delta^{18}O_P=\delta^{18}O_{water}+(111.4-T)/4.3$(其中 $T$ 单位：℃，$\delta^{18}O_{water}$：土壤水的氧同位素组成)(Kolodny et al., 1983)。上述的分馏反应会改变土壤环境中的 $\delta^{18}O_p$，甚至打破原有的同位素平衡，在无机磷($P_i$)上留下平衡的氧同位素标记(Blake et al., 2005)。磷酸盐氧同位素组成($\delta^{18}O_P$)反映了磷的微生物利用状况(McLaughlin et al., 2006)，因此可以用 $^{18}O/^{16}O$ 比值在不同磷源中的统计学差异，间接研究土壤中磷的来源及迁移转化过程(Kolodny et al., 1983)。

在地表环境中，生物作用几乎参与了磷循环的所有过程(如无机磷的同化、有机磷的矿化等)，并且生物作用会大大加速磷酸盐的氧同位素分馏(Blake et al., 2005)，使土壤中不同形态 $\delta^{18}O_P$ 值产生差异(Gross and Angert, 2015)。Gross et al.(2015)对巴拿马热带低地森林中不同施肥处理的土壤研究发现，长期接受 N、P、K 养分补充的土壤，会减缓土壤中由于磷过量微生物对磷酸盐的周转。Tian et al.(2020)通过分析中国不同地区的典型农业土壤中不同形态的磷酸盐氧同位素，发现肥料和土地利用是主要的影响因素。对于不同磷库，$H_2O-P_i$ 和 $NaHCO_3-P_i$ 是生物可利用的磷；$NaOH-P_i$ 有时参与

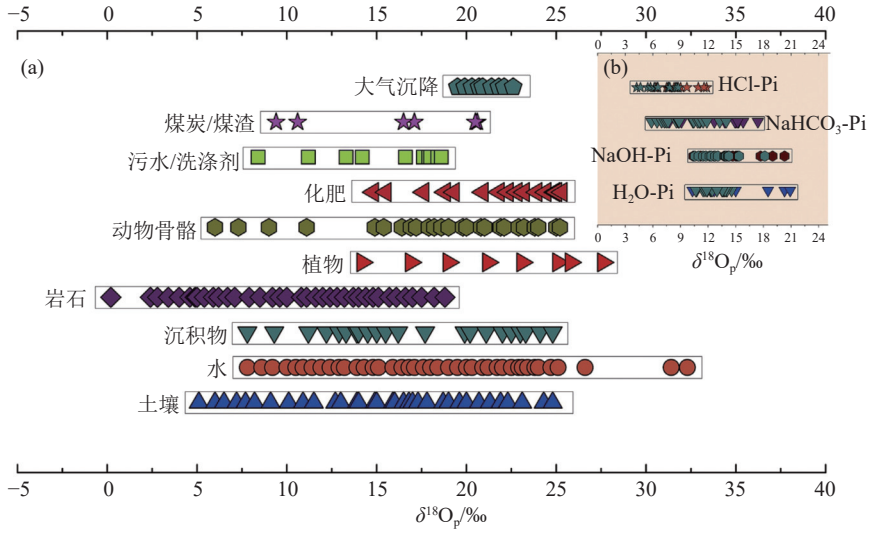


图 4 天然物质中磷酸盐的氧同位素组成(a)和土壤中不同部分的氧同位素组成(b, 据 Tian et al., 2020)
Fig.4 Oxygen isotope composition of phosphates in natural substances(a)and oxygen isotope composition of different parts of soil(b, after Tian et al., 2020)

生物转化; HCl–$P_i$ 与其他组分相比难以被微生物利用, 它主要反映母岩的 $\delta^{18}O_P$ 特征(Roberts et al., 2015)。由此可见, 土壤 $\delta^{18}O_P$ 特征不仅提供了磷的微生物利用信息, 也为土壤施加肥料提供理论依据。

$\delta^{18}O_P$ 技术也应用于上覆水以及沉积物领域(陈志刚等, 2010)。同土壤磷一样, 沉积物磷也可以划分为不同的形态, 这些形态具有不同的生物有效性(Cavalcante et al., 2018)。Yuan et al.(2019)利用 $\delta^{18}O_P$ 示踪沉积物磷的来源及其循环过程, 不同来源的 $\delta^{18}O_P$ 组成具有明显差异, 中国太湖磷的来源主要包括潜在的碎屑磷源(9.76‰~14.62‰), 自生磷源(15.28‰±0.56‰), 铝氧化物结合态(18.9‰~23.35‰)和铁氧化物结合态(18.7‰~20.8‰)(图 5)。研究表明, 内部磷负载(指通过重悬过程从沉积物中释放的磷, 以及通过吸附和解吸过程从悬浮颗粒中释放的磷)和外部磷输入(主要与人类活动有关)对于流域磷循环的贡献很大: 一方面由氧化还原电位和酶驱动的沉积物释放磷会增加上覆水中溶解的磷浓度; 另一方面, 随着人口增加和饮食改善, 在农田上增加肥料施用以满足粮食需求, 导致流域外部磷投入大幅增加(Wang et al., 2022b)。Wang et al.(2023)通过分析长江流域的水样得到河水的 $\delta^{18}O_P$ 值在雨季为 4.9‰~18.3‰, 旱季为 6.0‰~20.9‰, 表明季节对其影响较小, 而 $\delta^{18}O_P$ 的空间变化说明了人类活动, 如农业施肥、生活污水等对环境中磷循环的影响。Jin et al.(2023)对云南省滇池的采样研究, 也证实了 $\delta^{18}O_P$ 可以用于识别沉积物中不同组分的磷源。由此, 可知 $\delta^{18}O_P$ 技术为追踪土壤中磷酸盐的来源提供了信息。Yuan et al.(2022)发现水生环境中强烈的生物活动会改变 $\delta^{18}O_P$ 趋向均衡的值, 大多数水体样品中的 $\delta^{18}O_P$ 值不会达到平衡同位素, 表明河流源的特征不会轻易被叠加(McLaughlin et al., 2006)。因此, 磷酸氧同位素技术是追踪流域磷生物地球化学循环的有效途径。

自然条件下土壤磷循环的解释大多是对已知的来源和可能的影响过程进行推测, 难以从根本上揭示磷循环机制(赵甜甜等, 2022)。室内标记的培养实验在一定程度上可以更好地揭示磷循环机制。例如 Pistocchi et al.(2020)对富氧同位素水进行培养实验证实了, 在限磷条件下磷水解的同位素效应大于同位素平衡效应, 使微生物磷的 $\delta^{18}O_P$ 值低于平衡值。因此, 将多种方法融合, 如放射性磷标记(Pistocchi et al., 2020; Siegenthaler et al., 2020)、光谱技术与同位素技术结合(Helfenstein et al., 2018)等, 互相印证, 避免单一研究方法的不足, 可以让 $\delta^{18}O_P$ 技术发挥更大价值。

### 3.2 解析硝酸盐成因

氮是所有生物的基本元素, 在所有氮素形态

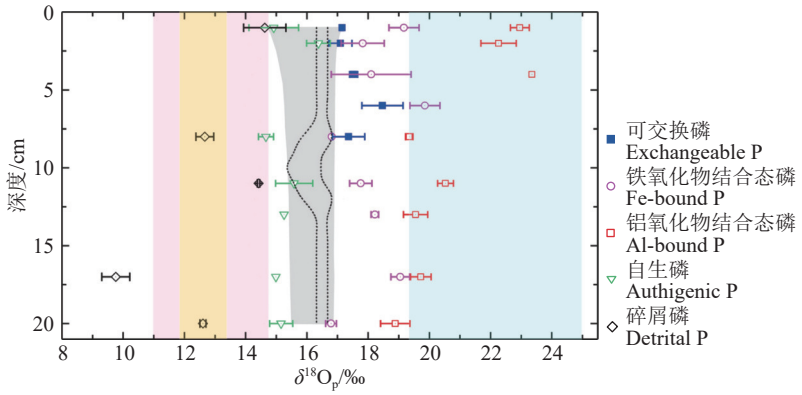


图 5 沉积物中不同磷库及潜在来源的 $\delta^{18}O_P$ 值(据 Yuan et al., 2019)

灰色阴影区表示使用沉积物-水界面季节平均温度数据计算的平衡 $\delta^{18}O_P$ 值区(Zeng et al., 2018); 灰色区域虚线之间的面积是根据沉积物-水界面实测温度和孔隙水同位素值计算出的平衡同位素值范围(95% 置信度); 浅粉色区域为火成岩/变质岩成因 $\delta^{18}O_P$ 值: 11‰ ~ 14.7‰(Jaisi et al., 2010); 浅黄色区域代表磷酸酯中新鲜再生的 $P_i$, $\delta^{18}O_P$ 值在 11.90‰~13.33‰(计算参考 Joshi et al., 2015); 浅青色区域代表化学肥料的 $\delta^{18}O_P$ 值总体范围为 19.4‰~25.0‰(Gruau et al., 2005; McLaughlin et al., 2006; Li et al., 2011; Gross et al., 2013)

Fig.5 $\delta^{18}O_P$ values in different P pools and potential sources in the sediment(after Yuan et al., 2019)

Gray shaded region represents the equilibrium $\delta^{18}O_P$ values zone calculated using season-average temperature data at sediment-water interface (Zeng et al., 2018). Area between dashed lines in grey zone denotes the range of equilibrium isotope values (with 95% confidence level) calculated using measured temperature at sediment-water interface and porewater isotope values in June. Light pink field refers to the $\delta^{18}O_P$ values of igneous/metamorphic origin (11‰−14.7‰; see (Jaisi et al., 2010)). Light yellow field represent freshly regenerated Pi with $\delta^{18}O_P$ values between 11.90 and 13.33‰ from phosphoesters (calculated as in Joshi et al., 2015) and light cyan field represents the ranges of chemical fertilizers with reported $\delta^{18}O_P$ values in overall range of 19.4‰−25.0‰ (Gruau et al., 2005; McLaughlin et al., 2006; Li et al., 2011; Gross et al., 2013)

中，由于较高的流动性，硝酸盐占主导地位(Frau et al., 2020)，其有效性取决于不同的转化反应，特别是硝化、反硝化和生物吸收(Kendall et al., 2007; Mayer et al., 2002)。硝酸盐是水体中常见的含氮化合物，高浓度的硝酸盐会引起湖泊富营养化、水生生物死亡等环境问题，同时也会对人体健康产生危害(Xu et al., 2016)。地表水体中 $NO_3^-$来源复杂，主要可分为大气沉降、土壤有机氮等自然源，以及动物粪便和生活污水、化学肥料、工业废水等人为源。传统识别硝酸盐污染来源的方法是通过一个区域研究对象的物理化学特征，并综合该区域土地的使用情况来识别硝酸盐的来源，但该方法在使用时耗时耗力，且不能准确的识别污染源(李智滔等, 2022)。

3.2.1 氧同位素追踪硝酸盐来源

随着同位素技术的发展，人们开始利用氧同位素示踪硝酸盐来源。在 Chen et al.(2020)和 Mayer et al.(2001)的研究中，大气沉降硝酸盐(AD)的 $\delta^{18}O-NO_3^-$范围为 25‰~75‰，明显高于硝基肥(17‰~25‰)和氮肥(NF)、土壤氮(SN)和牲畜排泄物与城市污水(MS的)硝化作用($\delta^{18}O-NO_3^-$= 10‰~15‰)。然而，由于 AD 中 $\delta^{18}O-NO_3^-$范围较广，以及氮循环过程中对$^{18}O$ 同位素分馏效应的影响，使得 $\delta^{18}O-NO_3^-$技术不能完全区分硝酸盐来源。为了克服这一局限性，$\Delta^{17}O-NO_3^-$被用作大气中硝酸盐沉积的示踪剂(Michalski et al., 2003)。其原理是当大气中的臭氧形成时，会发生与质量无关的同位素分馏，导致臭氧产物中$^{17}O$、$^{18}O$ 的富集(Marcus, 2008)，由此产生了氧同位素异常($\Delta^{17}O$)(Xia et al, 2019)，这导致了在 $NO_x$ 氧化过程中富集$^{17}O$ 的 $O_3$ 被转移到硝酸盐中。因此，来源于大气沉降的硝酸盐特点是$^{17}O$ 异常富集(Michalski et al., 2004)。

由于氧同位素异常仅在光化学反应中发生，它能够进一步量化硝酸盐形成过程中不同氧化路径的贡献比例(Kamezaki et al., 2017; Ishino et al., 2017)。通常情况下，AD 中的 $\Delta^{17}O-NO_3^-$为正值，在 17‰~35‰范围内；而一些陆地氮循环过程，如硝化和反硝化，都是质量相关分馏过程，这导致了 $\Delta^{17}O-NO_3^-$接近于 0‰(Ji et al., 2022)。Michalski et al.(2006)利用氧同位素异常研究发现，大气硝酸盐对太浩湖总硝酸盐的贡献约为 13%，还通过该贡献值与大气硝酸盐进入湖泊的沉积速率，估算了湖泊中的平均硝化作用速率。Liu et al.(2013)使用三重硝酸盐同位素确定，未经处理的大气硝酸盐占黄河硝酸盐的 0~7%。总体而言，$\Delta^{17}O-NO_3^-$比 $\delta^{18}O-NO_3^-$

对于加强河流硝酸盐污染源解析，尤其是大气硝酸盐贡献的识别更有效。原因如下：(1)$\Delta^{17}O-NO_3^-$值是稳定的，在陆地系统氮生物地球化学转化过程中不会发生变化。相反，AD 的初始 $\delta^{18}O-NO_3^-$值可能会因氮循环过程中$^{18}O$ 分馏而改变，这种动态变化特性可能导致硝酸盐来源解析结果的不确定性增加；(2)AD 中 $\Delta^{17}O-NO_3^-$的同位素范围比 $\delta^{18}O-NO_3^-$的同位素范围窄，有利于增强硝酸盐来源解析结果的准确性(Ji et al., 2022)。但由于单一元素的局限性，通常将 $NO_3^-$中的氧同位素与氮同位素结合使用，以便得到更可靠的源识别(张翠云等, 2003)。

3.2.2 氮氧双同位素追踪硝酸盐来源

氮氧双同位素也是识别硝酸盐污染源的一种方法。不同来源的 $NO_3^-$具有不同的 $\delta^{18}O$ 和 $\delta^{15}N$ 特征值，因此利用硝酸盐氮氧双同位素($\delta^{18}O-NO_3^-$和 $\delta^{15}N-NO_3^-$)技术分析氮氧同位素比值，可以确定地表水中 $NO_3^-$主要来源，解析地球化学循环规律(Zhang et al., 2018)。不同来源硝酸盐具有不同的同位素值域范围(李思远等, 2024)，据此可识别环境中氮素的主要来源(图 6)。无机化肥由大气 $N_2$ 通过工业固氮而来，其 $\delta^{15}N-NO_3^-$为−6‰~6‰，$\delta^{18}O-NO_3^-$为 17‰~25‰；受大气层中复杂的光化学作用影响，大气沉降通常表现出较高的 $\delta^{18}O-NO_3^-$值(25‰~75‰)(Amberger et al., 1987)，$\delta^{15}N-NO_3^-$为−13‰~13‰；人畜粪便 $\delta^{15}N-NO_3^-$为 5‰~25‰，$\delta^{18}O-NO_3^-$为 5‰~7‰；生活污水 $\delta^{15}N-NO_3^-$为 4‰~19‰，$\delta^{18}O-NO_3^-$为−5‰~10‰；土壤氮素受矿化及硝化作用综合影响，$\delta^{15}N-NO_3^-$为 0‰~8‰，$\delta^{18}O-NO_3^-$为−10‰~10‰(Blake et al., 2005; Elliott et al., 2006; Savarino et al., 2007)。

双同位素技术已成功地应用于水生生态系统中硝酸盐来源的识别，并极大地加深了人们对于氮循环的理解。中国地表水 $\delta^{15}N-NO_3^-$和 $\delta^{18}O-NO_3^-$特征值范围分别为−23.5‰~26.99‰和−12.7‰~83.5‰(张鑫等, 2020)。中国地表水系统主要分布在松花江流域、辽河流域、黄河流域、海河流域、淮河流域、长江流域和珠江流域这 7 个流域(表 3)。基于 $\delta^{18}O-NO_3^-$和 $\delta^{15}N-NO_3^-$特征，Li et al.(2010)首次成功评估了长江中硝酸盐的来源和变异性。结果表明，硝化作用和城市污水是长江流域硝酸盐的主要来源。Hu et al.(2019)首次采用双同位素技术鉴定了西藏河流、湖泊和湿地中硝酸盐的来源和转化过程，表明了不同地区硝酸盐来源存在显著差异，如该研究区湿地中硝化作用和反硝化作用是影响硝酸盐的主要因素，而湖泊中硝酸盐主要来源为粪便、污水等。李智滔等(2022)对鄱阳湖湿地硝酸盐来源的解析，$\delta^{18}O-NO_3^-$和 $\delta^{15}N-NO_3^-$值的关系显示，该地硝酸盐来源一定程度上受降水和化肥使用的影响。

氮氧双同位素解析硝酸盐来源时，还可以同步利用 $\Delta^{17}O-NO_3^-$加强硝酸盐来源解析，尤其是大气硝酸盐贡献的识别(Ji et al., 2022)。Hundey et al.(2016)应用 $\Delta^{17}O-NO_3^-$、$\delta^{18}O-NO_3^-$和 $\delta^{15}N-NO_3^-$对美国犹他州 Uinta 山的硝酸盐来源进行解析，发现水生系统中至少 70% 的硝酸盐来源于人类活动所导致的大气沉降输入。Ji et al.(2022)使用 $\Delta^{17}O-NO_3^-$、$\delta^{18}O-NO_3^-$和 $\delta^{15}N-NO_3^-$追踪中国东部流域中硝酸盐来源，发现城市污水(MS)是主要的硝酸盐来源(图 7)。其中，河水和降水的 $\Delta^{17}O-NO_3^-$值分别为−2.82‰~9.66‰和 14.83‰~31.39‰，表明 AD 是中国东部河流的重要硝酸盐来源。

利用氮、氧稳定同位素识别硝酸盐污染源弥补了传统方法无法定量化识别污染源的缺点，应用前景广阔。由于氮在迁移转化过程中同位素分馏效应复杂，增加了溯源结果的不确定性，有关氮循环过程中的硝化、反硝化、固氮、矿化、作物吸收等生物化学过程和氨挥发、水解、扩散等物理化学过程，其同位素分馏特征已有大量的研究成果，但是对于

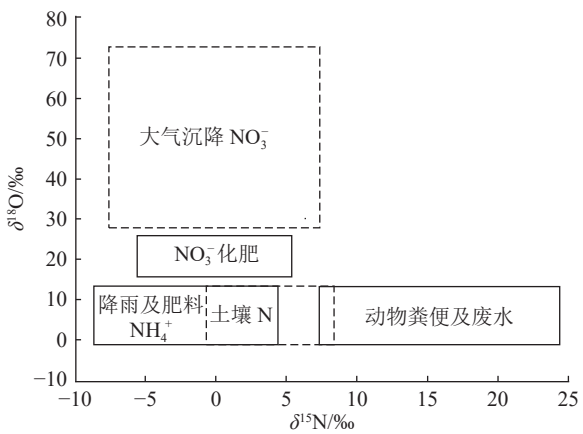


图 6 不同来源硝酸盐氮氧同位素特征值(据 Nestler et al., 2011)
Fig.6 Nitrogen and oxygen isotopes signatures of nitrate from different sources(after Nestler et al., 2011)

表 3 不同流域硝酸盐及氮氧同位素特征值

Table 3 Eigenvalues of nitrate and nitrogen and oxygen isotopes in different watersheds

| 流域 | $NO_3^-$/(mg/L) | $\delta^{15}N-NO_3^-$/‰ | $\delta^{18}O-NO_3^-$/‰ | 文献来源 |
|---|---|---|---|---|
| 松花江流域 | 11.43 | 6.27 | 3.18 | Yue et al., 2014 |
| 海河流域 | 22.96 | 16.28 | 5.05 | Peters et al., 2019 |
| 珠江流域 | 7.58 | 6.88 | 4.31 | Ye et al., 2015 |
| 黄河流域 | 19.84 | 7.26 | −0.96 | Yue et al., 2017 |
| 辽河流域 | 14.11 | 9.60 | 4.35 | Yue et al., 2015 |
| 长江流域 | 20.17 | 8.40 | 6.27 | Wang et al., 2017 |
| 淮河流域 | 10.16 | —— | —— | 毛剑英等，2003 |

硝酸盐异化还原、厌氧氨氧化等氮转化过程，其同位素分馏效应尚不明确。因此，需要进一步开展不同转化途径、不同环境要素对氮同位素分馏特征的影响研究。

### 3.3 追踪矿山环境污染物来源

随着全球范围内的大面积采矿活动的开展，其对生态环境和人类健康的影响日渐成为全球关注的一个重要问题(Cao et al., 2022)。富含金属硫化物的矿床(包括富含硫化物的煤矿和黑色岩系矿床)的采矿活动，产生的废弃物往往被堆放在地表或倾倒在地下(Ruhela et al., 2022)，会产生大量富含有害重金属的酸性矿山废水(AMD)，其特点是 pH 值低，$SO_4^{2-}$浓度、金属和准金属浓度高(Sierra et al., 2013; Maqsoud et al., 2016; Moyé et al., 2017)。这些废水通常会通过地表径流、淋滤等过程进入到环境中(Li et al., 2020a)，对人类健康和生态环境构成风险(Larkins et al., 2018)；还可以改变当地溪流和下游河流系统的水文、化学和生物组成(Newman et al., 2020; Li et al., 2022)。因此，查明矿山水的来源以及区域之间的联系，对于矿山污染源与 AMD 的识别以及区域生态环境可持续发展具有重要意义。

#### 3.3.1 氢氧同位素示踪水体来源

水体氢、氧同位素示踪技术是矿山水源解析、水力联系研究及 AMD 源识别的有效工具(赵睿涵等, 2022)。自然界的水中海水占 97.16%，陆地水占 2.83%(其中主要是冰川水，占 2.09%)，生物圈和大气圈的水含量微乎其微(郑永飞和陈江峰, 2000)。天然水环境中含有氢氧稳定同位素(陈陆望等, 2003)，来源相同的水体中氢氧稳定同位素特征具有相似的线性关系，而不同位置水体(如大气降水、河流/湖泊水体与地下水等)中的氢氧稳定同位

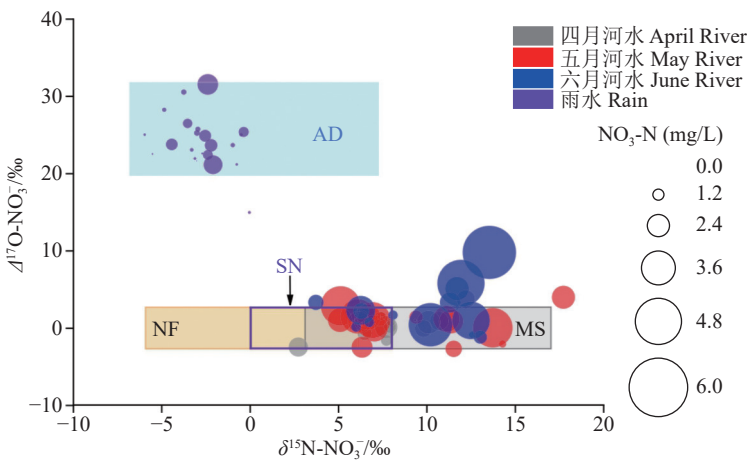


图 7 温瑞塘河流域河水、雨水和潜在硝酸盐来源中 $\delta^{15}N-NO_3^-$和 $\Delta^{17}O-NO_3^-$值散点图(据 Ji et al., 2022)

AD—大气沉降硝酸盐; NF—氮肥(氨基复合肥和尿素); SN—土壤氮; MS—城市污水

Fig.7 Scatter plot of $\delta^{15}N-NO_3^-$ and $\Delta^{17}O-NO_3^-$ values in river water, rainwater and potential nitrate sources in the Wen-Rui Tang River watershed(after Ji et al., 2022)

AD−atmospheric deposition nitrate; NF−nitrogen fertilizer (ammonia-based composite fertilizers and urea); SN−soil nitrogen; MS−municipal sewage.

素组成的变化规律往往不同，水的蒸发则会引起同位素分馏(汪敬忠等, 2013)。氢氧同位素示踪剂作为了解矿区污染物行为和相互作用以及从矿区到受体水域的传输和稀释的工具具有巨大潜力(Larkins et al., 2018)。因此，可以通过分析水中氢氧稳定同位素特征对区域内水体来源/混合、不同含水层地下水与矿井水之间的水力联系及是否存在蒸发作用等进行探究(樊娟等, 2021; 朱红艳等, 2021)。

氢氧稳定同位素作为示踪剂，可应用在矿山废弃物表征补给率或水在其中的移动，以及追踪场外矿山水的迁移(Dompierre et al., 2016)。$\delta$D、$\delta^{18}$O 组成与当地大气水线之间的相对位置揭示了补给源并提供了水样的循环信息(Bhatia et al., 2011)。Li et al.(2022)对湖南省冷水江市附近山区采样结果显示，河水 $\delta$D 介于 −41.3 ‰~−38.6 ‰，平均值为 −40.0 ‰；$\delta^{18}O_{H_2O}$ 介于 −7.8 ‰ 和 −5.9 ‰，平均值为 −6.6 ‰。相对于当地大气水线(LMWL, $\delta D = 8.38\delta^{18}O + 17.3$)和全球大气水线(GMWL, $\delta D = 8\delta^{18}O + 10$)，河水和矿井废水样品的同位素组成(图 8)显示：雨季的河流样品点在 LMWL 内或附近，表明河水来自降雨；而旱季样品与雨季样品的同位素相似，但$^{18}$O 略微富集，落在当地地下水的同位素范围内，表明地下水是枯水期河水的主要补给源。李小倩等(2014)测定广西合山矿区水体中的氢氧同位素数据显示，氢氧同位素组成均落在当地大气降水线右下方，表明水体接受大气降水补给后受到了显著的蒸发作用；而矿区矿井水及地下水较河水富集重同位素，表明其在接受大气降水及径流过程中受到更强烈的蒸发作用。同时矿区水体氢氧同位素组成间表现出较好的线性相关关系($\delta D = 6.69\delta^{18}O - 0.89$, $R^2=0.89$)，表明地下水和地表水间存在密切的水力联系。一般地下水中氢氧同位素组成主要受到补给来源、高程等的影响，受径流循环过程中水–岩相互作用等干扰较弱(张应华等, 2006)。综上可知，利用水体氢氧同位素示踪，矿山水主要来源于大气降水，且补给受发生在过去不同气候条件下当时的大气降水同位素组成、沉陷时间及蒸发作用所引起的同位素分馏等因素共同影响(赵睿涵等, 2022)。

除此之外，水体氢氧同位素还可以进行 AMD 源识别。Sanci et al.(2020)对阿根廷科布雷斯河流域水样调查发现，$\delta^{18}O-H_2O$ 和 $\delta D-H_2O$ 偏离大气水，表明蒸发量为 7%~17%。结合沿流域的 As 分布以及 $\delta^{18}O-SO_4^{2-}$，证实了天然硫化物氧化和温泉均导致 As 浓度大幅度上升。Doveri et al.(2019)采集阿普安阿尔卑斯山脉南部 Baccatoio 溪流集水区的雨水及地表水，获得相关 $\delta$D 和 $\delta^{18}$O 的数据，发现酸性矿井废水主要由当地补给并储存在碳酸盐含水层中的地下水供应，这些含水层在采矿后作业中流动。这些水通过与隧道中暴露的矿化物相互作用而受到污染(Doveri et al., 2019)。

### 3.3.2 硫氧同位素示踪硫酸盐来源

硫酸盐硫、氧同位素示踪技术是研究矿山环境中的硫酸盐来源、AMD 酸化过程及污染、细菌硫

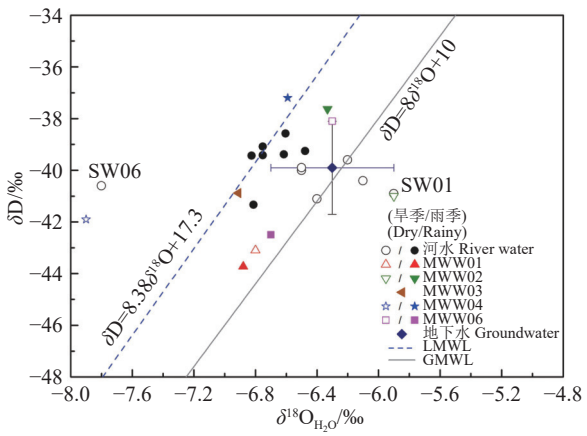


图 8 河水和矿井废水样本 $\delta$D 和 $\delta^{18}O_{H_2O}$ 之间的关系(据 Li et al., 2022)

MWW01—SW01 下游，岩石和熔渣垃圾场的渗滤液(碱性残渣)，取决于降雨量；MWW02—SW01 下游，MWW01 与矿井排水混合废水，大量排入河流；MWW03—受当地渣堆渗滤液和冶炼废水污染的混合废水，旱季无流量，雨季流量较大；MWW04—入河流量大，季节变化小；MWW05—定时入河，无季节变化；MWW06—SW06 下游，尾矿库渗滤液。SW01—上游河水，代表了当地的背景；SW06—下游矿山废水排入河流

Fig.8 The relationship between $\delta$D and $\delta^{18}O_{H_2O}$ of river water and mine wastewater samples(after Li et al., 2022)

MWW01−downstream of SW01, leachate (alkaline residue) from rock and slag dumps, depending on rainfall; MWW02−downstream of SW01, mixed wastewater from MWW01 and mine drainage, discharged in large quantities into the river; MWW03−mixed wastewater contaminated by local slag dump leachate and smelting wastewater, with no flow in the dry season and high flow in the rainy season; MWW04−high volume into the river, seasonal variation small; MWW05−regular flow into the river, no seasonal variation; MWW06−downstream of SW06, tailings pond leachate. SW01−upstream river, representing the local context; SW06−downstream mine wastewater discharged into the river

酸盐的还原作用与元素迁移转化等过程的重要工具(Kim et al., 2019; 赵睿涵等, 2022)。地下水硫酸盐的来源通常包括蒸发岩的溶解、硫化物氧化、大气降水、地下水渗透与淋滤及人类活动,其中蒸发岩硫酸盐的同位素组成通常明显富集重同位素(如二叠纪—三叠纪石膏 $\delta^{34}S$ 值为 10‰~28‰)(Krouse et al., 1991),而硫化物氧化生成的硫酸盐明显富集轻同位素($\delta^{34}S<0$)(李小倩等, 2014)。因此,河流 $SO_4^{2-}$的硫和氧同位素组成可以反映源混合的控制(Liu and Han, 2021)。Li et al.(2022)采集的河流硫酸盐和蒸发岩样品,两者的硫和氧同位素组成有显著差异,前者 $\delta^{18}O_{SO_4^{2-}}$ 值为(10.9±0.5)‰,$\delta^{34}S_{SO_4^{2-}}$ 值为(6.0±0.3)‰,而蒸发岩溶解产生 $\delta^{18}O_{SO_4^{2-}}$ 值从 10‰~20‰,$\delta^{34}S_{SO_4^{2-}}$ 值从 10‰~35‰,表明河水中的硫酸盐可以排除蒸发岩溶解源。任坤等(2021)对广西八步地下河流域中硫氧同位素分析发现,石膏溶解、硫化物氧化与大气降水是地表水与地下水中硫酸盐的主要来源,这三种来源在丰水期对流域硫酸盐的贡献率分别为 47%、40% 和 13%。同时,人类采矿活动也是矿山环境中硫酸盐的主要来源。Killingsworh and Bao(2015)对北美密西西比河中硫酸盐来源探究,认为其中自然来源的硫酸盐占 25%,人为来源占 75%,其中因煤矿开采产生的硫酸盐占比为 47%。对于以硫化物矿床为主的矿山中,硫化物矿物氧化是其环境中硫酸盐的主要来源(Haubrich et al., 2002; Junghans et al., 2009; Tichomirowa et al., 2010)。

已有研究表明,矿物氧化与地下水混合是造成水体酸化进而形成 AMD、污染地下水的主要原因(Ren et al., 2021)。相较于传统水质参数分析和水体稳定同位素测定,采用硫酸盐稳定同位素示踪硫化物矿物氧化形成 AMD 的运移途径更具灵敏性(Gammons et al., 2013; Yamaguchi et al., 2015; Tomiyama et al., 2019; Nishimoto et al., 2021)。Song et al.(2022)利用硫氧同位素与水体氢氧同位素,发现通过岩溶裂隙、管道渗透的 AMD 是地下水污染的主要原因;基于稳定同位素质量平衡模型($\delta^{18}O-\delta D$、$\delta^{34}S-SO_4^{2-}$)的分析,污染贡献率大小顺序为:巷道渗漏>矿井排污>尾矿淋滤。李小倩等(2014)利用硫酸盐浓度及其硫氧同位素组成的三元混合模型计算矿区地下水硫酸盐不同来源的贡献量,结果显示,大部分地下水样品均收到酸性矿山废水的入渗影响,酸性矿山废水对地下水硫酸盐的贡献比例为 16%~52%,平均贡献比例为 30%。由此可知,硫酸盐硫氧同位素不仅能够指示酸性矿山废水的产生机制与氧化途径,还能够准确量化污染源通过不同途径对地下水的贡献率,是示踪与评价矿山开采活动对地下水污染的有效分析工具。

## 4 氧同位素在古环境方面的应用

### 4.1 树木年轮氧同位素对古气候的响应

树木年轮稳定氧同位素作为一种高精度的古气候代用指标,具有时间分辨率高、反映环境参数多、精确度高等优点(Loader et al., 2003; Helle et al., 2004)。目前可以通过世界各地的树木获取一年的树木年轮年表,以评估树木生长与环境、极端气候事件的关系(Coulthard et al., 2020)。在树木附近采集以降水为主的土壤水样本时,由于光合过程中水通过根系吸收进入树木,因此土壤水具有与当地气候(相对湿度、温度)相关的同位素特征(Kortelainen, 2009; Gessler et al., 2014)。根部吸收的水分通过木质部运输不发生同位素分馏,但在叶片中蒸发富集(图 9),其中氧同位素比值可达 27‰(Barbour et al., 2001)。

由于树轮的化学成分相对比较稳定,结构和化学性质清楚,且易于从原木中提取,因此,广泛采用树轮 α-纤维素来分析 $\delta^{18}O$(Leavitt et al., 1993)。对于树轮 $\delta^{18}O$ 序列的建立,通常 4~5 棵树的样芯能够较好地反映样点水平的变化信息(Szymczak et al., 2012)。在中国干旱和半干旱地区,由于树木生长较慢,为了保证气体稳定同位素质谱分析的样品量以及样点序列的代表性,一般采用 4~10 棵树的样芯来建立树轮稳定同位素序列(Liu et al., 2014)。

二十世纪末以来,树轮氧同位素更多地关注于生态学和古气候学(Huang et al., 2022; Zhao et al., 2023)。树轮 $\delta^{18}O$ 对温度的响应主要出现在高纬度地区,这与温度是高纬度地区降水 $\delta^{18}O$ 主要影响因子是一致的(Schubert et al., 2015)。Treydte et al.(2006)研究揭示了生长在巴基斯坦喀喇昆仑山脉的杜松子树 1000 年来的降水记录。这一降水记录提供了上个千年后期降水量变化的证据,并且是目前已知最长的年度解析稳定同位素记录之一。在加

拿大西北部麦肯齐三角洲白云杉树木年轮的研究显示，在 1892—2003 年，树木年轮 $\delta^{18}O$ 解释了 4—7 月最低气温的 29% 的年际变率(Porter et al., 2014)。

亚洲中低纬的气候很大部分受到季风和热带海洋的影响，该区域多对流性降水，降水 $\delta^{18}O$ 显著的受到雨量效应的影响(Lawrence et al., 2004)，而湿度变化则通过叶片水蒸腾富集过程影响树轮 $\delta^{18}O$(McCarroll and Loader, 2004)。张芳芳等(2018)对湖北神农架巴山冷杉树轮纤维素氧同位素分析发现，树轮 $\delta^{18}O$ 序列较好地响应了 6—7 月降水、相对湿度以及 3—4 月温度($P<0.05$)的变化。因而，亚洲地区中低纬度树轮 $\delta^{18}O$ 主要记录与水分(降水、相对湿度、PDSI 等)有关的信号，且树轮 $\delta^{18}O$ 与温度呈显著正相关，与降水和相对湿度呈负相关(陈瑶等, 2017)。Bose et al.(2016)分析了从喜马拉雅西部收集的早期年轮纤维素样本的氧同位素，基于来自世界各地 12 个不同地点重叠时间的相似数据集，重建了 1901—2004 年间的土壤水 $\delta^{18}O$，将数据与现有的观测数据进行了比较，证明了该方法对于重建古土壤水分 $\delta^{18}O$ 的可行性。

当前，干旱是对森林生态系统造成重大破坏的最具经济和生态破坏性的极端事件之一(Hao et al., 2018)。树木年轮纤维素中的碳、氧同位素可以用来追踪干旱胁迫对树木生长的影响(Büntgen et al., 2021; Werner et al., 2021)。较低的相对湿度和/或较高的大气水汽压差促进蒸发性叶片水 $\delta^{18}O$ 的富集。Li et al.(2023)对半干旱环境中油松树轮稳定同位素研究表明，$\delta^{18}O$ 在生长季节后期与土壤水分同位素组成显著相关，$\delta^{13}C$ 反映了水分可用性对气孔导度的调节，在干(湿)年份 $\delta^{13}C$ 增加(减小)。因此，未来利用稳定的同位素重建过去季节性极端气候的能力将极大地提高我们预测未来森林生产力

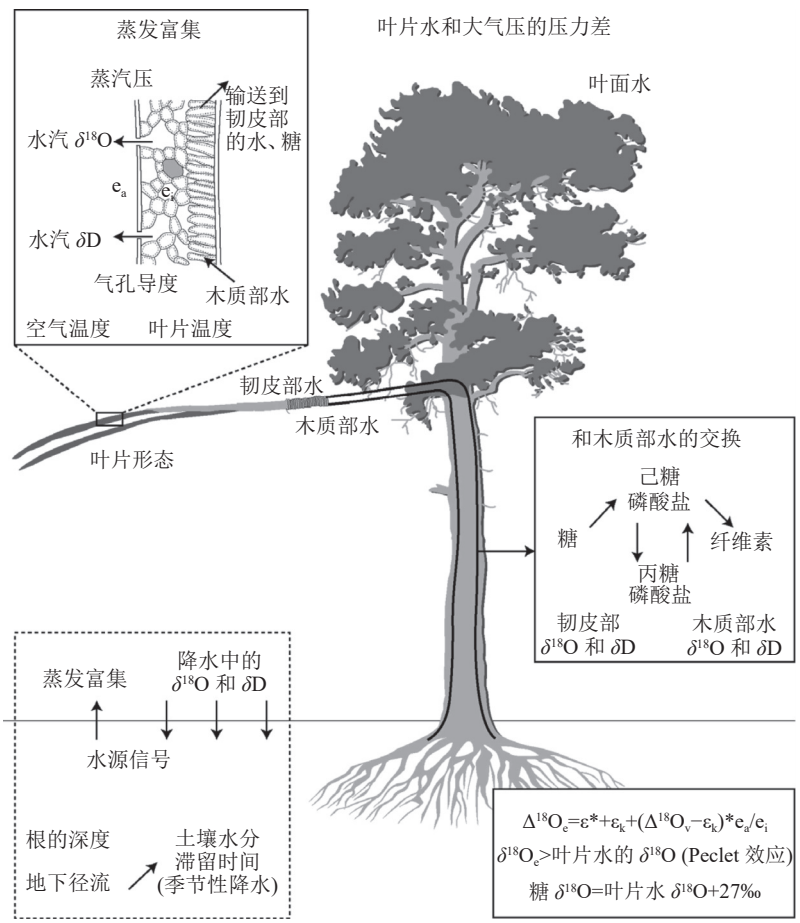


图 9 针叶树稳定氧同位素分馏模型(据 McCarroll and Loader, 2004)
Fig.9 Modeling stable oxygen isotope fractionation in conifers(after McCarroll and Loader, 2004)

的能力(Schönbeck et al., 2022)。

### 4.2 冰芯氧同位素气候环境记录

冰芯是在冰盖上钻孔获得的连续冰层,具有分辨率高、信息量大、保真度高的优势(朱大运等, 2013),它记录了包括气候、环境、生物地球化学循环、火山活动、温室效应气体、ENSO、太阳活动、宇宙事件、沙漠演化等重大事件,是研究古气候、古环境变化及其影响机制的良好载体(Yao et al., 2020; 张子洋等, 2021)。由于降水中的 $\delta^{18}$O、$\delta$D 是其形成时水汽凝结高度温度的函数(Dansgaard, 1964),而在极地水汽凝结高度气温与近地表气温密切相关(Epstein et al., 1965),因此,极地降水中的氢、氧稳定同位素成为反演古气候环境变化的温度指标(赵华标等, 2014; Siler et al., 2021)。张子洋等(2021)研究发现,1968—2001 年 LGB69 冰芯 $\delta^{18}$O 与邻近的戴维斯站气温距平 5 年滑动平均值之间具有明显的正相关关系(图 10),说明 $\delta^{18}$O 能有效指示当地气温变化。

南极 Dome C 冰芯重建了过去 80 万年 8 个冰期—间冰期旋回的温度变化,是目前全球冰芯中时间尺度最长的连续气候记录(Augustin et al., 2004; Schilt et al., 2010)。格陵兰冰盖记录的温度变化的时间尺度相对较短,如 GRIP 冰芯和 GISP2 冰芯的深度分别达到了 3022 m 和 3050 m,然而只记录了过去十几万年的温度变化(Ren et al., 2009);最新钻取的格陵兰 NEEM 冰芯也仅仅记录了过去约 13 万年的气候记录(Dahl-Jensen et al., 2013)。但是由于其积累率高,可用来探究短时间尺度的气候突变事件(如 D−O 循环等)(Johnsen et al., 2001; Ren et al., 2009)。

相较于两极地区,中低纬度冰芯由于受冰川表面积累量大的影响,时间分辨率更高(田立德和姚檀栋, 2016)。秘鲁安第斯山脉的 Quelccaya 冰盖是最早开展中低纬度冰芯研究的地区,其中提取的冰芯包含了过去 1500 年的记录(Thompson et al., 1986)。青藏高原及其周围的山脉,统称为第三极,拥有除极地以外最大的冰体(Pritchard, 2019)。青藏高原古里雅冰芯年代最老达 70 多万年,仅次于南极冰盖(Thompson et al., 1997)。与格陵兰和南极冰芯相比,古里雅冰芯记录在大的冷暖事件变化上是一致的,但冷暖变化幅度大于格陵兰和南极地区,表明青藏高原对气候变化比其他地区更加敏感(Yao, 1999)。基于对青藏高原地区降水和温度的检测,实现了关于氧同位素与温度的定量描述:降水中的 $\delta^{18}$O 每增加(或减少)1‰,温度上升(或下降)约 1.6℃(姚檀栋等, 1996)。同时,冰芯中的$\delta^{18}$O 记录显示海拔越高,气温上升的幅度越高(Liu et al., 2000)。过去 100 年北半球平均温度升高了约 0.6℃,同期青藏高原冰芯中 $\delta^{18}$O 增值为 1.3‰,进一步证实了青藏高原过去 100 年来明显升温的特征(Yao et al., 2006)。

由于夏季温度较高、蒸发较强,降水中 $\delta^{18}$O 含量高,冬季则与之相反,因此氧同位素比值在冰芯中形成夏高冬低的特征(Mosley−Thompson et al., 1990)。鉴于稳定同位素显著的季节特征能够在冰

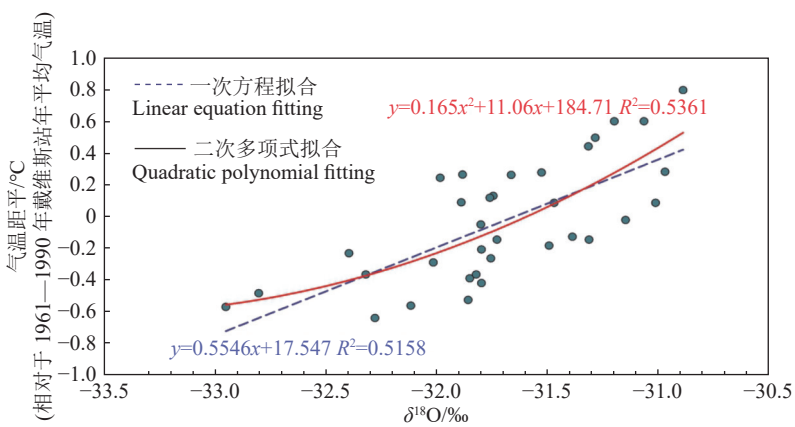


图 10 1968—2001 年 LGB69 冰芯 $\delta^{18}$O 与戴维斯站气温距平 5 年滑动平均散点图(据张子洋等, 2021)

Fig.10 The 5-year moving average scatter diagram of $\delta^{18}$O of LGB69 ice core and temperature departure of Davis Station from 1968 to 2001(after Zhang Ziyang et al., 2021)

芯中形成稳定的周期循环，据此对冰芯进行年层的划分(Li et al., 2021)。表 4 对比了两极地区和中低纬度地区典型冰芯用到的主要定年方法，可以看出，$\delta^{18}O$ 定年方法在不同积累率的冰芯定年中均被使用，但是在冰芯底部减薄速率加快后，$\delta^{18}O$ 应用变得非常有限，需要借助其它指标来辅助定年(刘科等, 2022)。

### 4.3 石笋氧同位素古气候记录

石笋是洞穴次生碳酸盐的一种，是由含 $Ca^{2+}$和 $HCO_3^-$的洞穴滴水滴到洞穴地面后，水中碳酸钙在一定条件下过饱和析出，年复一年沉积形成(Cheng et al., 2019)。在过去的十几年里，由于石笋具有空间分布广泛、气候代用指标丰富、记录较连续、时间跨度较大、相互对比性强、采用成本低等优势，使得晚更新世以来的古气候、古降水量及强度变化信息有高分辨率的重建结果(崔景伟等, 2008; Cheng et al., 2016)，可从千年精细到年际，甚至季节变化(汪永进和刘殿兵, 2016)，可以弥补树轮、冰芯等载体空间覆盖度不足和代用指标的局限性(Tan et al., 2014; Ridley et al., 2015)，在评估当今全球变暖的千年序列重建中有巨大发展潜力。

研究表明，在同位素平衡分馏状态时，洞穴石笋碳酸盐沉积的 $\delta^{18}O$ 值主要受控于年平均气温、年降水量(或湿度)以及降水气团的 $\delta^{18}O$ 值(O'Neil et al., 1969; Hendy, 1971)。Eren et al.(2021)对土耳其四个洞穴石笋进行了调查，结果显示稳定同位素值和微量元素含量主要受降雨量变化的控制，其微小变化主要受季节变化引起的降雨量和海水输入的控制。而位于日本的 Hiro-1 石笋 $\delta^{18}O$ 记录的温度变化(图 11a)与末次盛冰期至全新世后的气候阶段大致一致，但其基本不受降雨量的影响，温度效应本身可以导致 Hiro-1 观测到的位移小幅度的变化(Hori et al., 2013; Kato et al., 2021)。Hiro-1 的总体趋势与中国石笋中观察到的 $\delta^{18}O$ 趋势相似(图 11b)，但是其变化幅度大约是中国石笋的一半(Wang et al., 2001)。Fukugakuchi 洞穴石笋的 $\delta^{18}O$ 值显示了不同趋势(图 11c)，类似于中国西部黄土–古土壤序列(Maher et al., 2006)和中国南部的湖泊沉积物(Yancheva et al., 2007)中报告的东亚冬季风强度。高精度$^{230}Th$ 年龄控制的石笋氧同位素序列在轨道至千年尺度全球气候变化与突变事件的研究中发挥了重要作用(Cheng et al., 2012)。

在中国南方代表性的石笋记录中，南京葫芦洞石笋氧同位素序列记录了末次冰期(75~11 ka)完整的东亚季风变化历史(Wang et al., 2001)；湖北神农架三宝洞、贵州董哥洞等获得的石笋氧同位素序列，将高分辨率的亚洲季风记录逐步延伸至末次间冰期(Yuan et al., 2004)、倒数第二次间冰期(Wang et al., 2008)、倒数第四次间冰期(Cheng et al., 2009)乃至倒数第六次间冰期(Cheng et al., 2016)。其中，Cheng et al.(2016)的研究建立了目前全球最长时间尺度的石笋 $\delta^{18}O$ 连续记录，精细刻画了过去 7 个冰期—间冰期旋回中季风气候轨道—亚轨道尺度变化的高分辨率时间序列以及千年气候事件的内在联系共和性。

石笋中的 $\delta^{18}O$ 是否能反映降水的 $\delta^{18}O$ 变化，必须通过经典的 Hendy 检验(Yuan et al., 2004)，才可指示当时降水的氧同位素成分和洞穴温度。近

**表 4 两极地区和中低纬度地区典型冰芯定年方法**

**Table 4 Typical ice core dating methods in the polar regions and at low and middle latitudes**

| 区域 | 冰芯 | 钻取年份 | 钻取深度/m | 最老年代气候记录 | 主要定年方法 | 参考文献 |
|---|---|---|---|---|---|---|
| 中低纬度 | 古里雅冰芯 | 1992 | 308.6 | 约700 ka | $\delta^{18}O$、$^{36}C1$、离子、冰盖流体模型、$CH_4$、粉尘浓度等 | Thompson et al., 1997 |
| | 郭德冰芯 | 1987 | 140 | 约40 ka | $\delta^{18}O$、微粒浓度、电导率、离子等 | Shi et al., 2001 |
| 南极 | Dome C | 1999—2005 | 3190 | 800 ka | $\delta^{18}O$、电导率、粒度、粉尘、$\delta D$等 | Augustin et al., 2004 |
| | Vostok | 1998 | 3623 | 420 ka | $\delta^{18}O$、$\delta^{18}O_{atm}$、流动模型、离子、$^{10}Be$等 | Petit et al., 1999; Augustin et al., 2004 |
| 格陵兰 | GRIP | 1989—1992 | 2980 | 约250 ka | $\delta^{18}O$、$^{10}Be$、$^{36}Cl$、离子、冰层颜色、电导率等 | Yiou et al., 1997; Southon, 2002 |
| | GISP2 | 1989—1993 | 3053 | 150 ka | $\delta^{18}O$、冰层颜色、$^{14}C$、$^{10}Be$、电导率等 | Alley et al., 1997; Southon, 2002 |
| | NEEM | 2008 | 2540 | 约130 ka | $\delta^{18}O$、火山灰、电导率、层位对比法、$CH_4$、$\delta^{18}O_{atm}$、物理特征等 | Dahl-Jensen et al., 2013; Rasmussen et al., 2013 |

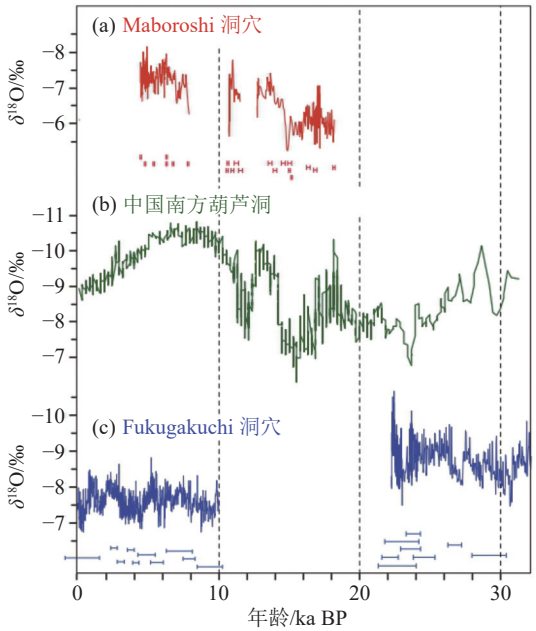


图 11 东亚三个洞穴更新世到全新世石笋 $\delta^{18}O$ 的最新记录
a—Maborishi 洞穴(据 Shen et al., 2010); b—葫芦洞穴(据 Wang et al., 2001), 以及 c—Fukugakuchi 洞穴(据 Sone et al., 2013; Amekawa et al., 2021)

Fig.11 Latest Pleistocene to Holocene records of stalagmite $\delta^{18}O$ from three caves in east Asia
a−Maborishi cave (after Shen et al., 2010), b−Hulu cave(after Wang et al., 2001), and c−Fukugakuchicave(Sone et al., 2013; after Amekawa et al., 2021)

来的研究发现，中国南方石笋氧同位素($\delta^{18}O_c$)不能直接指示降水量的变化(程海等, 2005)。一方面，绝大多数中国 $\delta^{18}O_c$ 序列无法与区域器测降水量进行校准(Tan, 2016)，根据“将今论古”原则，在时间尺度上 $\delta^{18}O_c$ 失去了可信度。另一方面，东部季风区在千年尺度上存在降水变化的南北差异(Ding et al., 2008; Chen et al., 2015)，而石笋氧同位素记录却表现出南北一致变化的空间特征(Dong et al., 2015; Liu et al., 2015)，再次说明 $\delta^{18}O_c$ 并不能反映当地降水量的变化。此外，在末次间冰期，中国$\delta^{18}O_c$ 记录与黄土记录存在明显差异(Rao et al., 2015)。因此，Chen et al.(2016)通过观测和模拟资料，对中国南方石笋氧同位素代表的是降水氧同位素而非降水量的变化，不宜作为东亚夏季风强度的代用指标。实际上，石笋 $\delta^{18}O$ 记录的是从水汽源到洞穴的全程水汽变化累计结果，理论上并不指示降水主要发生在水汽路径的哪一段(Cheng et al., 2016)。关于石笋水文气候意义的争议客观上促进了石笋古气候研究的发展，未来可以与争议来源的相关领域交叉融合，推动石笋古气候研究进程。

### 4.4 黄土碳酸盐中碳氧同位素古气候意义

黄土碳酸盐中的氧和碳同位素广泛用于重建古气候、古环境及古地貌(Beverly et al., 2021)，是研究第四纪气候变化的陆地档案之一(Zhou and Chafetz, 2009; Luo et al., 2020)。黄土碳酸盐有原生和次生之分，原生碳酸盐是指来源于黄土源区的碎屑颗粒中所固有的碳酸盐成分，一般指示源区气候条件；次生碳酸盐则是在黄土堆积过程中，受到后期降水的淋滤作用以及生物作用形成的碳酸盐(陈忠等, 2006)。由于成壤作用形成的次生碳酸盐的碳氧同位素才能反映沉积期后的气候环境特征，因此一般选用次生碳酸盐作为测试对象(苗甜等, 2021)。

韩家懋等(1995a, b)系统地研究了黄土次生碳酸盐的碳氧同位素。土壤中的重碳酸盐重新结晶形成次生碳酸盐后，在剖面的一定深度会相对富集钙结核。由于黄土中致密坚硬的钙结核中碳酸盐是自生的(不包括碎屑碳酸盐)，与形成时的环境水达到同位素平衡，且碳酸盐形成后处于封闭体系，其同位素组分在钙结核形成后没有改变，因此可以用钙结核 $\delta^{18}O$ 值研究古土壤形成时的古温度。Cerling(1984)测定了亚洲、非洲、美洲、欧洲等地的现代土壤样品中氧同位素值，并将土壤碳酸盐 $\delta^{18}O$ 与大气降水 $\delta^{18}O$ 进行了相关性分析，发现二者具有良好的线性关系($r$=0.98)：

$$\delta^{18}O_{H_2O} = -1.361 + 0.955\delta^{18}O_{CaCO_3} \quad (10)$$

式中，$\delta^{18}O_{H_2O}$ 和 $\delta^{18}O_{CaCO_3}$ 分别是大气降水和土壤碳酸盐的氧同位素组分，$\delta^{18}O_{H_2O}$ 以 SMOW 标准表示，$\delta^{18}O_{CaCO_3}$ 以 PDB 标准表示。中国北方黄土高原地区降水的 $\delta^{18}O$ 值与当地地表年平均温度的线性关系：

$$\delta^{18}O_{H_2O} = 0.31T - 12.96 \quad (11)$$

基于公式 11，可以得到碳酸钙结核的氧同位素组分每改变 0.3‰，代表环境温度约 1℃ 的变化。由此得到洛川地区土壤最为发育阶段形成时地表年平均温度约为 14.6℃，比现在高出约 5℃，而土壤最不发育形成时仅为 9.8℃，比现在只高出 0.5℃(韩家懋等, 1996)。土壤碳酸盐 $\delta^{18}O$ 指示成壤时期的古温度，较高表明碳酸盐形成时气候比较温暖，反

之则表明气候较为寒冷(Prud'homme et al., 2016; Ji et al., 2017); $\delta^{13}C$ 与土壤二氧化碳的碳同位素有关,其高值出现在黄土层中,低值出现在古土壤中,更多反映了植被发育程度(Ding et al., 2000; Li, 2003)。随后的研究认识到不同粒级黄土—古土壤中所含的碳酸盐具有不同的碳氧同位素组成,代表不同的成因和来源。陆生蜗牛响应气候环境变化敏感,其壳体化石碳氧同位素组成具有重建古生态和古大气水文条件的巨大潜力(鲍睿等, 2021)。盛雪芬等(2002)从黄土高原中部洛川和环县两个剖面选取若干黄土和古土壤样品,分为三种粒级(<2 μm、2~45 μm、>45 μm),与根状结核和蜗牛壳体碳酸盐同位素值相比,<2 μm 粒级组分的 $\delta^{18}O$ 值最为接近,代表了成壤时期形成的碳酸盐,其中氧同位素能反映古降水与古温度的定量信息,>45 μm 粒级组分代表碎屑成因碳酸盐。不同粒级中碳酸盐的碳氧同位素差异并不是偶然现象,其差异的趋势是一致的,次生碳酸盐更容易在细颗粒下聚集(Turpin et al., 2014)。

Nussloch 黄土—古土壤序列(德国莱茵河流域)因其极高的沉积速率和良好的年代学控制而被认为是西欧末次冰期最完整的记录之一。Prud'Homme et al.(2016)利用该序列重建了黄土环境中末次冰川冻土和古土壤形成过程中的土壤和空气温度,结果显示,5—9 月冻土层为(10.0±4.5)℃,古土壤为(12.1±3.9)℃,表明这些层位形成期间气候条件较温和,温度重建对于了解动植物对全球气候变化的响应具有重要意义。胡泉旭等(2018)对青藏高原东北部末次盛冰期和全新世早期黄土次生碳酸盐的研究显示,其 $\delta^{18}O$ 值(末次盛冰期平均值约为−1.38‰,全新世早期平均值约为−5.58‰)比该地区现代季风气候条件下形成的次生碳酸盐 $\delta^{18}O$ 理论值(末次盛冰期约为−5.30‰或−6.39‰,全新世早期比这个值更负)明显偏高,而温度的差异不足以影响,结果可能反映了东亚夏季风夹带的水汽不是青藏高原东北部末次盛冰期和全新世早期降水的最重要的直接来源,而西风降水和/或局部水汽蒸发循环对该地区的降水可能有重要贡献。

综上所述,黄土碳酸盐的研究为揭示第四纪气候环境变化提供了大量的证据,也仍然存在需要进一步探究的内容。碳酸盐中氧同位素虽然可以指示降水,但水汽来源、雨量效应、温度以及水汽运移过程中雨滴和水蒸气之间的分馏程度等都会对氧同位素产生影响;不同环境形成的碳酸盐的碳同位素组成也都存在差异,因此,环境中何种因素对于同位素组成起决定作用需要进一步厘定。

### 4.5 盐湖氧同位素对古气候演化的指示

在各类湖泊中,盐湖的形成于演化受特殊地质条件的影响,是水–岩相互作用的结果(Borzenko, 2021),具有成盐过程的多期性、长期性、沉积连续性、淡–盐化韵律性以及定向迁移扩张性等特点(郑绵平等, 1998),因此成为了古气候、古环境变化的重要研究对象。在使用氧同位素示踪盐湖古气候方面,氧与碳、氢同位素的联合使用发挥了重要作用。

#### 4.5.1 盐湖碳氧同位素示踪古气候

目前在盐湖沉积方面,主要应用碳氧同位素来指示古盐度、古水温等环境信息(苗青等, 2021)。内陆湖泊的盐度变化取决于流域降水、径流量与蒸发量之间的平衡关系,并直接表现为湖泊水位的变化(常凤琴等, 2010)。

通常,盐湖碳酸盐中 $\delta^{18}O$ 与当时的湖水 $\delta^{18}O$ 值以及温度有关(Dettman et al., 2003),湖水 $\delta^{18}O$ 值又由降水和蒸发比、地下水、河流注入水中的 $\delta^{18}O$ 值决定(Gasse et al., 1987)。碳酸盐中 $\delta^{18}O$ 高值指示干旱—半干旱气候,蒸发强烈,淡水汇入少,湖泊整体盐度较高;反之,则指示湿润气候,湖水淡化、盐度较低(Gasse et al., 1987; 侯战方等, 2011)。陆地湖泊体系中 $\delta^{18}O$ 值反映湖泊的水文平衡状态,即蒸发量与注入量的变化,这在封闭型湖泊中反映更加明显。这是因为蒸发作用会使较轻的氧同位素分子优先从湖水表面逸出转化为水蒸汽,造成湖水中沉淀的方解石氧同位素相应的变重。在潮湿气候条件下的开放湖泊环境中,降水量远大于蒸发量,湖水的 $\delta^{18}O$ 值就接近大气降水的同位素组成。反之,在干旱气候期,蒸发量增加,径流量减少,湖水的 $\delta^{18}O$ 值就会升高(Drummond et al., 1995; Liu et al., 1999)。湖泊碳酸盐中 $\delta^{13}C$ 值除了受湖水中 $\delta^{13}C$、注入水中 $\delta^{13}C$ 值和湖水蒸发的影响外(Miall, 2013),还受到以下因素的影响:陆源的 C3、C4 和 CAM 植物和内源的沉水植物、挺水植物及藻类(Farquhar et al., 1989),水–气界面 $CO_2$ 交换以及生

物生产力(Li et al., 1997)。在分析时,碳酸盐中 $\delta^{13}C$ 通常要与总有机碳和碳氮比等指标共同分析考虑。$\delta^{13}C$ 和 TOC 值高,指示暖湿气候;低值指示寒冷气候,有效湿度降低(吕凤琳等, 2018)。

湖泊沉积物的碳氧稳定同位素可以指示湖泊的封闭性与开放性(侯战方等, 2011)。研究表明,在开放性淡水湖泊中,碳酸盐 $\delta^{18}O$ 和 $\delta^{13}C$ 之间不相干或呈弱相关,在封闭性湖泊中,$\delta^{18}O$ 和 $\delta^{13}C$ 之间呈显著的相关关系(Hsieh et al., 1998)。王春连等(2013)对江陵凹陷盐湖样品分析得到(图 12),沙市组碳酸盐岩样品的 $\delta^{13}C$ 和 $\delta^{18}O$ 之间具有良好的正相关性,表明它们发育在蒸发作用明显的相对封闭的咸水湖泊体系中;而新沟嘴组 $\delta^{13}C$ 和 $\delta^{18}O$ 之间相关性差,指示该时期是水体滞留时间较短的开放型湖泊系统。Hou et al.(2011)测试天水盆地沉积物碳酸盐中 $\delta^{18}O$ 值在 8.5~10.92 Ma 较 10.92 Ma 之前偏重 1.5‰,可能指示了当时青藏高原南部隆升到可以改变大气环流的高度,阻遏了西南印度洋和南太平洋携带湿润气流达到或者很少到达该区域。

#### 4.5.2 盐湖氢氧同位素示踪古气候

在盐湖体系中,卤水的氢氧同位素直接代表了水体的起源、成因和演化过程,同位素组成的差异可用于识别水体的来源和补给过程(Shi et al., 2014)。王弭力等(1996)对柴达木盆地北部昆特依地区淡水和卤水进行了氢氧同位素的研究,认为卤水成因主要分为三类:(1)古湖水蒸发浓缩成因;(2)大气降水沿断裂下渗并溶解围岩中的盐分而形成的具一定盐度的卤水,即大气循环淋滤水,在一定的构造条件下又返回地表并补给盐湖;(3)由深部水补给,而后又受蒸发浓缩而形成。通常来说,由于大气降水形成的地下水,上涌过程中会发生水岩反应,并溶滤一些盐类物质,地表会出露有益元素,形成低 $\delta D$、$\delta^{18}O$ 值卤水;强蒸发环境下浓缩形成的卤水往往具有高的 $\delta D$、$\delta^{18}O$ 值;若受到古近纪—新近纪古卤水补给的现代盐湖晶间卤水则具有低 $\delta D$、高 $\delta^{18}O$ 值的特征(李建森等, 2022)。

对比研究区的氢氧同位素拟合线与区域大气降水线的斜率关系,是了解盐湖经历地质作用的一个重要途径(表 5)。付昌昌和刘聪(2022)对可可西里盐湖水体研究得到,该流域大气降水是水体主要补给源,由于河水和湖水的氢氧同位素拟合线(LEL)斜率小于区域大气降水线(LMWL),表明湖水和河水经历了一定程度的蒸发作用(图 13)。由于干旱条件,$\delta^{18}O$ 的蒸发分馏要大于 $\delta D$,因此干旱区的 $\delta D$ 更为贫化(崔蕊等, 2019)。

### 4.6 三重氧同位素示踪水循环

近些年,同位素地球化学中使用三重氧同位素($^{16}O$、$^{17}O$、$^{18}O$)示踪,重建古环境有了显著的扩展(Joussaume et al., 1984)。最新的技术和分析进展表明,$^{17}O/^{16}O$ 和 $^{18}O/^{16}O$ 之间较小的、与质量相关的偏差包含有关水循环和古环境条件的新信息(Barkan et al., 2005)。

在现代水域中,动力学分馏的程度通常使用氘过量($d_{excess}=\delta D-8\times\delta^{18}O$)进行量化(Dansgaard, 1964),这是一个由于水循环过程蒸发动力分馏产生的指标,在瑞利降雨期间,它保持相对不变;对于源地不同的海气相互作用条件导致了一系列平行的大气水线(Gat, 1981),每一种情况下的 $d_{excess}$ 都与水汽来源有关,继承自气团的初始同位素组成,尤其是与气团含水量获得地界面上方的水汽亏缺有关(Merlivat et al., 1975)。根据 IAEA1992 年的数据,冬季降水的 $d_{excess}$ 值通常稍高,夏季较低,这主要是由于雪中高 $d_{excess}$ 值的影响(Jouzel et al., 1984),同时冬季下降的雨滴蒸发程度通常盖过海

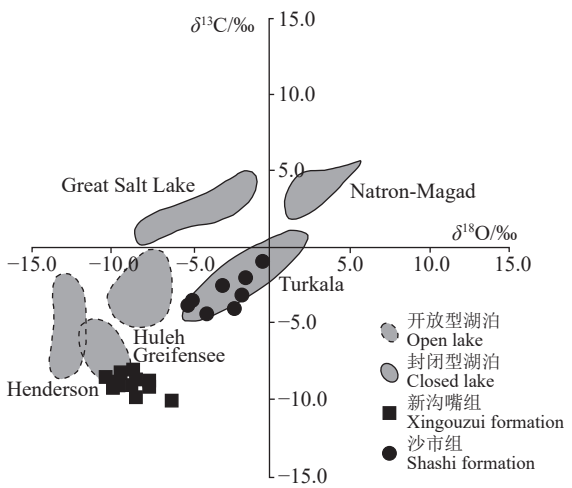


图 12 不同地层单元湖相碳酸盐岩 $\delta^{18}O$ 和 $\delta^{13}C$ 平均值在现代开放型和封闭型湖泊中原生碳酸盐 $\delta^{18}O$ 和 $\delta^{13}C$ 分布区的投影(据王春连等, 2013)

Fig.12 Plot of average $\delta^{18}O$ and $\delta^{13}C$values of lacustrine carbonate rocks in different stratigraphic units in comparison with $\delta^{18}O$ and $\delta^{13}C$ domains of primary lacustrine carbonates in modern open and closed lakes(after Wang Chunlian et al., 2013)

**表 5 当地大气降水线与盐湖氢氧同位素拟合线关系**

**Table 5 Relationship between local atmospheric precipitation lines and hydroxide isotope fitting lines in salt lakes**

| 地区 | 当地大气降水线方程（LMWL） | 盐湖氢氧同位素拟合线 | 参考文献 |
|---|---|---|---|
| 美国天然湖泊 | $\delta D=8\delta^{18}O+10$<br>（大气降水线） | $\delta D=5.3\delta^{18}O-37.91$ | Brooks et al., 2014 |
| 美国内华达州 | $\delta D=8\delta^{18}O+10$<br>（大气降水线） | $\delta D=5.49\delta^{18}O-37.1$<br>$\delta D=6.75\delta^{18}O-7.69$ | Newman et al., 2020<br>Springer et al., 2017 |
| 俄罗斯外贝加尔湖 | $\delta D=8.0\delta^{18}O+9.2$ | 氯化物湖$\delta D=4.5\delta^{18}O-32$<br>硫酸盐湖$\delta D=4.9\delta^{18}O-34$<br>苏打湖$\delta D=5.4\delta^{18}O-32$<br>新鲜湖泊$\delta D=5.1\delta^{18}O-35$ | Borzenko et al., 2022 |
| 青海省可可西里盐湖 | $\delta D=8.07\delta^{18}O+17.74$ | $\delta D=5.80\delta^{18}O-8.42$ | 付昌昌和刘聪，2022 |
| 青海省柴达木盆地 | - | $\delta D=5.0\delta^{18}O-25$ | 李建森等，2022 |
| 内蒙古哈达贺休盐湖 | $\delta D=7.30\delta^{18}O+2.14$ | $\delta D=5.32\delta^{18}O-20.08$ | 马正明等，2021 |
| 甘肃省苏干湖盆地 | $\delta D=8\delta^{18}O+10$<br>（大气降水线） | $\delta D=6.44\delta^{18}O-14.48$ | Craig, 1961<br>喻生波和屈君霞，2021 |
| 内蒙古吉兰泰盐湖 | $\delta D=7.9\delta^{18}O+8.2$ | $\delta D=7.54\delta^{18}O+1.87$ | 崔蕊等，2019 |

洋源区的较高湿度(Merlivat et al., 1979)，也会导致 $d_{excess}$ 值的冬高夏低。$d_{excess}$ 随温度和相对湿度而变化，这种多因素耦合效应导致其环境指示意义的解释具有显著的不确定性。

大气水同位素间的线性关系在同位素水文学中是普遍存在的，为评估同位素变异性、量化非平衡分馏提供了重要参考价值(Gat, 1996)。然而，在特定环境条件下，某些水体间也可能表现出非线性的同位素关系(Craig, 1961)。因为地球上的同位素值范围相对较小，围绕明显线性关系的数据点散布太广，无法分辨出轻微的弯曲，但同位素范围足够大时会出现曲率(图 14a、c)。当同位素组成之间的斜率大于 1 时，曲率呈凹形(图 14b)；当同位素组成之间的斜率小于 1 时，曲率呈凸形(图 14d)。因此，引入对数 $\delta'$表示法将同位素组成之间的指数关系线性化(Hulston et al., 1965; Miller, 2002)，这种 $\delta'$表示法用于三重氧同位素研究和部分 $d_{excess}$ 的研究中(Dütsch et al., 2017)。

$$\delta' = \ln(\delta+1) \qquad (12)$$

与 $d_{excess}$ 非常相似，三重氧同位素为古气候记录增加了自由度($^{17}O/^{16}O$)，三氧同位素分馏指数很好地表征了平衡($\theta_{eq}$)和动力学过程($\theta_{diff}$)(图 15)(Marrero et al., 1972; Young et al., 2002)。$\theta_{eq}$ 和 $\theta_{diff}$ 值之间具有统计学意义的差异意味着三重氧同位素可以区分含有氧原子的材料中的平衡和动力学分馏(Aron et al., 2021)。$\delta'^{18}O$($\delta'^{18}O = \ln(\delta^{18}O + 1)$)和 $\delta'^{17}O$($\delta'^{17}O = \ln(\delta^{17}O + 1)$)的测量补充了氘过

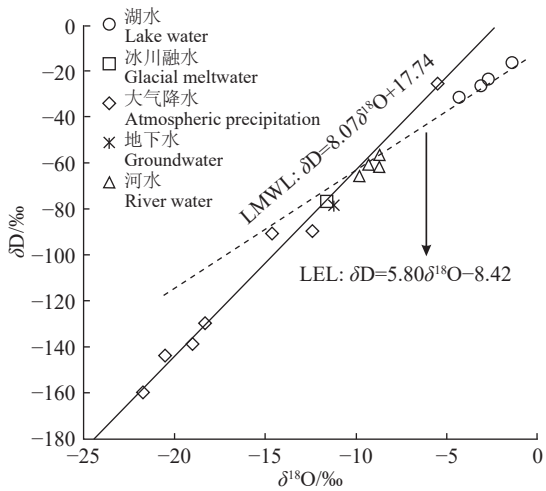


图 13 盐湖流域不同水体 $\delta D-\delta^{18}O$ 关系(据付昌昌和刘聪, 2022)

Fig.13 The relationship of $\delta D-\delta^{18}O$ of the different water samples in Yanhu Lake basin (after Fu Changchang and Liu Cong, 2022)

量等传统指标，用于跟踪蒸发量、水分输送和降水过程等(Galewsky et al., 2016)，并且可以阐明一些仅用传统氧同位素比值无法识别的动力学分馏的同位素效应(Rech et al., 2019)，有助于从地质记录中重建古环境。由于 $\delta'^{18}O$ 和 $\delta'^{17}O$ 的关系几乎总是呈线性，因此解释三重氧同位素数据的最实用方法是考虑与参考线的偏差 $\Delta'^{17}O$(Barkan et al., 2007)：

$$\Delta'^{17}O = \delta'^{17}O - \lambda_{ref}\,\delta'^{18}O \qquad (13)$$

其中，参考斜率($\lambda_{ref}$)值通常使用为 0.528，即全球大气降水线斜率(Meijer et al., 1998; Luz et al.,

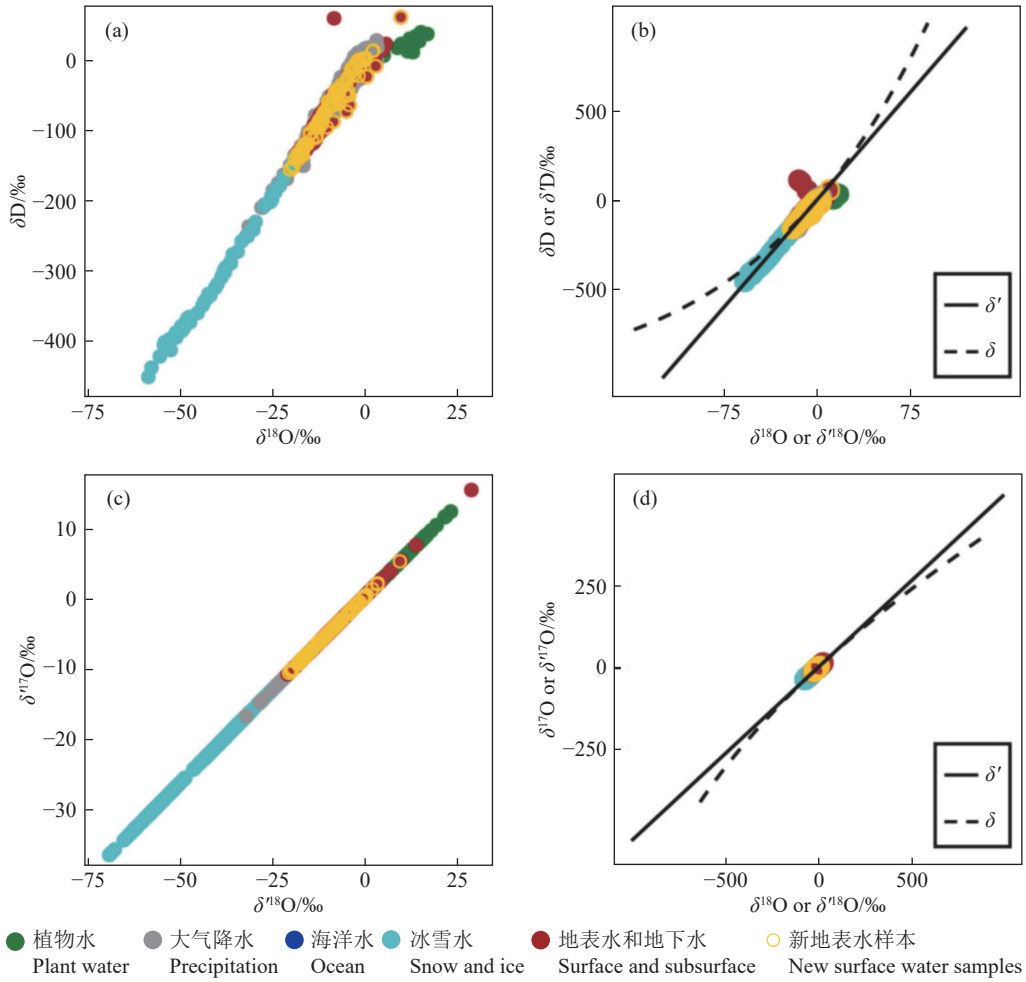


图 14 大气水同位素散点值(据 Aron et al., 2021)
Fig.14 Scatterplots of meteoric water isotope values (after Aron et al., 2021)

2010)。

Luz et al.(2010)定义了一条关于 $\delta^{17}O$ 和 $\delta^{18}O$ 全球大气水线(GMWL),建立了 $\lambda_{ref}$ 作为这条线的斜率,并设定了 $\Delta'^{17}O$ 值在 $\delta'^{18}O$ 的约 70‰范围内相对不变的预期。

$$\ln(\delta^{17}O+1)=0.528\ln(\delta^{18}O+1)+0.000033\ (R^2=0.99999) \quad (14)$$

水中过量(或耗尽)$^{17}O$ 的定义为:

$$^{17}O-\text{excess}=\ln(\delta^{17}O+1)-0.528(\delta^{18}O+1) \quad (15)$$

因此,近十年的大部分时间里,人们假设所有未蒸发的大气水 $\delta'^{18}O$ 和 $\delta'^{17}O$ 值都绘制在一条全球大气降水水线上,即观测斜率($\lambda_{obs}$)等于参考斜率($\lambda_{ref}$)(Aron et al., 2021)。而最新的观测资料表明,大气水 $\delta'^{18}O$ 和 $\delta'^{17}O$ 值并不总是在单一的全球大气降水线上,它们可以拟合多条回归线,其中的 $\lambda_{obs}$ 值是变化的(表 6)(Miller, 2018; Sharp et al., 2018),这表明 2010 年定义的全球大气水位线实际上可能并不代表全球大气降水。

现有的三重氧同位素数据不符合全球任何一条大气水线。Hayles et al.(2022)研究发现,$^{16}O$–$^{17}O$–$^{18}O$ 系统中的动力学同位素效应可以导致超出平衡限制的分馏。Aron et al.(2021)更新后的气象水线中包含的河流和降水数据的 $\delta'^{18}O$–$\delta'^{17}O$ 回归为:

$$\delta'^{17}O=0.5267\times\delta'^{18}O(\pm0.0002)+0.013(\pm0.002‰) \quad (16)$$

### 4.7 重建海相环境

海洋是全球能量和物质循环的关键环节,对全球气候系统产生了深远影响(Wang et al., 2022a)。海水中最常用的代用指标是有孔虫、贝壳等碳酸盐

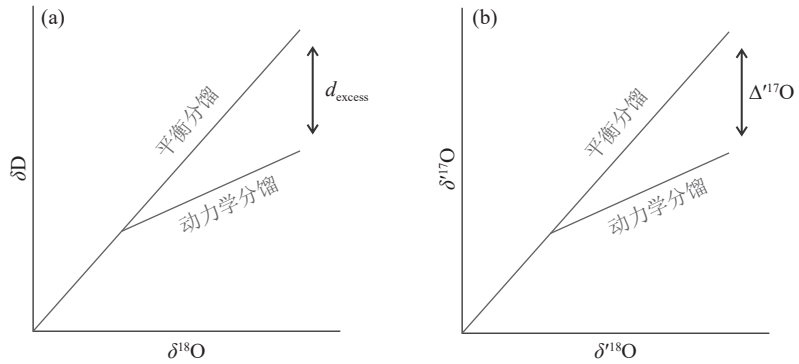


图 15 $d_{excess}$(a) 和 $\Delta'^{17}O$ 之间的相似性(b, 据 Aron et al., 2021)
Fig.15 Schematic showing the similarities between (a) $d_{excess}$ and $\Delta'^{17}O$ (b, after Aron et al., 2021)

沉积物的 $\delta^{18}O$(Miller et al., 2020; Agterhuis et al., 2022)。浮游生物在表层水中生活,死亡后沉入水底,逐渐堆积形成沉积物,这些沉积物的 $\delta^{18}O$ 能成为解读历史时期表层海水 $\delta^{18}O$ 信息的有效指标。

4.7.1 有孔虫的氧同位素重建古海平面演化

深海沉积物中钙质有孔虫的氧同位素与全球大陆冰量的变化具有相关性,具有连续、高分辨率、准确定量的优势,并且与古气候波动的海平面记录相关,提供了有关过去百万年以来详细的气候变化信息(Bergé et al., 1984; Rohling et al., 2009; Miller et al., 2012)。保存完好的白垩纪、古近纪和新近纪海底有孔虫测试的氧同位素组成被用作古代海水温度、古气候波动的指示物(Dubicka et al., 2021),并与浮游生物有孔虫数据相结合,重建古海水温度和海洋生物生产力的垂直梯度(Cramer et al., 2009; Friedrich et al., 2012; MacLeod et al., 2013; Falzoni et al., 2016)。

4.7.1.1 有孔虫氧同位素指示意义

有孔虫的氧同位素比值对全球冰量较为敏感,可以作为全球冰量变化的指标——低值表明冰量小,是全球暖期,高值表明冰量大,全球温度较低,是冷期(Shackleton, 1967; Mix et al., 1984),与其相关的水文循环过程如图 16 所示(Rohling, 2013)。如果冰盖体积发生变化,冰盖的同位素成分保持稳定,并且温度变化和海洋水团保持不变,则可通过氧同位素记录估算海平面变化(Falzoni et al., 2016; Trofimova et al., 2021)。

有孔虫组合和 $\delta^{18}O$ 的时间序列变化揭示了海面环境变化的影响因素(Kuwano et al., 2022)。海洋有孔虫壳体 $\delta^{18}O$ 变化的主要与温度效应和冰期效应的共同作用有关(Epstein et al., 1953),其中冰期效应占主导地位(Shackleton et al., 1973),这也是各海洋钻孔中底栖有孔虫壳体的 $\delta^{18}O$ 呈现出同步变化的主要原因,为重建古海平面奠定了理论基础(郭启梅等, 2020)。目前,常用的氧同位素地层标尺有 HAYS et al.(1984)、Prell et al.(1986)以及 Lisiecki et al.(2005)。将研究区域有孔虫壳体 $\delta^{18}O$ 变化曲线与标准相比,确定相邻氧同位素界线处深度对应的年龄,利用内插法即可获得每个沉积物样品对应的年龄,即确定了研究区的地层年代框架(郭启梅等, 2020)。窦衍光等(2022)将冲绳海槽中北部 CSHC-15 孔底栖有孔虫 $\delta^{18}O$ 曲线与全球标准底栖有孔虫氧同位素曲线(Lisiecki et al., 2005)进行对比,选取了 3 个控制点,结果显示该孔保存了近 200 ka 以来的连续沉积记录,同时其氧同位素值具有冰期—间冰期旋回变化特征,冰期偏重,间冰期偏轻。有孔虫 $\delta^{18}O$ 值还可以反映降水量等气候信息,$\delta^{18}O$ 值低于现今值,表明流域盐度较低(Liu et al., 2016)。

现有的重建方法主要包括:有孔虫氧同位素比值与海平面遗迹之间建立关系的方法(Labeyrie et al., 1987; Lea et al., 2002; Cutler et al., 2003)、红海

**表 6 不同体系中三重氧同位素的 $\lambda_{obs}$ 值**

**Table 6 $\lambda_{obs}$values of triple oxygen isotopes in different systems**

| 样本 | $\lambda_{obs}$ | 参考文献 |
|---|---|---|
| 大气降水 | 0.5273 ± 0.0001 | Landais et al., 2010 |
| 湖泊 | 0.5229 ± 0.001 | Passey et al., 2019 |
| 植物水（茎和叶） | 0.5188 ± 0.0004 | Landais et al., 2006 |
| 雪水、冰水 | 0.5285 ± 0.00006 | Touzeau et al., 2016 |
| 地下水 | 0.5261 ± 0.0001 | Bershaw et al., 2020 |
| 海水 | 0.513±0.037 | Galili et al., 2022 |
| 碳酸盐岩 | 0.5247±0.0007 | Miller et al. 2002 |

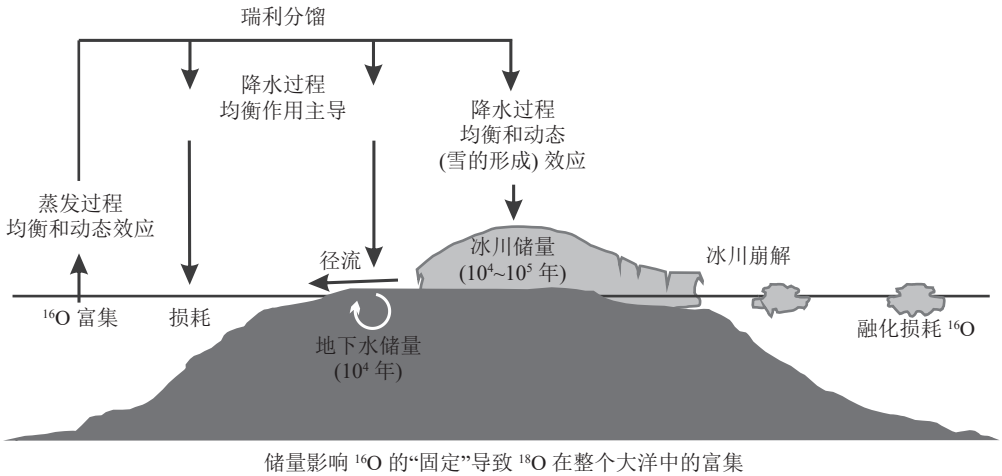


图 16 水文循环对氧同位素比值影响的示意图(据 Rohling, 2013; 李悦等, 2016)

Fig.16 Schematic representation of the effect of the hydrologic cycle on oxygen isotope ratios (after Rohling, 2013; Li Yue et al., 2016)

和地中海水力模型与有孔虫氧同位素结合的重建方法(Siddall et al., 2003; Grant et al., 2012)、利用北半球冰盖和海水温度耦合模型的重建方法(Bintanja et al., 2005)。实际上,影响海水中氧同位素比值变化的因素除了大陆冰体变化以外,还有海水温度、有孔虫栖息水体的性质、蒸发和降水的变化等(Guo et al., 2020; Yu and Li et al., 2022),在实际应用中需要全方位考虑,剔除其他的影响因素,才可能获得较为准确的结果。

除有孔虫外,海洋沉积物中贝壳化石在地质记录中同样分布广泛,其氧同位素组成也可用来重建季节性、当地气候和海拔条件(Roy et al., 2019)。根据经验得出的软体动物的最流行的古温度方程是 Epstein et al.(1953)经 Anderson and Arthur(1983)为钙化双壳类开发的方程:

$$T(^{\circ}\mathrm{C}) = 16 - 4.14 \times \left(\delta^{18}\mathrm{O}_{\mathrm{Shell}} - \delta^{18}\mathrm{O}_{\mathrm{water}}\right) + 0.13 \times \left(\delta^{18}\mathrm{O}_{\mathrm{Shell}} - \delta^{18}\mathrm{O}_{\mathrm{water}}\right)^2 \quad (17)$$

$\delta^{18}\mathrm{O}_{\mathrm{Shell}}$ 是碳酸钙和磷酸在 25℃ 下反应释放的 $CO_2$ 的 $\delta^{18}$O 值(与 Vienna Peedee Belemnite (VPDB)相比),$\delta^{18}\mathrm{O}_{\mathrm{water}}$ 是在 25°C 下与水平衡的 $CO_2$ 的 $\delta^{18}$O 值(与维也纳标准平均海水(VSMOW)相比)。Kim 等在 2007 年提出的文石-水同位素分馏关系,根据贝壳和湖水的 $\delta^{18}$O 值计算生长温度(Kim et al., 2007):

$$1000\ln\alpha_{\mathrm{aragonite-water}} = 17.88 \pm 0.13(10^3/T) - 31.14 \pm 0.46 \quad (18)$$

其中,$\alpha_{\mathrm{aragonite\text{-}water}}$ 是文石和水之间的平衡氧同位素分馏因子,$T$ 是水的开尔文温度。将计算出的温度与测量的湖水温度进行比较,以研究选定淡水软体动物的生长模式以及季节性温度变化对贝壳生长的影响(Kim et al., 2007)。Roy et al.(2019)根据贝壳和水的氧同位素组成,利用 Kim et al.(2007)提出的公式,计算出温度范围为(14±2)°C 至(27±2)°C(图 17),在湖水温度平均范围内(Gu, 2008);计算温度的平均值为(21±4)°C,非常接近年平均地表水温(19.1±1.2)°C(Cui et al., 2008),表明 *Bellamya* (>2.2 cm)这种淡水软体动物能准确地记录了水温的季节性变化,是湖泊环境条件的极好档案,适合古环境研究。

4.7.1.2 有孔虫氧碳同位素指示意义

有孔虫氧碳同位素比值测试可作为重建海水温度和生物生产力的工具(Dubicka et al., 2021)。有孔虫壳体 $\delta^{18}$O 与底层水温度、盐度相关,其信号幅度的变化很大程度上反映了大陆冰量和温度的变化。与 $\delta^{18}$O 变化的控制因素不同,有孔虫壳体 $\delta^{13}$C 的变化主要受生命效应(生长、繁殖、光合作用、新陈代谢等)的控制,其次为物理因素(冰期效应、温度、盐度)的影响。表层浮游有孔虫壳体高的 $\delta^{13}$C 值,指示了光合作用过程营养利用率较高,进而反映了高的表层初级生产力(Maiorano et al., 2015)。而由于全球效应只会改变整个大洋的 $\delta^{13}$C 平均值,因此,底栖有孔虫壳体 $\delta^{13}$C 数据可以深入了解全球碳循环的本质以及深海环流模式的一级变化(郭启梅等, 2023)。底栖有孔虫根据微生

境的不同，可大致分为表生种和内生种（Corliss, 1985）。由于表生底栖有孔虫在钙化过程中与海水始终保持 $\delta^{13}C$ 平衡，因此是记录大洋底层海水 $\delta^{13}C$ 的重要载体（Zahn et al., 1986）；内生底栖有孔虫壳体 $\delta^{13}C$ 与沉积物孔隙水 $\delta^{13}C$ 有关，因沉积物内部有机质呼吸作用和矿物反应而有别于沉积物上部的底层水 $\delta^{13}C$（Tachikawa et al., 2002）。

相比较氧同位素，底栖有孔虫的碳同位素可以补充研究全球植被消长、表层海水初级生产力和底层水溶解氧含量、有机质通量等方面的信息（Hesse et al., 2011）。在古海洋研究中，底栖有孔虫壳体的氧碳稳定同位素与海水性质密切相关，使其成为研究古海洋学的有力工具之一（Duplessy et al., 1985; 郭启梅等, 2020）。Zachos et al.（2001）通过搜集的不同地质时间段的 40 多个全球各大洋深海钻探项目（DSDP）和海洋钻探计划（ODP）站位的底栖有孔虫 $\delta^{18}O$、$\delta^{13}C$ 数据，汇编成单一的的新生代全球深海同位素记录（图 18），这条记录显示了 6500 万年以来全球气候在逐渐变冷，这与前人研究结果一致（Emiliani,1955; Shackleton,1975）。

前人研究表明，不是所有的底栖有孔虫属种的氧碳同位素可以用于古海洋学研究。用于重建古温度、盐度的底栖有孔虫最好与海水保持 $\delta^{18}O$ 平衡，如内生种 *U. mediterranea*（Shackleton, 1974）；用于重建古洋流模式的底栖有孔虫必须与海水溶解

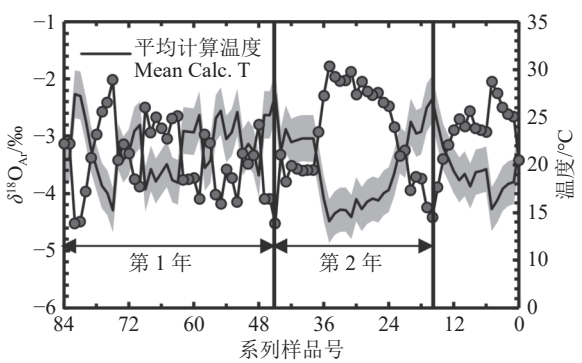


图 17 抚仙湖 *Bellamya* 大贝壳生命周期中单个贝壳系列样品的 $\delta^{18}O_{Ar}$ 值以及计算出的沿贝壳生长方向的温度（黑色平滑线）变化（据 Roy et al., 2019）

阴影区域表示计算的温度范围

Fig.17 $\delta^{18}O_{Ar}$ values of serial samples from*Bellamya* shell and the calculated temperature (black smooth line) variation along the direction of shell growth from Fuxian Lake（after Roy et al., 2019）

Shaded area represents the range of calculated temperature

无机碳的 $\delta^{13}C$ 保持平衡，如表生种 *C. wuellerstorfi*（McCorkle et al., 1990）。曹超等（2012）对南海北部 2 个区块的沉积柱样有孔虫碳氧同位素组成和测年发现，底栖有孔虫 *Uvigerina* spp.碳同位素值为 −2.12‰~−0.21‰，浮游有孔虫 *Globigerinoidesruber*. 氧同位素值为−3.11‰~−0.60‰，分析认为该区为典型的甲烷渗漏环境，在氧同位素的Ⅱ、Ⅳ期，由于全球海平面下降，导致海底压力减小，天然气水合物分解释放，具轻碳同位素的大量甲烷释放进入海底溶解无机碳池并记录在有孔虫壳体内，造成有孔虫碳同位素负偏。

有孔虫壳体稳定氧碳同位素在指示水团来源、建立氧同位素地层框架、查明新生代全球气候变化趋势、恢复区域古洋流模式等方面发挥着巨大作用。但这些指标在古海洋学研究的应用中存在着局限性，如海水性质、有孔虫生命效应等的限制。因此，在具体研究中，可以采用多指标的方法，如结合微量元素与 Ca 的比值（Mg/Ca、Cd/Ca、Mn/Ca）等，以规避这些限制因素对解释古气候变化的影响。

4.7.2 海相碳酸盐氧同位素演化

碳、氧同位素是海相碳酸盐岩研究的重要地化指标之一，在反映全球气候、海平面升降、成岩环境及层序地层划分和对比等方面发挥着重要作用（Li et al., 2017; Shao et al., 2019）。海相碳酸盐岩在成岩后生作用中会伴生微量元素的增多或减少，比如在成岩作用过程中会出现 Mn 含量的增多及 Sr 含量的减少。因此，不同类型的海相碳酸盐岩对古海水信息保存性存在明显差异，在沉积演化中易遭受成岩蚀变（黄思静等, 2003）。影响海相碳酸盐中 $\delta^{18}O$ 值的因素较多，有成岩作用、古海水组成及古温度等（董庆民等, 2021）。

由于海相盆地碳酸盐层系缺乏古温度导致很难对其热史进行恢复，因此研究中往往使用碳酸盐团簇同位素（$\Delta_{47}$）示踪古温度（Eiler et al., 2004）。在碳酸盐矿物当中具有 $^{13}C–^{18}O$ 键的基团称为团簇，实验室通常利用 105% 过饱和磷酸将其酸解为 $CO_2$ 利用质谱仪进行间接测量（Passey et al., 2012; Henkes et al., 2014）。$\Delta_{47}$ 是碳酸盐团簇同位素的丰度与其理想状态下随机分布丰度值之间的偏差（Affek et al., 2006）：

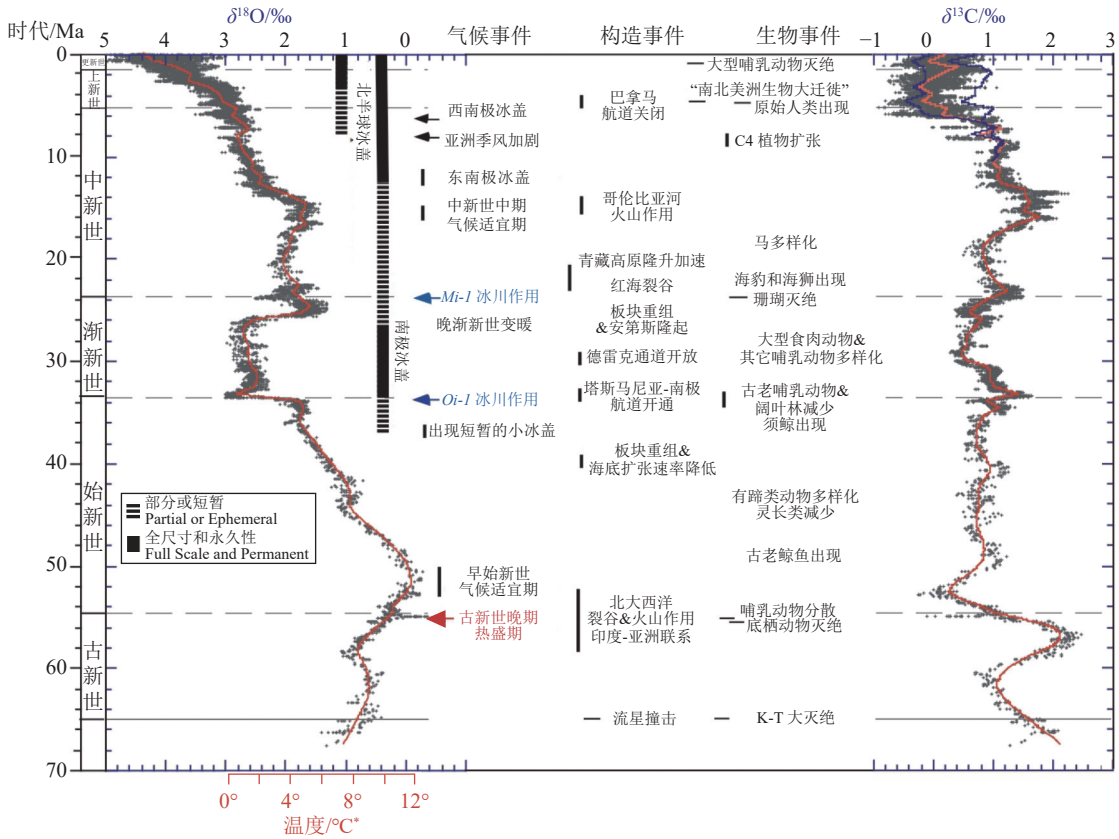


图 18 全球深海氧和碳同位素记录(据 Zachos et al., 2001)

垂直条粗略地表示了每个半球相对于末次盛冰期的冰量,虚线条表示最小冰覆盖时期(≤50%),实线条代表接近最大冰盖覆盖率(大于目前的 50%);*表示 $\delta^{18}O$ 温标是针对无冰海洋计算的 [~1.2‰标准平均海水(SMOW)],因此仅适用于南极洲大规模冰川作用开始之前(~35 Ma)

Fig.18 Global deep-sea oxygen and carbon isotope records(after Zachos et al., 2001)

The vertical bars provide a rough qualitative representation of ice volume in each hemisphere relativeto the LGM, with the dashed bar representing periods of minimal icecoverage (≤50%), and the full bar representing close to maximum icecoverage (>50% of present).The $\delta^{18}O$ temperature scale was computed for an ice−free ocean [~1.2‰ Standard Mean Ocean Water (SMOW)], and thus only applies to the time preceding the onset of large−scale glaciation on Antarctica (~35 Ma)

$$\Delta_{47}=\left[\left(\frac{R^{47}}{R^{47*}}-1\right)-\left(\frac{R^{46}}{R^{46*}}-1\right)-\left(\frac{R^{45}}{R^{45*}}-1\right)\right]\times 1000‰ \quad (19)$$

$R^i$ 是 $CO_2$ 中质量分数为 $i$ 的同位素体与质量分数为 44 的同位素体的丰度比,*表示经过持续 2 h、1000℃ 的高温加热,反应中各同位素组成达到随机分布(Came et al., 2007)。$\Delta_{47}$ 也是温度的函数(邱楠生等, 2023)。二者关系式(适用于 20~250℃, $R^2$=0.99)为(Kluge et al., 2015):

$$\Delta_{47}=0.98\left(-\frac{3.407\times 10^9}{T^4}+\frac{2.365\times 10^7}{T^3}-\frac{2.607\times 10^3}{T^2}-\frac{5.88}{T}\right)+0.293(\pm 0.04) \quad (20)$$

由于碳酸盐矿物中 $CO_2$ 质量数为 47 的同位素(主要是 $^{13}C\,^{18}O^{16}O$, 占 $^{47}CO_2$ 质量的 96%)与成岩流体的 $\delta^{18}O$ 和 $\delta^{13}C$ 无关,而是通过 $^{13}C$–$^{18}O$ 配对的形式将温度信息记录在化学键中,通过其丰度变化反映温度(Eiler, 2007; Henkes et al., 2013)。该方法主要应用于古海水温度、古气候变化和成岩流体示踪研究等(MacDonald et al., 2018; Swart et al., 2019; Al-Ramadan et al., 2020; Fiebig et al., 2021)。同时由于碳酸盐矿物 $\delta^{18}O$ 受温度、成岩流体属性和分馏系数控制,通过团簇同位素测试获取矿物形成温度,再测试矿物的 $\delta^{18}O$ 值,就能求解成岩流体属性,因此碳酸盐矿物团簇同位素还可为成岩流体属性示踪提供参数(乔占峰等, 2023)。

Schauble et al.(2006)第一次尝试对团簇同位素重排率与温度的关系进行定量研究,结果表明在时间超过百万年、温度超过 100~120℃ 的条件下,方

解石将发生 $^{13}C–^{18}O$ 键的重排及 $\Delta_{47}$ 值的变化。Mangenot et al.(2018)将碳酸盐团簇同位素(约束温度)和 U–Pb 定年(约束时间)结合,精细揭示了巴黎盆地碳酸盐岩层的古温度演化史,为沉积盆地热历史恢复提供了新思路。邱楠生等(2023)利用团簇同位素研究四川海相盆地的热史,结果表明,川东地区二叠系茅口组经历中三叠世、晚三叠世和晚白垩世 3 次抬升降温,地层温度在晚白垩世抬升前达到最大(图 19)。

碳酸盐团簇同位素作为一种新兴的古温标,在碳酸盐地层热史恢复中展现了巨大潜力,也仍存在一些不足。通过将碳酸盐团簇同位素与其它古温标结合,如镜质体反射率、沥青反射率等,以及 U–Pb 定年结合元素、同位素分析,以精确重建海相盆地热史(Mangenot et al., 2019; Naylor et al., 2020; Cong et al., 2021)。

## 5　追踪食物/动物的地理来源

氧同位素适用于地理起源的表征,因为 $\delta^{18}O$ 具有很强的纬度依赖性,主要受当地环境条件的影响,可以提供有关水源(如当地降水、地下水)、气候(凝结和降水期间的环境温度)和蒸散程度的关键信息(Dansgaard,1964; Gat,1996; Clark et al., 1997),是反映其生存环境的理想指标(Kelly et al., 2005; Liu et al., 2011)。大气降水经过蒸发、凝结和降水等过程,呈现出系统的地理同位素变化(Yuntseover et al., 1981)。当赤道地区海洋中的水蒸气移动到更高的纬度和高度时,温度下降导致降水中的重同位素逐渐减少(Craig,1961)。

### 5.1　示踪食物来源

同位素分析已被证明是鉴定和追踪农作物、食品的有力工具(Gatzert et al., 2021; Suzuki et al., 2022)。地理原产地在葡萄酒行业中占有非常重要的地位,因为葡萄酒的特性,都高度依赖于地理位置(Kamiloglu, 2019)。目前,使用氧同位素来评估葡萄酒真实性,已被欧盟认定为官方方法,包括掺假行为以及与标签中所示原产地的一致性(European Commission, 2008)。自来水或泉水的 $\delta^{18}O$ 值低于来自植物的酒水中的 $\delta^{18}O$(Horacek et al., 2021),且该值不受人类活动以及酿酒过程或储存的影响(Coelho et al., 2023),因此常用 $\delta^{18}O$ 追踪葡萄酒的

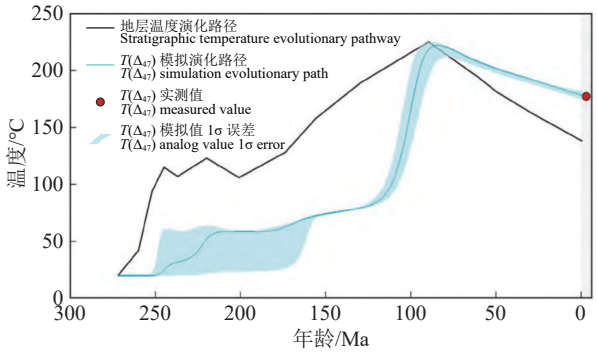


图 19　川东二叠系茅口组钻井样品团簇同位素对地层温度的热模拟结果(据邱楠生等, 2023)

Fig.19　Thermal modeling results of clumped isotope of drilling sample from Permian Maokou Formation in eastern Sichuan Basin on strata temperature(after Qiu Nansheng et al., 2023)

地理来源和检测葡萄酒的水分,是一种良好的天然示踪剂。该值受气候条件和地理位置的影响,主要是纬度、降水、与海洋的距离和温度(Orellana et al., 2019)。通常中欧和北欧国家的 $\delta^{18}O$ 值比南欧国家低,这是因为随着纬度、海拔、离海洋距离的增加,雨水中的 $\delta^{18}O$ 值通常会降低,因此葡萄酒中的 $\delta^{18}O$ 值也会降低;此外,炎热的气温和干燥的气候有助于葡萄藤的水分蒸发增加,导致 $\delta^{18}O$ 值变大(Santesteban et al., 2015)。

根据来源动物的饮食以及生产处理方法的不同,牛奶品质会有显著差异(Hullar et al., 1993; Liu et al., 2016),因此对牛奶的地理来源追溯具有重要意义。Rossmann et al.(1999)报道的酒水中 $\delta^{18}O$ 与 $(D/H)_I$ 密切相关,证实了乙醇分子甲基位点氘/氢的同位素比($(D/H)_I$)可以用作地理示踪剂(Ishida-Fujii et al., 2005; LeGrande et al., 2006)。Perini et al.(2022)对欧洲国家(意大利、德国、奥地利、法国、西班牙)的 120 份牛奶进行乳糖分离发酵,测定发酵得到的酒精中的稳定同位素比值。乙醇($(D/H)_I$)与牛奶水的 $\delta^{18}O$ 相关性高,牛奶水的 $\delta^{18}O$ 值又与饮用水 $\delta^{18}O$ 密切相关,进而证实了 $(D/H)_I$ 参数可成为潜在的牛奶地理示踪剂(Masud et al., 1999)。$\delta^{18}O$ 与 $(D/H)_I$ 比率表现为从赤道到极地递减的趋势(图 20),牛奶水 $\delta^{18}O$ 与乙醇中 $(D/H)_I$ 相关性显著($R^2$=0.7)。其中,氢同位素携带与动物饮食习惯相关的特征,而氧同位素特征更多地反映动物的生理水分平衡(Vander et al., 2016)。

表 7 中列出了常见食物不同地理区域的 $\delta^{18}O$

特征。由于植物蒸腾作用涉及到环境中的水分流失，较轻的同位素更倾向于气相，因此更多的$^{16}O$将从叶子中流失。在这种情况下，可能导致植物蒸腾速率在低压条件下大幅增加，因此在海拔较高的植物样品中$^{18}O$含量更高。在广泛的地理区域上，食物$\delta^{18}O$差值明显。对于大米样品，通常来说，澳大利亚的大米样品中的$\delta^{18}O$值明显高于其他国家的大米样品(Korenaga et al., 2010; Li et al., 2015)。在一些情况中，仅凭氧同位素无法精准示踪，此时则需要使用多元素($\delta^{13}C$、$\delta^{15}N$、$\delta D$、$\delta^{18}O$)稳定同位素比分析(Ehtesham et al., 2015)。

### 5.2 追踪动物生长环境

稳定同位素已成为追踪双壳类和其他水生物种(包括鱼、虾和海参)当地来源的有力工具(del Rio-Lavín et al., 2022)。动物体内氢氧同位素的来源是饮用水、食物以及食物水，对于氧而言，还有$O_2$来源(Hobson et al., 2015)。在海洋哺乳动物中，最大的$O_2$供应来源于水，进入体内的主要途径是摄取(Costa, 2018)。此外，海洋哺乳动物的$\delta^{18}O$值在种群内几乎没有差异(Clementz et al., 2001)。目前，海洋中氧稳定同位素比值大部分变化与热梯度无关，而是由轻同位素的优先蒸发引起的(Bowen, 2010)。大气水蒸发和降水过程中的分馏作用导致淡水环境相对于海水更富$^{16}O$(Bowen, 2010; Trueman et al., 2019)。此外，由于海水中的盐度和$\delta^{18}O$受同一蒸发过程控制，因此海洋$\delta^{18}O$值的总体变化与盐度呈线性正相关(Delaygue et al., 2001; Conroy et al., 2014; Belem et al., 2019)。这表明，氧同位素可以作为盐度梯度较大地区海洋物种栖息地使用的示踪剂(Trueman et al., 2012; Wheatley et al., 2012; Zenteno et al., 2013)。生活在半咸淡水或淡水栖息地的物种应该具有较低的水体$\delta^{18}O$值(Roe et al., 1998; Newsome et al., 2010)，因此，氧同位素的比值可以用于研究在海洋、半咸淡水和淡水生态系统之间移动的海洋哺乳动物栖息地。

Drago et al.(2020)评估了Río de la Plata河口和南大西洋西部13种海洋哺乳动物栖息地的稳定氧同位素比值(图21)，结果显示，大陆架物种的$\delta^{18}O$值介于海洋和河口–沿海物种之间，且海洋物种的搁浅点到河口最内点的距离明显小于其他物种，而河口—沿海物种的搁浅点最大(Drago et al., 2020)。基于Río de la Plata河的强盐度梯度(Acha et al., 2008)，表明氧同位素在盐度梯度上是强有力的栖息地示踪剂，二者总体呈正相关关系，证实了氧同位素可以很好地示踪栖息地的利用(Zenteno et al., 2013; Belem et al., 2019)。海洋哺乳动物的$\delta^{18}O$值在种群内表现出很小的变异性(Clementz et al., 2001)，因此它们将经常使用近岸河口—沿海生态系统的物种与仅限于近海远洋水域的物种区分开来。相比之下，采样位置不足以描述物种的栖息地，因为动物被运送到远离其典型栖息地的搁浅地

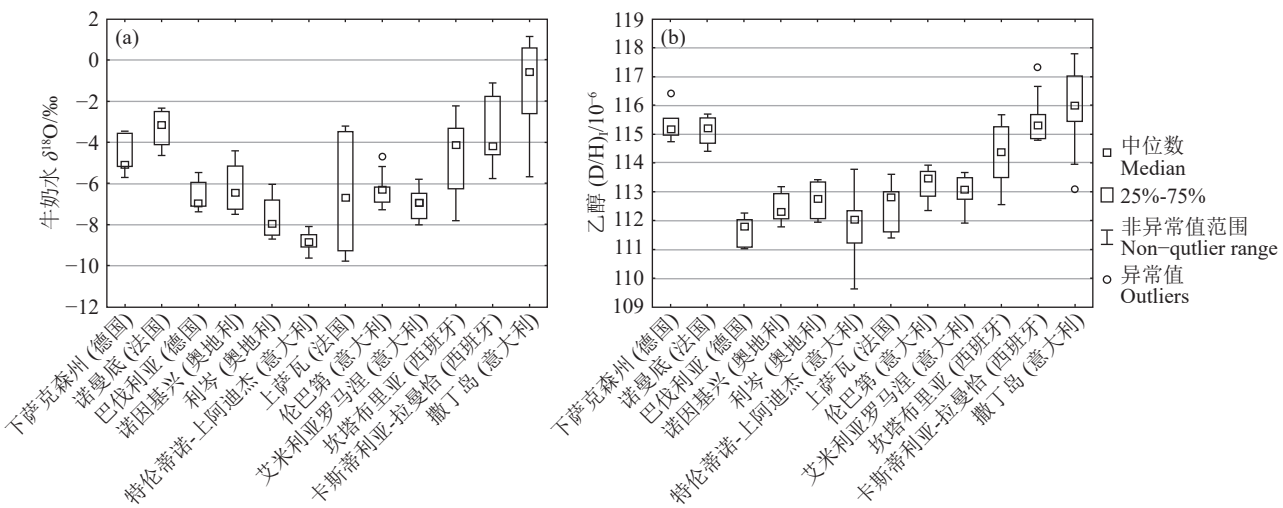


图 20 欧洲不同地区牛奶水$\delta^{18}O$(a)及乙醇的$(D/H)_I$(b)随纬度(从北到南)的变化(据 Perini et al., 2022)

Fig.20 Variation of $\delta^{18}O$ content in milk water (a) and $(D/H)_I$ of ethanol(b)of different European regions according to their latitude (from North to South)(after Perini et al., 2022)

**表 7 常见食物的氧同位素 $\delta^{18}O$ 特征**

**Table 7 Oxygen isotope $\delta^{18}O$ characterization of common foods**

| 种类 | 地区 | $\delta^{18}O$值/‰ | 参考文献 |
|---|---|---|---|
| 苹果 | 德国 | −5.2~−2.9 | Gatzert et al., 2021 |
| | 罗马尼亚 | −4.2 | Magdas et al., 2012 |
| | 斯洛文尼亚 | −4.8~+0.9 | Bat et al., 2016 |
| | 意大利 | +1.1~+3.0 | Mimmo et al., 2015 |
| 大米 | 澳大利亚 | +33.6 | Korenaga et al., 2010 |
| | 中国 | +24.1 | Suzuki et al., 2022 |
| | 孟加拉 | +26.6 | |
| | 日本 | +23.7 | |
| | 泰国 | +24.2 | Kukusamude et al., 2018 |
| | 美国 | +21.9 | Li et al., 2015 |
| 葡萄酒 | 澳大利亚 | +1.694~+14.225 | Wu et al., 2019 |
| | 葡萄牙 | +0.25~+7.27 | Coelho et al., 2023 |
| | 斯洛文尼亚 | − 8.24~4.31 | Ogrinc et al., 2001 |
| | 奥地利 | 1.3 | Horacek et al., 2021 |
| | 中国云川藏 | −10.148~−4.468 | Su et al., 2020 |
| | 中国河西走廊 | +2.054~+6.428 | |
| 牛奶 | 斯洛文尼亚 | −9.2~−0.04 | Hamzić et al., 2020 |
| | 立陶宛 | −7.275 | Garbaras et al., 2019 |
| | 加拿大 | −13.5~−5.7 | Stevenson et al., 2015 |
| | 美国 | −7.8~−6.5 | Chesson et al., 2010 |
| | 澳大利亚和新西兰 | −11.457~−10.747 | Luo et al., 2016 |
| | 中国 | −13.658~−12.462 | |

点可能涉及其他因素。

Martino et al.(2022)对来自东南亚和澳大利亚南部的野生章鱼样品，使用了碳氧同位素组合，对内部钙化结构耳石进行同位素分析，并与软组织进行 ITRAXX 射线荧光元素分析。结果显示，从赤道附近的低纬度地区到澳大利亚南部的高纬度地区，耳石中的 $\delta^{18}O$ 显著降低；除越南样品外，耳石中的 $\delta^{13}C$ 也表现出类似的特征(图 22)。基于 CAP 分析表明，除 $\delta^{18}O$ 外，$\delta^{13}C$、Br、K 和 As 也存在显著的区域性差异(图 23)，即使在不同的物种之间也是如此，章鱼原产地分类率较高(约 95%)。这项研究证实，同位素和多元素分析是章鱼的有效来源工具，可用于支持海产品供应链的透明度和问责制，从而鼓励可持续利用海洋资源。

## 6 展　望

近几十年来，氧同位素示踪技术在土壤−植被−生态系统中的应用取得了重大进展。未来，这项工作在以下三方面仍有较大的发展潜力：

一、示踪环境污染物。(1)$\delta^{18}O_P$ 技术为示踪土壤磷循环提供了新思路，而土壤磷形态分级方法的不统一限制了 $\delta^{18}O_P$ 比值的测定，因此亟需建立统

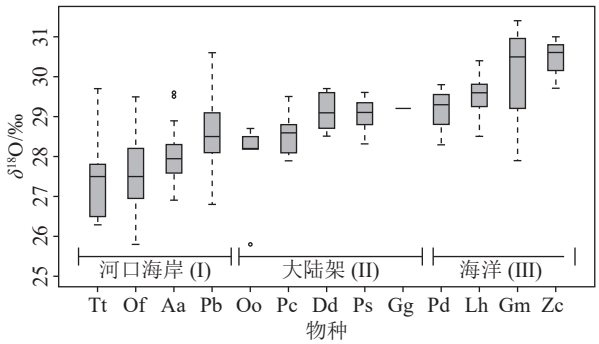


图 21 13 种海洋哺乳动物骨骼的 $\delta^{18}O_{SMOW}$ 值箱线图(据 Drago et al., 2020)

物种：Tt—拉希尔宽吻海豚；Of—南美洲海狮；Aa—南美洲毛海豹；Pb—方济各海豚；Oo—虎鲸；Pc—伪虎鲸；Dd—普通海豚；Ps—伯迈斯特江豚；Gg—里索海豚；Pd—眼镜江豚；Lh—弗雷泽海豚；Gm—长鳍领航鲸；Zc—库维尔喙鲸

Fig.21 Boxplots of the $\delta^{18}O_{SMOW}$ values in the bones of the thirteen marine mammal species considered(after Drago et al., 2020)

Species: Tt−Lahille's bottlenose dolphins; Of−South American sea lions, Aa−South American fur seals; Pb−Franciscana dolphins; Oo−killer whales; Pc−false killer whales; Dd−common dolphins; Ps−Burmeister's porpoises; Gg−Risso's dolphins; Pd−spectacled porpoises; Lh−Fraser's dolphins; Gm−long−finned pilot whales; Zc−Cuvier's beaked whales

一的标准方法。(2)硝酸盐氮氧同位素的发展加深了我们对于水生生态系统氮循环的认识，而对于硝酸盐异化还原、厌氧氨氧化等氮转化过程，其同位素分馏效应尚不明确。(3)与传统方法相比，在矿区环境中应用氧同位素示踪可以得到不同端元的贡献率，在污染源识别、迁移机制等方面发挥了重要作用，但是现有措施对地下水环境充分改善可能性不大，未来可着重为解决 AMD 引起的环境问题提供实践参考。

二、恢复古环境、古气候和古地貌。在树木年轮、有孔虫、黄土碳酸盐、盐湖、冰芯、石笋、海相碳酸盐等介质以及三重氧同位素中，氧同位素组成随气候、环境条件的变化而改变。然而各类介质都存在一些局限性。当前，结合多种代用指标进行综合分析已成为一种具有前瞻性和潜力的研究方法，在古气候学以及其它领域取得了显著的实践结果。因此，今后可结合不同介质研究氧同位素的应用，探索其生态学价值。同时，发展新的模型方法，例如动力学模型、质量守恒模型等，方法学的进步将有助于稳定同位素为科学研究提供更加合理和明确的证据。

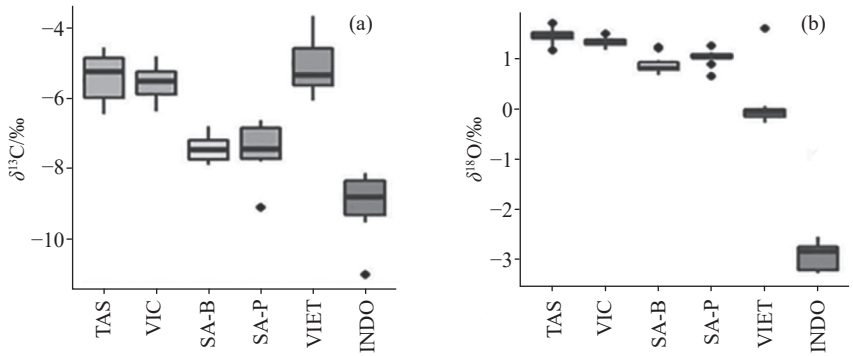


图 22 章鱼中碳和氧同位素的箱形图(据 Martino et al., 2022)
这些地区从高纬度到低纬度排列,包括 TAS—塔斯马尼亚州、VIC—维多利亚州、SA—南澳大利亚州、VIET—越南和 INDO—印度尼西亚
Fig.22 Boxplots of carbon ($\delta^{13}C$) and oxygen isotopes ($\delta^{18}O$) in octopus statoliths(after Martino et al., 2022)
The regions are arranged from high to low latitude and include TAS−Tasmania, VIC−Victoria, SA−South Australia, VIET−Vietnam, and INDO−Indonesia

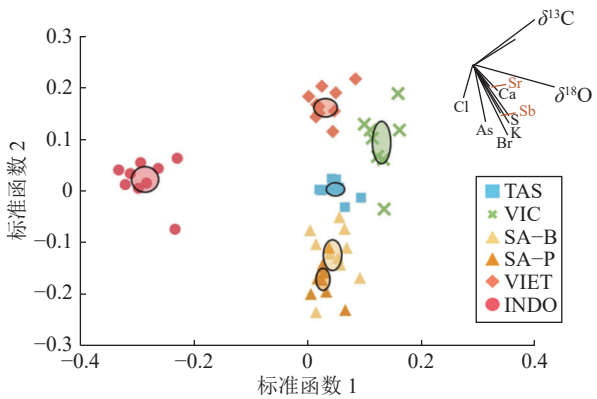


图 23 不同地理来源章鱼化学特征的 CAP 图(据 Martino et al., 2022)
TAS—塔斯马尼亚州;VIC—维多利亚州;SA—南澳大利亚州;VIET—越南;INDO—印度尼西亚;南澳样本包括两个物种 SA−B 和 SA−P 以阐明物种特异性效应
Fig.23 CAP plot of chemical characteristics of octopus from different geographical origins(after Martino et al., 2022)
TAS−Tasmania; VIC−Victoria; SA−South Australia; VIET−Vietnam; INDO−Indonesia; South Australian samples includes two species – Octopus berrima (SA−B) and Octopus Pallidus (SA−P) – to elucidate species−specific effects

三、追踪动物、食物地理来源。由于氧同位素的纬度依懒性,动物、食物 $\delta^{18}O$ 值随环境变化灵敏。随着数据库的扩大和分析样本数量的增加,元素组成和同位素比值的自然变化也会增加,从而导致对地理起源的解释变得更为复杂。因此,为了进行有意义的来源分配,对元素和同位素测量的重复性和再现性极其重要。此外,对于一些气候条件相似的地区,如中国和日本,通过稳定同位素分析很难清楚地区分产品产地,需要结合其他分析方法,例如使用微量元素分析和锶同位素值来区分产品的不同来源。

## 7 结 论

(1)氧同位素分析技术与氧同位素示踪技术目前已经建立了成熟体系,稳定同位素技术在理解生物圈的关键过程中起着重要作用。

(2)氧同位素技术作为一种强有力的示踪方法,已被用于追踪水体氮循环、土壤磷循环、矿山污染源和 AMD 的运移途径。此外,在第四纪古气候研究领域,通过分析介质中氧同位素的特征,为重建古气候、古环境提供了重要依据。同时氧同位素技术也是追溯各种农产品和动物产品地理来源的有力工具。

(3)未来氧同位素的应用不仅可以结合碳、氢、氮、磷、硫、锶等多种同位素示踪技术,还可以在树轮、有孔虫、黄土、盐湖、极地冰芯、海洋沉积物等多种介质中联合使用,从而推动氧同位素技术在全球变化和生态环境研究中的进步与发展。

## References

Agterhuis T, Ziegler M, de Winter N J, Lourens L J. 2022. Warm deep−sea temperatures across Eocene Thermal Maximum 2 from clumped isotope thermometry[J]. Communications Earth & Environment, 3(1): 39.

Acha E M, Mianzan H, Guerrero R, Carreto J, Giberto D, Montoya N, Carignan M. 2008. An overview of physical and ecological processes in the Rio de la Plata Estuary[J]. Continental Shelf Research, 28(13): 1579−1588.

Affek H P, Eiler J M. 2006. Abundance of mass 47 $CO_2$ in urban air,

car exhaust, and human breath[J]. Geochimica et Cosmochimica Acta, 70(1): 1−12.

Alexander B, Thiemens M, Farquhar J, Kaufman A, Savarino J, Delmas R. 2003. East Antarctic ice core sulfur isotope measurements over a complete glacial−interglacial cycle[J]. Journal of Geophysical Research: Atmospheres, 108(D24): 4786.

Alley R, Shuman C, Meese D, Gow A, Taylor K, Cuffey K, Fitzpatrick J, Grootes P, Zielinski G, Ram M. 1997. Visual−stratigraphic dating of the GISP2 ice core: Basis, reproducibility, and application[J]. Journal of Geophysical Research: Oceans, 102(C12): 26367−26381.

Al–Ramadan K, Koeshidayatullah A, Cantrell D, Swart P K. 2020. Impact of basin architecture on diagenesis and dolomitization in a fault–bounded carbonate platform: outcrop analogue of a pre–salt carbonate reservoir, Red Sea rift, NW Saudi Arabia[J]. Petroleum Geoscience, 26(3): 448−461.

Amberger A, Schmidt H–L. 1987. Natürliche isotopengehalte von Nitrat als Indikatoren für dessen Herkunft[J]. Geochimica et Cosmochimica Acta, 51(10): 2699−2705.

Amekawa S, Kashiwagi K, Hori M, Sone T, Kato H, Okumura T, Yu T–L, Shen C–C, Kano A. 2021. Stalagmite evidence for East Asian winter monsoon variability and $^{18}O$–depleted surface water in the Japan Sea during the last glacial period[J]. Progress in Earth and Planetary Science, 8: 1−15.

Anderson T F, Arthur M A. 1983. Stable isotopes of oxygen and carbon and their application to sedimentologic and paleoenvironmental problems[C]//Arthur M A, Anderson T F, Kaplan I R, Veizer J, Land L S. Stable Isotopes in Sedimentary Geology (Vol. 10). SEPM Society for Sedimentary Geology.

Angert A, Weiner T, Mazeh S, Sternberg M. 2012. Soil phosphate stable oxygen isotopes across rainfall and bedrock gradients[J]. Environmental Science & Technology, 46(4): 2156−2162.

Aron P G, Levin N E, Beverly E J, Huth T E, Passey B H, Pelletier E M, Poulsen C J, Winkelstern I Z, Yarian D A. 2021. Triple oxygen isotopes in the water cycle[J]. Chemical Geology, 565: 120026.

Assonov S, Brenninkmeijer C. 2005. Reporting small $\Delta^{17}O$ values: existing definitions and concepts[J]. Rapid Communications in Mass Spectrometry: An International Journal Devoted to the Rapid Dissemination of Up−to−the−Minute Research in Mass Spectrometry, 19(5): 627−636.

Augustin L, Barbante C, Barnes P R F, Barnola J M, Bigler M, Castellano E, Cattani O, Chappellaz J, DahlJensen D, Delmonte B, Dreyfus G, Durand G, Falourd S, Fischer H, Flückiger J, Hansson M E, Huybrechts P, Jugie R, Johnsen S J, Jouzel J, Kaufmann P, Kipfstuhl J, Lambert F, Lipenkov V Y, Littot G V C, Longinelli A, Lorrain R, Maggi V, Masson–Delmotte V, Miller H, Mulvaney R, Oerlemans J, Oerter H, Orombelli G, Parrenin F, Peel D A, Petit J R, Raynaud D, Ritz C, Ruth U, Schwander J, Siegenthaler U, Souchez R, Stauffer B, Steffensen J P, Stenni B, Stocker T F, Tabacco I E, Udisti R, van de Wal R S W, van den Broeke M, Weiss J, Wilhelms F, Winther J G, Wolff E W, Zucchelli M, Members E C. 2004. Eight glacial cycles from an Antarctic ice core[J]. Nature, 429(6992): 623−628.

Bao H, Cao X, Hayles J A. 2016. Triple oxygen isotopes: fundamental relationships and applications[J]. Annual Review of Earth and Planetary Sciences, 44: 463−492.

Bao Rui, Sheng Xuefen, Chen Jun. 2021. Carbon and oxygen isotopic composition of land snail shells and climate[J]. Quaternary Sciences, 41(4): 903−915 (in Chinese with English abstract).

Barbour M M, Andrews T J, Farquhar G D. 2001. Correlations between oxygen isotope ratios of wood constituents of Quercus and Pinus samples from around the world[J]. Australian Journal of Plant Physiology, 28(5): 335−348.

Barkan E, Luz B. 2005. High precision measurements of $^{17}O/^{16}O$ and $^{18}O/^{16}O$ ratios in $H_2O$[J]. Rapid Communications in Mass Spectrometry: An International Journal Devoted to the Rapid Dissemination of Up−to−the−Minute Research in Mass Spectrometry, 19(24): 3737−3742.

Barkan E, Luz B. 2007. Diffusivity fractionations of $H_2{}^{16}O$ $H_2{}^{17}O$ and $H_2{}^{16}O/H_2{}^{18}O$ in air and their implications for isotope hydrology[J]. Rapid Communications in Mass Spectrometry: An International Journal Devoted to the Rapid Dissemination of Up−to−the−Minute Research in Mass Spectrometry, 21(18): 2999−3005.

Bat K B, Eler K, Mazej D, Vodopivec B M, Mulič I, Kump P, Ogrinc N. 2016. Isotopic and elemental characterisation of Slovenian apple juice according to geographical origin: Preliminary results[J]. Food Chemistry, 203: 86−94.

Beer C, Reichstein M, Tomelleri E, Ciais P, Jung M, Carvalhais N, Rödenbeck C, Arain M A, Baldocchi D, Bonan G B. 2010. Terrestrial gross carbon dioxide uptake: Global distribution and covariation with climate[J]. Science, 329(5993): 834−838.

Belem A L, Caricchio C, Albuquerque A L S, Venancio I M, Zucchi M, Santos T H R, Alvarez Y G. 2019. Salinity and stable oxygen isotope relationship in the Southwestern Atlantic: Constraints to paleoclimate reconstructions[J]. Anais da Academia Brasileira de Ciências, 91: e20180226.

Bender M, Sowers T, Labeyrie L. 1994. The Dole effect and its variations during the last 130, 000 years as measured in the Vostok ice core[J]. Global Biogeochemical Cycles, 8(3): 363−376.

Bergé A, Imbrie J, Hays J, Kukla G, Salzman B. 1984. Milankovitch and Climate[M]. D. In: Reidel Publishing Company, Dordrecht.

Bershaw J, Hansen D D, Schauer A J. 2020. Deuterium excess and $^{17}O$–excess variability in meteoric water across the Pacific Northwest, USA[J]. Tellus B: Chemical and Physical Meteorology, 72(1): 1−17.

Beverly E J, Levin N E, Passey B H, Aron P G, Yarian D A, Page M, Pelletier E M. 2021. Triple oxygen and clumped isotopes in modern

soil carbonate along an aridity gradient in the Serengeti, Tanzania[J]. Earth and Planetary Science Letters, 567: 116952.

Bhatia M P, Das S B, Kujawinski E B, Henderson P B, Burke A, Charette M A. 2011. Seasonal evolution of water source contributions to subglacial outflow: Insight from a new isotope–mixing model[J]. Journal of Glaciology, 57(205): 929−941.

Bintanja R, Van De Wal R S, Oerlemans J. 2005. Modelled atmospheric temperatures and global sea levels over the past million years[J]. Nature, 437(7055): 125−128.

Blake R E, O'Neil J R, Surkov A V. 2005. Biogeochemical cycling of phosphorus: insights from oxygen isotope effects of phosphoenzymes[J]. American Journal of Science, 305(6/8): 596−620.

Blunier T, Bender M L, Barnett B, Von Fischer J C. 2012. Planetary fertility during the past 400 ka based on the triple isotope composition of $O_2$ in trapped gases from the Vostok ice core[J]. Climate of the Past, 8(5): 1509−1526.

Boering K, Jackson T, Hoag K, Cole A, Perri M, Thiemens M, Atlas E. 2004. Observations of the anomalous oxygen isotopic composition of carbon dioxide in the lower stratosphere and the flux of the anomaly to the troposphere[J]. Geophysical Research Letters, 31(3): L03109.

Borzenko S V. 2021. The main formation processes for different types of salt lakes: Evidence from isotopic composition with case studies of lakes in Transbaikalia, Russia[J]. Science of the Total Environment, 782: 146782.

Borzenko S, Zamana L, Posokhov V. 2022. The Isotope Composition, Nature, and Main Mechanisms of Formation of Different Types and Subtypes of Salt Lakes in Transbaikalia[J]. Russian Geology and Geophysics, 63(6): 706−725.

Bose T, Sengupta S, Chakraborty S, Borgaonkar H. 2016. Reconstruction of soil water oxygen isotope values from tree ring cellulose and its implications for paleoclimate studies[J]. Quaternary International, 425: 387−398.

Bowen G J, Cai Z, Fiorella R P, Putman A L. 2019. Isotopes in the water cycle: regional–to global–scale patterns and applications[J]. Annual Review of Earth and Planetary Sciences, 47: 453−479.

Bowen G J. 2010. Isoscapes: spatial pattern in isotopic biogeochemistry[J]. Annual Review of Earth and Planetary Sciences, 38: 161−187.

Brooks J R, Gibson J J, Birks S J, Weber M H, Rodecap K D, Stoddard J L. 2014. Stable isotope estimates of evaporation: inflow and water residence time for lakes across the United States as a tool for national lake water quality assessments[J]. Limnology and Oceanography, 59(6): 2150−2165.

Büntgen U, Urban O, Krusic P J, Rybníček M, Kolář T, Kyncl T, Ač A, Koňasová E, Čáslavský J, Esper J. 2021. Recent European drought extremes beyond Common Era background variability[J]. Nature Geoscience, 14(4): 190−196.

Came R E, Eiler J M, Veizer J, Azmy K, Brand U, Weidman C R. 2007. Coupling of surface temperatures and atmospheric $CO_2$ concentrations during the Palaeozoic era[J]. Nature, 449(7159): 198−201.

Cao Chao, Lei Huaiyan. 2021. Respondence between carbon and oxygen isotopic characteristics of *Foraminifera* from the Northern South China Sea and Late Quaternary hydrate released[J]. Journal of Jilin University (Earth Science Edition), 42(S1): 162–171 (in Chinese with English abstract).

Cao J, Xie C, Hou Z. 2022. Ecological evaluation of heavy metal pollution in the soil of Pb–Zn mines[J]. Ecotoxicology, 31(2): 259−270.

Cao Jialu, Niu Zhenchuan, Liang Dan, Feng Xue, Lü Mengni, Wang Guowei, Liu Wanyu. 2023. Progress on mass independent fractionation of oxygen isotope in $CO_2$ related researches[J]. Journal of Earth Environment, 14(6): 714−724 (in Chinese with English abstract).

Cappa C D, Hendricks M B, DePaolo D J, Cohen R C. 2003. Isotopic fractionation of water during evaporation[J]. Journal of Geophysical Research: Atmospheres, 108(D16): 4525.

Capuano R M. 1992. The temperature dependence of hydrogen isotope fractionation between clay minerals and water: Evidence from a geopressured system[J]. Geochimica et Cosmochimica Acta, 56(6): 2547−2554.

Cavalcante H, Araújo F, Noyma N, Becker V. 2018. Phosphorus fractionation in sediments of tropical semiarid reservoirs[J]. Science of the Total Environment, 619: 1022−1029.

Cerling T E. 1984. The stable isotopic composition of modern soil carbonate and its relationship to climate[J]. Earth and Planetary Science Letters, 71(2): 229−240.

Chang Fengqin, Zhang Hucai, Lei Guoliang, Pu Yang, Chen Guangjie, Zhang Wenxiang, Yang Lunqing. 2010. Geochemical behaviors of strontium isotope and related elements of the lacustrine deposits and their application to paleoenvironment reconstruction[J]. Quaternary Sciences, 30(5): 962−971 (in Chinese with English abstract).

Chen J, Chen F, Feng S, Huang W, Liu J, Zhou A. 2015. Hydroclimatic changes in China and surroundings during the Medieval Climate Anomaly and Little Ice Age: Spatial patterns and possible mechanisms[J]. Quaternary Science Reviews, 107: 98−111.

Chen J, Rao Z, Liu J, Huang W, Feng S, Dong G, Hu Y, Xu Q, Chen F. 2016. On the timing of the East Asian summer monsoon maximum during the Holocene——Does the speleothem oxygen isotope record reflect monsoon rainfall variability?[J]. Science China Earth Sciences, 59: 2328−2338.

Chen Luwang, GuiHerong, Xu Guangquan, Song Xiaomei, Yuan Wenhua. 2003. Characteristics of the hydrogen and oxygen stable isotopes in karst water of seam floor in the mining district of the

northern Anhui Province[J]. Journal of Hefei University of Technology(Natural Science)(3): 374–378 (in Chinese with English abstract).

Chen X, Jiang C, Zheng L, Dong X, Chen Y, Li C. 2020. Identification of nitrate sources and transformations in basin using dual isotopes and hydrochemistry combined with a Bayesian mixing model: Application in a typical mining city[J]. Environmental Pollution, 267: 115651.

Chen Yao, Gou Xiaohua, Liu Wenhuo, Chen Qiaomei, SuJiajia, Lin Wei. 2017. Advances in tree−ring stable oxygen isotope study in Asia[J]. Journal of Glaciology and Geocryology, 39(2): 308−316 (in Chinese with English abstract).

Chen Zhigang, Huang Yipu, Liu Guangshan, Cai Yihua, Lu Yangyang, Liu Run. 2010. Advances in the measurement methods and fractionation mechanism of the oxygen isotope composition of phosphate[J]. Advances in Earth Science, 25(10): 1040 (in Chinese with English abstract).

Chen Zhong, Ma Haizhou, Cao Guangchao, Zhou Dujun, Zhang Xiying, Tan Hongbing, Yao yuan. 2006. Study on Carbonates in Loess: A Review[J]. Journal of Salt Lake Research, (4): 66–72 (in Chinese with English abstract).

Cheng H, Edwards R L, Broecker W S, Denton G H, Kong X, Wang Y, Zhang R, Wang X. 2009. Ice age terminations[J]. Science, 326(5950): 248−252.

Cheng H, Edwards R L, Sinha A, Spötl C, Yi L, Chen S, Kelly M, Kathayat G, Wang X, Li X. 2016. The Asian monsoon over the past 640, 000 years and ice age terminations[J]. Nature, 534(7609): 640−646.

Cheng H, Sinha A, Wang X, Cruz F W, Edwards R L. 2012. The Global Paleomonsoon as seen through speleothem records from Asia and the Americas[J]. Climate Dynamics, 39: 1045−1062.

Cheng H, Zhang H, Zhao J, Li H, Ning Y, Kathayat G. 2019. Chinese stalagmite paleoclimate researches: A review and perspective[J]. Science China Earth Sciences, 62: 1489−1513.

Cheng Hai, R L Edwards, Wang Xianfeng, Wang Yongjin, Kong Xinggong, Yuan Daoxian, Zhang Meiliang, Lin Yushi, Qin Jiaming, Ran Jingcheng. 2005. Oxygen isotope records of stalagmites from Southern China[J]. Quaternary Sciences, 25(2): 157−163 (in Chinese with English abstract).

Chesson L A, Valenzuela L O, O'Grady S P, Cerling T E, Ehleringer J R. 2010. Hydrogen and oxygen stable isotope ratios of milk in the United States[J]. Journal of Agricultural and Food Chemistry, 58(4): 2358−2363.

Chiba H, Sakai H. 1985. Oxygen isotope exchange rate between dissolved sulfate and water at hydrothermal temperatures[J]. Geochimica et Cosmochimica Acta, 49(4): 993−1000.

Clark I D, Fritz P. 1997. Environmental Isotopes in Hydrogeology[M]. CRC press: London, UK.

Clayton D. 2003. Handbook of Isotopes in the Cosmos: Hydrogen to Gallium[M]. Cambridge, UK: Cambridge Univ. Press.

Clayton R N, Grossman L, Mayeda T K. 1973. A component of primitive nuclear composition in carbonaceous meteorites[J]. Science, 182(4111): 485−488.

Clementz M T, Koch P L. 2001. Differentiating aquatic mammal habitat and foraging ecology with stable isotopes in tooth enamel[J]. Oecologia, 129: 461−472.

Cliff S S, Brenninkmeijer C A M, Thiemens M H. 1999. First measurement of the $^{18}O/^{16}O$ and $^{17}O/^{16}O$ ratios in stratospheric nitrous oxide: A mass−independent anomaly[J]. Journal of Geophysical Research: Atmospheres, 104(D13): 16171−16175.

Coelho I, Matos A S, Epova E N, Barre J, Cellier R, Ogrinc N, Castanheira I, Bordado J, Donard O F. 2023. Multi–element and multi–isotopic profiles of Port and Douro wines as tracers for authenticity[J]. Journal of Food Composition and Analysis, 115: 104988.

Cong F, Tian J, Hao F, Licht A, Liu Y, Cao Z, Eiler J M. 2021. A thermal pulse induced by a Permian mantle plume in the Tarim Basin, Northwest China: Constraints from clumped isotope thermometry and In situ calcite U−Pb dating[J]. Journal of Geophysical Research: Solid Earth, 126(4): e2020JB020636.

Conroy J L, Cobb K M, Lynch–Stieglitz J, Polissar P J. 2014. Constraints on the salinity–oxygen isotope relationship in the central tropical Pacific Ocean[J]. Marine Chemistry, 161: 26−33.

Cook G, Lauer C. 1968. The encyclopedia of the chemical elements[M]. Reinhold B. Corp. , New York.

Coplen T B, Kendall C, Hopple J. 1983. Comparison of stable isotope reference samples[J]. Nature, 302: 236−238.

Coplen, TylerB. 1994. Reporting of stable hydrogen, carbon, and oxygen isotopic abundances (technical report)[J]. Pure & Applied Chemistry, 66(2): 273−276.

Corliss B H. 1985. Microhabitats of benthic foraminifera within deep–sea sediments[J]. Nature, 314(6010): 435−438.

Costa D P, 2018. Osmoregulation. In: Würsig B, Thewissen J G M, Kovacs K M. Encyclopedia of Marine Mammals [M]. Third ed. Academic Press, San Diego, 659–664.

Coulthard B L, George S S, Meko D M. 2020. The limits of freely–available tree–ring chronologies[J]. Quaternary Science Reviews, 234: 106264.

Craig H, Gordon L I. 1964. Deuterium and oxygen 18 variations in the ocean and the marine atmosphere[C]// Symposium on Marine Geochemistry.

Craig H. 1961. Standard for reporting concentrations of deuterium and oxygen–18 in natural waters[J]. Science, 133(3467): 1833−1834.

Cramer B, Toggweiler J, Wright J, Katz M, Miller K. 2009. Ocean overturning since the Late Cretaceous: Inferences from a new benthic foraminiferal isotope compilation[J]. Paleoceanography,

24(4): PA4216.

Criss R E, Farquhar J. 2008. Abundance, notation, and fractionation of light stable isotopes[J]. Reviews in Mineralogy and Geochemistry, 68(1): 15−30.

Cui Jingwei, Huang Junhua, Hu Chaoyong. 2008. Environment substitute indexes and the paleoclimate and paleoenvironment contained in stalagmite[J]. Bulletin of Geological Science and Technology (1): 93–98 (in Chinese with English abstract).

Cui Y D, Liu X Q, Wang H Z. 2008. Macrozoobenthic community of Fuxian Lake, the deepest lake of southwest China[J]. Limnologica, 38(2): 116−125.

Cui Rui, Wang Ji, Zhang Chengfu, Shi Xiaohong, Han Zhiming. 2019. Analysis on hydrogen and oxygen isotopes and lake water source in Girantai saline lake[J]. Journal of Inner Mongolia Forestry ScienceandTechnology, 45(1): 17−21 (in Chinese with English abstract).

Cutler K, Edwards R, Taylor F, Cheng H, Adkins J, Gallup C, Cutler P, Burr G, Bloom A. 2003. Rapid sea–level fall and deep–ocean temperature change since the last interglacial period[J]. Earth and Planetary Science Letters, 206(3/4): 253−271.

Dahl–Jensen D, Albert M R, Aldahan A, Azuma N, Balslev–Clausen D, Baumgartner M, Berggren A M, Bigler M, Binder T, Blunier T, Bourgeois J C, Brook E J, Buchardt S L, Buizert C, Capron E, Chappellaz J, Chung J, Clausen H B, Cvijanovic I, Davies S M, Ditlevsen P, Eicher O, Fischer H, Fisher D A, Fleet L G, Gfeller G, Gkinis V, Gogineni S, Goto–Azuma K, Grinsted A, Gudlaugsdottir H, Guillevic M, Hansen S B, Hansson M, Hirabayashi M, Hong S, Hur S D, Huybrechts P, Hvidberg C S, Iizuka Y, Jenk T, Johnsen S J, Jones T R, Jouzel J, Karlsson N B, Kawamura K, Keegan K, Kettner E, Kipfstuhl S, Kjær H A, Koutnik M, Kuramoto T, Köhler P, Laepple T, Landais A, Langen P L, Larsen L B, Leuenberger D, Leuenberger M, Leuschen C, Li J, Lipenkov V, Martinerie P, Maselli O J, Masson–Delmotte V, McConnell J R, Miller H, Mini O, Miyamoto A, Montagnat–Rentier M, Mulvaney R, Muscheler R, Orsi A J, Paden J, Panton C, Pattyn F, Petit J R, Pol K, Popp T, Possnert G, Prié F, Prokopiou M, Quiquet A, Rasmussen S O, Raynaud D, Ren J, Reutenauer C, Ritz C, Röckmann T, Rosen J L, Rubino M, Rybak O, Samyn D, Sapart C J, Schilt A, Schmidt A M Z, Schwander J, Schüpbach S, Seierstad I, Severinghaus J P, Sheldon S, Simonsen S B, Sjolte J, Solgaard A M, Sowers T, Sperlich P, Steen–Larsen H C, Steffen K, Steffensen J P, Steinhage D, Stocker T F, Stowasser C, Sturevik A S, Sturges W T, Sveinbjörnsdottir A, Svensson A, Tison J L, Uetake J, Vallelonga P, van de Wal R S W, van der Wel G, Vaughn B H, Vinther B, Waddington E, Wegner A, Weikusat I, White J W C, Wilhelms F, Winstrup M, Witrant E, Wolff E W, Xiao C, Zheng J, Community N. 2013. Eemian interglacial reconstructed from a Greenland folded ice core[J]. Nature, 493(7433): 489−494.

Dansgaard W. 1953. The abundance of $O^{18}$ in atmospheric water and water vapour[J]. Tellus, 5(4): 461−469.

Dansgaard W. 1964. Stable isotopes in precipitation[J]. Tellus, 16(4): 436−468.

del Rio–Lavín A, Weber J, Molkentin J, Jiménez E, Artetxe–Arrate I, Pardo M A. 2022. Stable isotope and trace element analysis for tracing the geographical origin of the Mediterranean mussel (Mytilus galloprovincialis) in food authentication[J]. Food Control, 139: 109069.

Delaygue G, Bard E, Rollion C, Jouzel J, Stiévenard M, Duplessy J C, Ganssen G. 2001. Oxygen isotope/salinity relationship in the northern Indian Ocean[J]. Journal of Geophysical Research: Oceans, 106(C3): 4565−4574.

Delgado A, Reyes E. 1996. Oxygen and hydrogen isotope compositions in clay minerals: A potential single–mineral geothermometer[J]. Geochimica et Cosmochimica Acta, 60(21): 4285−4289.

Dettman D L, Fang X, Garzione C N, Li J. 2003. Uplift–driven climate change at 12 Ma: A long $\delta^{18}O$ record from the NE margin of the Tibetan plateau[J]. Earth and Planetary Science Letters, 214(1−2): 267−277.

Ding Y, Wang Z, Sun Y. 2008. Inter−decadal variation of the summer precipitation in East China and its association with decreasing Asian summer monsoon. Part I: Observed evidences[J]. International Journal of Climatology: A Journal of the Royal Meteorological Society, 28(9): 1139−1161.

Ding Z L, Yang S L. 2000. $C_3/C_4$ vegetation evolution over the last 7.0 Myr in the Chinese Loess Plateau: evidence from pedogenic carbonate $\delta^{13}C$[J]. Palaeogeography, Palaeoclimatology, Palaeoecology, 160(3/4): 291–299.

Dompierre K A, Barbour S L. 2016. Characterization of physical mass transport through oil sands fluid fine tailings in an end pit lake: a multi–tracer study[J]. Journal of Contaminant Hydrology, 189: 12−26.

Dong J, Shen C C, Kong X, Wang H C, Jiang X. 2015. Reconciliation of hydroclimate sequences from the Chinese Loess Plateau and low–latitude East Asian Summer Monsoon regions over the past 14, 500 years[J]. Palaeogeography, Palaeoclimatology, Palaeoecology, 435: 127–135.

Dong Qinming, Hu Zhonggui, Chen Shiyue, Li Shilin, Cai Jialan, Zhu Yixin, Zhang Yuying. 2021. Isotope geochemical responses and their geological significance of Changxing–Feixianguan Formation carbonates, northeastern Sichuan Basin[J]. Oil Gas Geology, 42(6): 1307−1320 (in Chinese with English abstract).

Dou Yanguang, Li Qing, Wu Yonghua, Zhao Jingtao, Sun Chenghui, Cai Feng, Chen Xiaohui, Zhang Yong, Fan Jiahui, Shi Xuefa. 2022. Carbon and oxygen isotopic characteristics of benthic foraminifera in the Okinawa Trough since MIS6 and their palaeoceanographical significance[J]. Earth Science Frontiers, 29(4): 84−92 (in Chinese

with English abstract).

Doveri M, Stenni B, Petrini R, Giannecchini R, Dreossi G, Menichini M, Ghezzi L. 2019. Oxygen and hydrogen isotopic composition of waters in a past–mining area of southern Apuan Alps (Italy): Hydrogeological characterization and implications on the fate of potentially toxic elements[J]. Journal of Geochemical Exploration, 205: 106338.

Drago M, Valdivia M, Bragg D, González E M, Aguilar A, Cardona L. 2020. Stable oxygen isotopes reveal habitat use by marine mammals in the Río de la Plata estuary and adjoining Atlantic Ocean[J]. Estuarine, Coastal and Shelf Science, 238: 106708.

Drummond C N, Patterson W P, Walker J C. 1995. Climatic forcing of carbon–oxygen isotopic covariance in temperate–region marl lakes[J]. Geology, 23(11): 1031−1034.

Dubicka Z, Wierzbowski H, Pałczyńska A. 2021. Can oxygen and carbon isotope ratios of Jurassic foraminifera be used in palaeoenvironmental reconstructions?[J]. Palaeogeography, Palaeoclimatology, Palaeoecology, 577: 110554.

Duplessy J C, Shackleton N J. 1985. Response of global deep–water circulation to Earth's climatic change 135, 000–107, 000 years ago[J]. Nature, 316(6028): 500−507.

Dütsch M, Pfahl S, Sodemann H. 2017. The impact of nonequilibrium and equilibrium fractionation on two different deuterium excess definitions[J]. Journal of Geophysical Research: Atmospheres, 122(23): 12732−12746.

Ehtesham E, Hayman A, Van Hale R, Frew R. 2015. Influence of feed and water on the stable isotopic composition of dairy milk[J]. International Dairy Journal, 47: 37−45.

Eiler J M, Schauble E. 2004. $^{18}O^{13}C^{16}O$ in Earth's atmosphere[J]. Geochimica et Cosmochimica Acta, 68(23): 4767−4777.

Eiler J M. 2007. "Clumped–isotope" geochemistry—— The study of naturally–occurring, multiply–substituted isotopologues[J]. Earth and Planetary Science Letters, 262(3/4): 309−327.

Elliott E, Kendall C, Burns D, Boyer E, Harlin K, Wankel S, Butler T, Carlton R. 2006. Nitrate isotopes in precipitation to distinguish NOx sources, atmospheric processes, and source areas in the United States[C]// American Geophysical Union, Fall Meeting 2007. San Francisco, AGU.

Emiliani C. 1955. Pleistocene temperatures[J]. The Journal of Geology, 63(6): 538−578.

Emsley J. 2011. Nature's Building Blocks: An AZ Guide to the Elements[M]. Oxford University Press, USA.

Epstein S, Buchsbaum R, Lowenstam H A, Urey H C. 1953. Revised carbonate–water isotopic temperature scale[J]. Geological Society of America Bulletin, 64(11): 1315−1326.

Epstein S, Sharp R P, Gow A J. 1965. Six−year record of oxygen and hydrogen isotope variations in South Pole firn[J]. Journal of Geophysical Research, 70(8): 1809−1814.

Eren M, Akgöz M, Kadir S, Kapur S. 2021. Primary characteristics of selected stalagmites from four caves located between Erdemli and Silifke (Mersin), southern Turkey——Implications on their formation[J]. Carbonates and Evaporites, 36(2): 20.

European Commission. 2008. Commission Regulation (EC)[EB/OL]. No 555/2008 of 27 June 2008.

Falzoni F, Petrizzo M R, Clarke L J, MacLeod K G, Jenkyns H C. 2016. Long–term Late Cretaceous oxygen–and carbon–isotope trends and planktonic foraminiferal turnover: A new record from the southern Midlatitudes[J]. Bulletin, 128(11/12): 1725−1735.

Fan Juan, Nan Shenghui, Liu Yingfeng, Zhou Tianwei, Zhang Guangming. 2021. Water–filling conditions of Xiaotun Coal Mine based on hydrochemical and isotopic characteristics[J]. Safety and Environmental Engineering, (4): 80–87 (in Chinese with English abstract).

Farquhar G D, Ehleringer J R, Hubick K T. 1989. Carbon isotope discrimination and photosynthesis[J]. Annual Review of Plant Biology, 40(1): 503−537.

Fiebig J, Daëron M, Bernecker M, Guo W, Schneider G, Boch R, Bernasconi S M, Jautzy J, Dietzel M. 2021. Calibration of the dual clumped isotope thermometer for carbonates[J]. Geochimica et Cosmochimica Acta, 312: 235−256.

Frau F, Cidu R, Ghiglieri G, Caddeo G A. 2020. Characterization of low–enthalpy geothermal resources and evaluation of potential contaminants. RendicontiLincei[J]. ScienzeFisiche e Naturali, 31(4): 1055−1070.

FriedmanI, O'Nei J R. 1977. Data of Geochemistry. Chapter KK, Compilation of Stable Isotope Fractionation Factors of Geochemical Interest[M]. Washington DC: US GPO.

Friedrich O, Norris R D, Erbacher J. 2012. Evolution of middle to Late Cretaceous oceans—— a 55 my record of Earth's temperature and carbon cycle[J]. Geology, 40(2): 107−110.

Fu Changchang, Liu Cong. 2022. Hydrochemical characteristics and formation mechanism of saline lakes in Hoh Xil region[J]. Yangtze River, 53(7): 36−41 (in Chinese with English abstract).

Galewsky J, Steen−Larsen H C, Field R D, Worden J, Risi C, Schneider M. 2016. Stable isotopes in atmospheric water vapor and applications to the hydrologic cycle[J]. Reviews of Geophysics, 54(4): 809−865.

Galili N, Sade Z, Halevy I. 2022. Equilibrium fractionation of triple–oxygen and hydrogen isotopes between ice and water[J]. Earth and Planetary Science Letters, 595: 117753.

Gammons C H, Brown A, Poulson S R, Henderson T H. 2013. Using stable isotopes (S, O) of sulfate to track local contamination of the Madison karst aquifer, Montana, from abandoned coal mine drainage[J]. Applied Geochemistry, 31: 228−238.

Garbaras A, Skipitytė R, Šapolaitė J, Ežerinskis Ž, Remeikis V. 2019. Seasonal variation in stable isotope ratios of cow milk in Vilnius

region, Lithuania[J]. Animals, 9(3): 69.

Gasse F, Fontes J C, Plaziat J, Carbonel P, Kaczmarska I, De Deckker P, Soulié–Marsche I, Callot Y, Dupeuble P. 1987. Biological remains, geochemistry and stable isotopes for the reconstruction of environmental and hydrological changes in the Holocene lakes from North Sahara[J]. Palaeogeography, Palaeoclimatology, Palaeoecology, 60: 1–46.

Gat J R. 1996. Oxygen and hydrogen isotopes in the hydrologic cycle[J]. Annual Review of Earth and Planetary Sciences, 24(1): 225−262.

Gat J. 1981. Paleoclimate conditions in the Levant as revealed by the isotopic composition of paleowaters[J]. Israel Meteorological Research Papers, 3: 13−28.

Gatzert X, Chun K P, Boner M, Hermanowski R, Mäder R, Breuer L, Gattinger A, Orlowski N. 2021. Assessment of multiple stable isotopes for tracking regional and organic authenticity of plant products in Hesse, Germany[J]. Isotopes in Environmental and Health Studies, 57(3): 281−300.

Gedney N, Cox P M, Betts R A, Boucher O, Huntingford C, Stott P. 2006. Detection of a direct carbon dioxide effect in continental river runoff records[J]. Nature, 439(7078): 835−838.

Gessler A, Ferrio J P, Hommel R, Treydte K, Werner R A, Monson R K. 2014. Stable isotopes in tree rings: towards a mechanistic understanding of isotope fractionation and mixing processes from the leaves to the wood[J]. Tree Physiology, 34(8): 796−818.

Gonfiantini R. 1978. Standards for stable isotope measurements in natural compounds[J]. Nature, 271(5645): 534−536.

Gonfiantini R. 1984. Stable isotope reference samples for geochemicaland hydrological investigations[J].International Journal of AppliedRadiation and Isotopes, 35(5): 426−426.

Grant K, Rohling E, Bar–Matthews M, Ayalon A, Medina–Elizalde M, Ramsey C B, Satow C, Roberts A. 2012. Rapid coupling between ice volume and polar temperature over the past 150, 000 years[J]. Nature, 491(7426): 744−747.

Gross A, Angert A. 2015. What processes control the oxygen isotopes of soil bio–available phosphate?[J]. Geochimica et Cosmochimica Acta, 159: 100−111.

Gross A, Nishri A, Angert A. 2013. Use of phosphate oxygen isotopes for identifying atmospheric–P sources: A case study at Lake Kinneret[J]. Environmental Science & Technology, 47(6): 2721−2727.

Gross A, Turner B L, Wright S J, Tanner E V, Reichstein M, Weiner T, Angert A. 2015. Oxygen isotope ratios of plant available phosphate in lowland tropical forest soils[J]. Soil Biology and Biochemistry, 88: 354−361.

Gruau G, Legeas M, Riou C, Gallacier E, Martineau F, Hénin O. 2005. The oxygen isotope composition of dissolved anthropogenic phosphates: A new tool for eutrophication research?[J]. Water Research, 39(1): 232−238.

Gu G H. 2008. Water temperature record and trend analysis of Fuxian Lake[R]. Yuxi City Water Resources District.

Guo H, Yu X, Lin M. 2022. Kinetic isotope effects in $H_2O_2$ self–decomposition: Implications for triple oxygen isotope systematics of secondary minerals in the solar system[J]. Earth and Planetary Science Letters, 594: 117722.

Guo Q, Li B, Voelker A H, Kim J–K. 2020. Mediterranean Outflow Water dynamics across the middle Pleistocene transition based on a 1.3 million–year benthic foraminiferal record off the Portuguese margin[J]. Quaternary Science Reviews, 247: 106567.

Guo Qimei, Li Baohua, Wang Xiaoyan, Yu Zhoufei, Xu Ye, Zhang Kai. 2020. Applications of benthic foraminifera in paleoceanography[J]. Acta Palaeontologica Sinica, 59(3): 365−379 (in Chinese with English abstract).

Guo Qimei, Liu Jing, Li Baohua. 2023. Single/Multi–shell benthic foraminiferal stable oxygen and carbon isotopic composition, difference and its significance[J]. Acta Micropalaeontologica Sinica, 40(1): 53−65 (in Chinese with English abstract).

Hamzić Gregorčič S, Potočnik D, Camin F, Ogrinc N. 2020. Milk authentication: Stable isotope composition of hydrogen and oxygen in milks and their constituents[J]. Molecules, 25(17): 4000.

Han Jiamao, Jiang Wenying, Liu Dongsheng, Lü Houyuan, Guo Zhengtang, Wu Naiqin. 1996. The isotopic record of paleoclimate change in loess carbonates[J]. Scientia Sinica (Terrae), (5): 399−404 (in Chinese).

Han Jiamao, Jiang Wenying, Lü Houyuan, Wu Naiqin, Guo Zhengtang. 1995a. Carbon and oxygen isotope compositions of carbonate concretions in loess part 2: Carbon isotope and paleo–aridity[J]. Quaternary Sciences(4): 367–377 (in Chinese with English abstract).

Han Jiamao, Jiang Wenying, Wu Naiqin, Guo Zhengtang. 1995b. Carbon and oxygen isotope compositions of carbonate concretions in loss part 1: Oxygen isotope and paleotemperature[J]. Quaternary Sciences(2): 130–138 (in Chinese with English abstract).

Hao Z, Singh V P, Xia Y. 2018. Seasonal drought prediction: Advances, challenges, and future prospects[J]. Reviews of Geophysics, 56(1): 108−141.

Haubrich F, Tichomirowa M. 2002. Sulfur and oxygen isotope geochemistry of acid mine drainage—— the polymetallic sulfide deposit “ HimmelfahrtFundgrube” in Freiberg (Germany)[J]. Isotopes in Environmental and Health Studies, 38(2): 121−138.

Hayes J M. 1982. An introduction to isotopic measurements and terminology[J]. Spectr, 8: 3−8.

Hayles J A, Killingsworth B A. 2022. Constraints on triple oxygen isotope kinetics[J]. Chemical Geology, 589: 120646.

Hays I J. 1984. The orbital theory of Pleistocene climate: Support from a revised chronology of the marine $\delta^{18}O$ record[J]. Milankouitch

and Climate, NATO ASI Series, Series C: Mathematical and Physical Sciences, 126: 269–305.

Helfenstein J, Tamburini F, von Sperber C, Massey M S, Pistocchi C, Chadwick O A, Vitousek P M, Kretzschmar R, Frossard E. 2018. Combining spectroscopic and isotopic techniques gives a dynamic view of phosphorus cycling in soil[J]. Nature Communications, 9(1): 3226.

Helle G, Schleser G H. 2004. Interpreting Climate Proxies from Tree–rings[M]. In The Climate in Historical Times: Towards a Synthesis of Holocene Proxy Data and Climate Models (129–148): Springer.

Hendy C H. 1971. The isotopic geochemistry of speleothems——I. The calculation of the effects of different modes of formation on the isotopic composition of speleothems and their applicability as palaeoclimatic indicators[J]. Geochimica et Cosmochimica Acta, 35(8): 801−824.

Henkes G A, Passey B H, Grossman E L, Shenton B J, Pérez–Huerta A, Yancey T E. 2014. Temperature limits for preservation of primary calcite clumped isotope paleotemperatures[J]. Geochimica et Cosmochimica Acta, 139: 362−382.

Henkes G A, Passey B H, Wanamaker Jr A D, Grossman E L, Ambrose Jr W G, Carroll M L. 2013. Carbonate clumped isotope compositions of modern marine mollusk and brachiopod shells[J]. Geochimica et Cosmochimica Acta, 106: 307−325.

Hesse T, Butzin M, Bickert T, Lohmann G. 2011. A model−data comparison of $\delta^{13}C$ in the glacial Atlantic Ocean[J]. Paleoceanography, 26(3): 3220.

Hoag K, Still C, Fung I, Boering K. 2005. Triple oxygen isotope composition of tropospheric carbon dioxide as a tracer of terrestrial gross carbon fluxes[J]. Geophysical Research Letters, 32(2): L02802.

Hobson K A, Koehler G. 2015. On the use of stable oxygen isotope ($\delta^{18}O$) measurements for tracking avian movements in North America[J]. Ecology and Evolution, 5(3): 799−806.

Hoefs J. 1997. Stable Isotope Geochemistry[M]. Berlin: Springer: 58–66.

Horacek M, Ogrinc N, Magdas D A, Wunderlin D, Sucur S, Maras V, Misurovic A, Eder R, ˇCuˇs F, Wyhlidal S, Papesch W. 2021. Isotope analysis ($^{13}C$, $^{18}O$) of wine from central and eastern Europe and Argentina, 2008 and 2009 Vintages: Differentiation of origin, environmental indications, and variations within countries[J]. Frontiers in Sustainable Food Systems, 5: 638941.

Hori M, Ishikawa T, Nagaishi K, Lin K, Wang B S, You C F, Shen C C, Kano A. 2013. Prior calcite precipitation and source mixing process influence Sr/Ca, Ba/Ca and $^{87}Sr/^{86}Sr$ of a stalagmite developed in southwestern Japan during 18.0–4.5 ka[J]. Chemical Geology, 347: 190−198.

Horváth B, Hofmann M, Pack A. 2012. On the triple oxygen isotope composition of carbon dioxide from some combustion processes[J]. Geochimica et Cosmochimica Acta, 95: 160−168.

Hou Zhanfang, Zhang Jun, Song Chunhui, Li Jijun, Liu Jia, Liu Shanpin, Hui Zhengchuang, Peng Tingjiang. 2011. The oxygen and carbon isotopic records of Miocene sediments in the Tianshui Basin of the Northestern Tibetan Plateau and their paleoclimatic implications[J]. Marine Geology & Quaternary Geology, 31(3): 69−78 (in Chinese with English abstract).

Hsieh J C, Chadwick O A, Kelly E F, Savin S M. 1998. Oxygen isotopic composition of soil water: Quantifying evaporation and transpiration[J]. Geoderma, 82(1/3): 269−293.

Hu M, Wang Y, Du P, Shui Y, Cai A, Lv C, Bao Y, Li Y, Li S, Zhang P. 2019. Tracing the sources of nitrate in the rivers and lakes of the southern areas of the Tibetan Plateau using dual nitrate isotopes[J]. Science of the Total Environment, 658: 132−140.

Hu Quanxu, Wang Xianyan, Meng Xianqiang, Liu Quanyu, Lu Huayu. 2018. Paleoclimatic implications of oxygen isotope from authigenic carbonates in loess deposit of northeastern Tibetan Plateau[J]. Earth Science, 43(11): 4128−4137 (in Chinese with English abstract).

Huang R, Zhu H, Liang E, Bräuning A, Zhong L, Xu C, Feng X, Asad F, Sigdel S R, Li L. 2022. Contribution of winter precipitation to tree growth persists until the late growing season in the Karakoram of northern Pakistan[J]. Journal of Hydrology, 607: 127513.

Huang Sijing, Shi He, Mao Xiaodong, Zhang Meng, Shen Licheng, Wu Wenhui. 2003. Diagenetic alteration of earlier Palaeozoic marine carbonate and preservation for the information of sea water[J]. Journal of Chengdu University of Technology(Science & Technology Edition), 30(1): 9−18 (in Chinese with English abstract).

Hullar I, Brand A. 1993. Nutritional factors affecting milk quality, with special regard to milk protein: A review[J]. Acta Veterinaria Hungarica, 41(1−2): 11−32.

Hulston J R, Thode H G. 1965. Variations in the $S^{33}$, $S^{34}$, and $S^{36}$ contents of meteorites and their relation to chemical and nuclear effects[J]. Journal of Geophysical Research, 70(14): 3475−3484.

Hundey E J, Russell S, Longstaffe F J, Moser K A. 2016. Agriculture causes nitrate fertilization of remote alpine lakes[J]. Nature Communications, 7(1): 10571.

Ishida–Fujii K, Goto S, Uemura R, Yamada K, Sato M, Yoshida N. 2005. Botanical and geographical origin identification of industrial ethanol by stable isotope analyses of C, H, and O[J]. Bioscience, Biotechnology, and Biochemistry, 69(11): 2193–2199.

Ishino S, Hattori S, Savarino J, Jourdain B, Preunkert S, Legrand M, Caillon N, Barbero A, Kuribayashi K, Yoshida N. 2017. Seasonal variations of triple oxygen isotopic compositions of atmospheric sulfate, nitrate, and ozone at Dumont d'Urville, coastal Antarctica[J]. Atmospheric Chemistry and Physics, 17(5): 3713−3727.

Jaisi D P, Blake R E. 2010. Tracing sources and cycling of phosphorus in Peru margin sediments using oxygen isotopes in authigenic and detrital phosphates[J]. Geochimica et Cosmochimica Acta, 74(11): 3199−3212.

Jameel Y, Brewer S, Good S P, Tipple B J, Ehleringer J R, Bowen G J. 2016. Tap water isotope ratios reflect urban water system structure and dynamics across a semiarid metropolitan area[J]. Water Resources Research, 52(8): 5891−5910.

Ji S, Nie J, Breecker D O, Luo Z, Song Y. 2017. Intensified aridity in northern China during the middle Piacenzian warm period[J]. Journal of Asian Earth Sciences, 147: 222−225.

Ji X, Shu L, Li J, Zhao C, Chen W, Chen Z, Shang X, Dahlgren R A, Yang Y, Zhang M. 2022. Tracing nitrate sources and transformations using $\Delta^{17}O$, $\delta^{15}N$, and $\delta^{18}O$–$NO_3^-$ in a coastal plain river network of eastern China[J]. Journal of Hydrology, 610: 127829.

Jin Z, Wang J, Zhang R, Liao P, Liu Y, Yang J, Chen J. 2023. Identification of the sources of different phosphorus fractions in lake sediments by oxygen isotopic composition of phosphate[J]. Applied Geochemistry, 151: 105627.

Johnsen S J, Dahl−Jensen D, Gundestrup N, Steffensen J P, Clausen H B, Miller H, Masson-Delmotte V, Sveinbjörnsdottir A E, White J. 2001. Oxygen isotope and palaeotemperature records from six Greenland ice−core stations: Camp Century, Dye−3, GRIP, GISP2, Renland and NorthGRIP[J]. Journal of Quaternary Science: Published for the Quaternary Research Association, 16(4): 299−307.

Joshi S R, Kukkadapu R K, Burdige D J, Bowden M E, Sparks D L, Jaisi D P. 2015. Organic matter remineralization predominates phosphorus cycling in the mid–bay sediments in the Chesapeake Bay[J]. Environmental Science & Technology, 49(10): 5887−5896.

Joussaume S, Jouzel J, Sadourny R. 1984. Erratum: A general circulation model of water isotope cycles in the atmosphere[J]. Nature, 311(5987): 680−680.

Jouzel J, Merlivat L. 1984. Deuterium and oxygen 18 in precipitation: Modeling of the isotopic effects during snow formation[J]. Journal of Geophysical Research: Atmospheres, 89(D7): 11749−11757.

Junghans M, Tichomirowa M. 2009. Using sulfur and oxygen isotope data for sulfide oxidation assessment in the Freiberg polymetallic sulfide mine[J]. Applied Geochemistry, 24(11): 2034−2050.

Kamezaki K, Hattori S, Iwamoto Y, Ishino S, Furutani H, Miki Y, Miura K, Uematsu M, Yoshida N. 2017. Nitrogen and Triple Oxygen Isotopic Analyses of Atmospheric Particulate Nitrate over the Pacific Ocean[C]. Paper presented at the EGU General Assembly Conference Abstracts.

Kamiloglu S. 2019. Authenticity and traceability in beverages[J]. Food Chemistry, 277: 12−24.

Kato H, Amekawa S, Hori M, Shen C C, Kuwahara Y, Senda R, Kano A. 2021. Influences of temperature and the meteoric water $\delta^{18}O$ value on a stalagmite record in the last deglacial to Middle Holocene period from southwestern Japan[J]. Quaternary Science Reviews, 253: 106746.

Kelly S, Heaton K, Hoogewerff J. 2005. Tracing the geographical origin of food: The application of multi–element and multi–isotope analysis[J]. Trends in Food Science & Technology, 16(12): 555−567.

Kendall C, Elliott E M, Wankel S D. 2007. Tracing anthropogenic inputs of nitrogen to ecosystems[J]. Stable Isotopes in Ecology and Environmental Science, 2(1): 375−449.

Kendall C, McDonnell J J. 1998. Isotope Tracers in Catchment Hydrology[M]. Amsterdam: Elsevier.

Killingsworth B A, Bao H. 2015. Significant human impact on the flux and $\delta^{34}S$ of sulfate from the Largest River in North America[J]. Environmental Science & Technology, 49(8): 4851−4860.

Kim D M, Yun S T, Yoon S, Mayer B. 2019. Signature of oxygen and sulfur isotopes of sulfate in ground and surface water reflecting enhanced sulfide oxidation in mine areas[J]. Applied Geochemistry, 100: 143−151.

Kim S T, O'Neil J R, Hillaire–Marcel C, Mucci A. 2007. Oxygen isotope fractionation between synthetic aragonite and water: Influence of temperature and $Mg^{2+}$ concentration[J]. Geochimica et Cosmochimica Acta, 71(19): 4704−4715.

Kluge T, John C M, Jourdan A L, Davis S, Crawshaw J. 2015. Laboratory calibration of the calcium carbonate clumped isotope thermometer in the 25–250 C temperature range[J]. Geochimica et Cosmochimica Acta, 157: 213−227.

Kolodny Y, Luz B, Navon O. 1983. Oxygen isotope variations in phosphate of biogenic apatites, I. Fish bone apatite——Rechecking the rules of the game[J]. Earth and Planetary Science Letters, 64(3): 398−404.

Korenaga T, Musashi M, Nakashita R, Suzuki Y. 2010. Statistical analysis of rice samples for compositions of multiple light elements (H, C, N, and O) and their stable isotopes[J]. Analytical Sciences, 26(8): 873−878.

Kortelainen N. 2009. Isotopic composition of atmospheric precipitation and shallow groundwater in Olkiluoto: O–18, H–2 and H–3[R]. Posiva Oy.

Krouse H R, Grinenko V A. 1991. Stable Isotopes: Natural and Anthropogenic Sulphur in the Environment[M]. New York: John Wiley and Sons Ltd, 1991: 1–40.

Kukusamude C, Sola P, Kongsri S. 2018. Stable isotope ratio of local rice samples in Thailand[C]//Journal of Physics: Conference Series. IOP Publishing, 1144(1): 012168.

Kuwano D, Tsuchiya Y, Kameo K, Hayashi H, Kubota Y, Mantoku K, Oura Y. 2022. Early Pleistocene (marine isotope stage 40–36) paleoceanography in the northwestern Pacific: Evidence from

faunal and oxygen isotope analyses of planktonic foraminifera[J]. Palaeogeography, Palaeoclimatology, Palaeoecology, 592: 110873.

Labeyrie L, Duplessy J C, Blanc P. 1987. Variations in mode of formation and temperature of oceanic deep waters over the past 125, 000 years[J]. Nature, 327(6122): 477−482.

Landais A, Barkan E, Yakir D, Luz B. 2006. The triple isotopic composition of oxygen in leaf water[J]. Geochimica et Cosmochimica Acta, 70(16): 4105−4115.

Landais A, Risi C, Bony S, Vimeux F, Descroix L, Falourd S, Bouygues A. 2010. Combined measurements of $^{17}O_{excess}$ and d–excess in African monsoon precipitation: Implications for evaluating convective parameterizations[J]. Earth and Planetary Science Letters, 298(1/2): 104−112.

Larkins C, Turunen K, Mänttäri I, Lahaye Y, Hendriksson N, Forsman P, Backnäs S. 2018. Characterization of selected conservative and non–conservative isotopes in mine effluent and impacted surface waters: implications for tracer applications at the mine–site scale[J]. Applied Geochemistry, 91: 1−13.

Laskar A H, Maurya A S, Singh V, Gurjar B R, Liang M–C. 2020. A new perspective of probing the level of pollution in the megacity Delhi affected by crop residue burning using the triple oxygen isotope technique in atmospheric $CO_2$[J]. Environmental Pollution, 263: 114542.

Lawrence J R, Gedzelman S D, Dexheimer D, Cho H K, Carrie G D, Gasparini R, Anderson C R, Bowman K P, Biggerstaff M I. 2004. Stable isotopic composition of water vapor in the tropics[J]. Journal of Geophysical Research: Atmospheres, 109(D6): D06115.

Lea D W, Martin P A, Pak D K, Spero H J. 2002. Reconstructing a 350 ky history of sea level using planktonic Mg/Ca and oxygen isotope records from a Cocos Ridge core[J]. Quaternary Science Reviews, 21(1−3): 283−293.

Leavitt S W, Danzer S R. 1993. Method for batch processing small wood samples to holocellulose for stable–carbon isotope analysis[J]. Analytical Chemistry, 65(1): 87−89.

LeGrande A N, Schmidt G A. 2006. Global gridded data set of the oxygen isotopic composition in seawater[J]. Geophysical research letters, 33(12): L12604.

Li A, Keely B, Chan S, Baxter M, Rees G, Kelly S. 2015. Verifying the provenance of rice using stable isotope ratio and multi–element analyses: A feasibility study[J]. Quality Assurance and Safety of Crops & Foods, 7(3): 343−354.

Li C, Ren J, Shi G, Pang H, Wang Y, Hou S, Li Z, Du Z, Ding M, Ma X. 2021. Spatial and temporal variations of fractionation of stable isotopes in East–Antarctic snow[J]. Journal of Glaciology, 67(263): 523−532.

Li H C, Ku T L. 1997. $\delta^{13}C$–$\delta^{18}C$ covariance as a paleohydrological indicator for closed–basin lakes[J]. Palaeogeography, Palaeoclimatology, Palaeoecology, 133(1–2): 69–80.

Li J, Li Z, Brandis K J, Bu J, Sun Z, Yu Q, Ramp D. 2020a. Tracing geochemical pollutants in stream water and soil from mining activity in an alpine catchment[J]. Chemosphere, 242: 125167.

Li Jiansen, Cai Jinfu, Fan Qishun, Shan Fashou, Ling Zhiyong, Han Yuanhong, Zhang Yongxing. 2022. Metallogenic geochemical system of K, B and Li resources in salt lakes of Qaidam Basin[J]. Journal of Salt Lake Research, 30(3): 12−20 (in Chinese with English abstract).

Li S L, Liu C Q, Li J, Liu X, Chetelat B, Wang B, Wang F. 2010. Assessment of the sources of nitrate in the Changjiang River, China using a nitrogen and oxygen isotopic approach[J]. Environmental Science & Technology, 44(5): 1573−1578.

Li Siyuan, Hou Qingye, Yang Zhongfang, Yu Tao. 2024. Nitrogen isotope fractionation mechanism, analysis measurement tracer technology and itsapplication in ecological environment[J]. Geology in China, 51(5): 1617−1643 (in Chinese with English abstract).

Li Tong, Qiu Guoyu. 2018. Hydrogen and oxygen stable isotope study on the difference of evaporation between salt and pure water[J]. Tropical Geography, 38(6): 857−865 (in Chinese with English abstract).

Li X, Pan G, Zhou A, Fang L, He N. 2022. Stable sulfur and oxygen isotopes of sulfate as tracers of antimony and arsenic pollution sources related to antimony mine activities in an impacted river[J]. Applied Geochemistry, 142: 105351.

Li X, Wang Y, Stern J, Gu B. 2011. Isotopic evidence for the source and fate of phosphorus in Everglades wetland ecosystems[J]. Applied Geochemistry, 26(5): 688−695.

Li Xiaoqian, Zhang Bin, Zhou Aiguo, LiuYunde. 2014. Using sulfur and oxygen isotopes of sulfate to track groundwater contamination from coal mine drainage in Heshan[J]. Hydrogeology & Engineering Geology, 41(6): 103−109 (in Chinese with English abstract).

Li Y, Liu T, Wu W, Hna J, Hong Y. 2003. Paleoenvironment in Chinese loess plateau during mis 3: Evidence from Malan Loess[J]. Quaternary Sciences, 23(1): 69−76.

Li Y, Zeng X, Liu X, Evans M N, Xu G, Szejner P, Ni P. 2023. A seasonally varying tree physiological response to environmental conditions: Results from semi−arid China[J]. Journal of Geophysical Research: Biogeosciences, 128(7): e2023JG007455.

Li Yue, Wang Rujian, Li Wenbao. 2016. Review on research on paleo–sea level reconstruction based on foraminiferal oxygen isotope in deep sea sediments[J]. Advances in Earth Science, 31(3): 310−319 (in Chinese with English abstract).

Li Z, Ou J, Chen X, Li F, Wang X, Tan X. 2017. Characteristics and main development controlling factors for Lower Permian dolomite reservoirs in Chuanzhong region[J]. Petroleum Geology & Oilfield Development in Daqing, 36(4): 1−8.

Li Z, Zhang R, Liu C, Zhang R, Chen F, Liu Y. 2020b. Phosphorus spatial distribution and pollution risk assessment in agricultural soil around the Danjiangkou reservoir, China[J]. Science of the Total Environment, 699: 134417.

Li Zhitao, Xiao Hongwei, Wu Zuoting, Ma Yan, Xiao Yangning, Chen Zhenping, Tao Jihua. 2022. Hydrochemistry, nitrogen and oxygen isotope composition of nitrate to trace its source in Poyang Lake wetland[J]. China Environmental Science, 42(9): 4315−4322 (in Chinese with English abstract).

Liang M C, Laskar A H, Barkan E, Newman S, Thiemens M H, Rangarajan R. 2023. New constraints of terrestrial and oceanic global gross primary productions from the triple oxygen isotopic composition of atmospheric $CO_2$ and $O_2$[J]. Scientific Reports, 13(1): 2162.

Liang M C, Mahata S, Laskar A H, Bhattacharya S K. 2017. Spatiotemporal variability of oxygen isotope anomaly in near surface air $CO_2$ over urban, semi–urban and ocean areas in and around Taiwan[J]. Aerosol and Air Quality Research, 17(3): 706−720.

Liang M C, Mahata S. 2015. Oxygen anomaly in near surface carbon dioxide reveals deep stratospheric intrusion[J]. Scientific Reports, 5(1): 11352.

Liang M C, Yung Y L. 2007. Sources of the oxygen isotopic anomaly in atmospheric $N_2O$[J]. Journal of Geophysical Research: Atmospheres, 112(D13): D13307.

Lin M, Thiemens M H. 2024. 40 years of theoretical advances in mass–independent oxygen isotope effects and applications in atmospheric chemistry: A critical review and perspectives[J]. Applied Geochemistry, 161: 105860.

Lisiecki L E, Raymo M E. 2005. A Pliocene−Pleistocene stack of 57 globally distributed benthic $\delta^{18}O$ records[J]. Paleoceanography, 20(2): PA2007.

Liu C L, Wang M L, Jiao P C. 1999. Hydrogen, oxygen, strontium and sulfur isotopic geochemistry and potash–forming material sources of lop salt lake, Xinjiang[J]. Mineral Deposits, 18(3): 268−275.

Liu J, Chen J, Zhang X, Li Y, Rao Z, Chen F. 2015. Holocene East Asian summer monsoon records in northern China and their inconsistency with Chinese stalagmite $\delta^{18}O$ records[J]. Earth–Science Reviews, 148: 194−208.

Liu J, Han G. 2021. Tracing riverine sulfate source in an agricultural watershed: Constraints from stable isotopes[J]. Environmental Pollution, 288: 117740.

Liu Ke, Hou Shugui, Pang Hongxi, Shi Guitao, Geng Lei, Hu Huanting, Song Jing, Zhang Wangbin, Zou Xiang, An Chunlei, Yu Jinhai. 2022. Polar ice core–based climate and environmental research: A review and perspective[J]. Chinese Journal of Polar Research, 34(4): 530−545 (in Chinese with English abstract).

Liu S, Zhang R, Kang R, Meng J, Ao C. 2016. Milk fatty acids profiles and milk production from dairy cows fed different forage quality diets[J]. Animal Nutrition, 2(4): 329−333.

Liu T, Wang F, Michalski G, Xia X, Liu S. 2013. Using $^{15}N$, $^{17}O$, and $^{18}O$ to determine nitrate sources in the Yellow River, China[J]. Environmental Science & Technology, 47(23): 13412−13421.

Liu X F, Xue C H, Wang Y M, Li Z J, Xue Y, Xu J. 2011. Principal component analysis and cluster analysis of inorganic elements in sea cucumber Apostichopus japonicus[J]. Spectroscopy and Spectral Analysis, 31(11): 3119−3122.

Liu X, Chen B. 2000. Climatic warming in the Tibetan Plateau during recent decades[J]. International Journal of Climatology: A Journal of the Royal Meteorological Society, 20(14): 1729−1742.

Liu Y, Wang Y, Li Q, Song H, Linderholm H W, Leavitt S W, Wang R, An Z. 2014. Tree–ring stable carbon isotope–based May–July temperature reconstruction over Nanwutai, China, for the past century and its record of 20th century warming[J]. Quaternary Science Reviews, 93: 67−76.

Loader N, Robertson I, McCarroll D. 2003. Comparison of stable carbon isotope ratios in the whole wood, cellulose and lignin of oak tree–rings[J]. Palaeogeography, Palaeoclimatology, Palaeoecology, 196(3/4): 395–407.

Lü Fenglin, Liu Chenglin, Jiao Pengcheng, Zhang Hua, Sun Xiaohong, Zhang Yongming. 2018. Carbon and oxygen isotopic compositions of the lacustrine carbonate in Lop Nur since the Mid–Pleistocene and their paleoenvironment significance[J]. Acta Geologica Sinica, 92(8): 1589−1604 (in Chinese with English abstract).

Luo D, Dong H, Luo H, Xian Y, Guo X, Wu Y. 2016. Multi–element (C, N, H, O) stable isotope ratio analysis for determining the geographical origin of pure milk from different regions[J]. Food Analytical Methods, 9: 437−442.

Luo X, Wang H, An Z, Zhang Z, Liu W. 2020. Carbon and oxygen isotopes of calcified root cells, carbonate nodules and total inorganic carbon in the Chinese loess–paleosol sequence: The application of paleoenvironmental studies[J]. Journal of Asian Earth Sciences, 201: 104515.

Luz B, Barkan E, Bender M L, Thiemens M H, Boering K A. 1999. Triple–isotope composition of atmospheric oxygen as a tracer of biosphere productivity[J]. Nature, 400(6744): 547−550.

Luz B, Barkan E. 2010. Variations of $^{17}O/^{16}O$ and $^{18}O/^{16}O$ in meteoric waters[J]. Geochimica et Cosmochimica Acta, 74(22): 6276−6286.

Ma Zhengming, Jiang Panwu, Li Qingkuan, Wei Haicheng, Li Yongshou, Shan Fashou. 2021. Hydrogen and oxygen isotope characteristics and origin of Hadahexiu Salt Lake Brine[J]. Journal of Salt Lake Research, 29(1): 80−87 (in Chinese with English abstract).

MacDonald G K, Bennett E M, Potter P A, Ramankutty N. 2011. Agronomic phosphorus imbalances across the world's croplands[J]. Proceedings of the National Academy of Sciences, 108(7):

3086−3091.

MacDonald J M, John C M, Girard J–P. 2018. Testing clumped isotopes as a reservoir characterization tool: A comparison with fluid inclusions in a dolomitized sedimentary carbonate reservoir buried to 2–4 km[J]. Geological Society, London, Special Publications, 468(1): 189–202.

MacLeod K G, Huber B T, Berrocoso Á J, Wendler I. 2013. A stable and hot Turonian without glacial $\delta^{18}O$ excursions is indicated by exquisitely preserved Tanzanian foraminifera[J]. Geology, 41(10): 1083−1086.

Magdas DA, Dehelean A, Puscas R. 2012. Isotopic and elemental determination in some Romanian apple fruit juices[J]. Scientific World Journal, 2012: 1−7.

Mahecha M D, Reichstein M, Carvalhais N, Lasslop G, Lange H, Seneviratne S I, Vargas R, Ammann C, Arain M A, Cescatti A. 2010. Global convergence in the temperature sensitivity of respiration at ecosystem level[J]. Science, 329(5993): 838−840.

Maher B A, Hu M. 2006. A high–resolution record of Holocene rainfall variations from the western Chinese Loess Plateau: Antiphase behaviour of the African/Indian and East Asian summer monsoons[J]. The Holocene, 16(3): 309−319.

Maiorano P, Marino M, Balestra B, Flores J–A, Hodell D, Rodrigues T. 2015. Coccolithophore variability from the Shackleton Site (IODP Site U1385) through MIS 16–10[J]. Global and Planetary Change, 133: 35−48.

Majoube M. 1971. Fractionnementenoxygène–18 et endeutérium entre l'eau et savapeur[J]. Journal de Chimie Physique, 68: 1423−1436.

Mangenot X, Deçoninck J F, Bonifacie M, Rouchon V, Collin P Y, Quesne D, Gasparrini M, Sizun J P. 2019. Thermal and exhumation histories of the northern subalpine chains (Bauges and Bornes——France): Evidence from forward thermal modeling coupling clay mineral diagenesis, organic maturity and carbonate clumped isotope (Δ47) data[J]. Basin Research, 31(2): 361−379.

Mangenot X, Gasparrini M, Gerdes A, Bonifacie M, Rouchon V. 2018. An emerging thermochronometer for carbonate–bearing rocks: Δ47/(U–Pb)[J]. Geology, 46(12): 1067−1070.

Mao Jianying, Zhu Jianping, Xiao Jianjun. 2003. The relationship between nitrogen contamination and dissolved oxygen in mainstream of the Huaihe River[J]. Environmental Monitoring in China, (5): 41−43 (in Chinese with English abstract).

Maqsoud A, Neculita C M, Bussière B, Benzaazoua M, Dionne J. 2016. Impact of fresh tailing deposition on the evolution of groundwater hydrogeochemistry at the abandoned Manitou mine site, Quebec, Canada[J]. Environmental Science and Pollution Research, 23: 9054−9072.

Marcus R. 2008. Mass–independent oxygen isotope fractionation in selected systems. Mechanistic considerations[J]. Advances in Quantum Chemistry, 55: 5−19.

Marrero T R, Mason E A. 1972. Gaseous diffusion coefficients[J]. Journal of Physical and Chemical Reference Data, 1(1): 3−118.

Martino J C, Mazumder D, Gadd P, Doubleday Z A. 2022. Tracking the provenance of octopus using isotopic and multi–elemental analysis[J]. Food Chemistry, 371: 131133.

Masud Z, Vallet C, Martin G J. 1999. Stable isotope characterization of milk components and whey ethanol[J]. Journal of Agricultural and Food Chemistry, 47(11): 4693−4699.

Mayer B, Bollwerk S M, Mansfeldt T, Hütter B, Veizer J. 2001. The oxygen isotope composition of nitrate generated by nitrification in acid forest floors[J]. Geochimica et Cosmochimica Acta, 65(16): 2743−2756.

Mayer B, Boyer E W, Goodale C, Jaworski N A, Van Breemen N, Howarth R W, Seitzinger S, Billen G, Lajtha K, Nadelhoffer K. 2002. Sources of nitrate in rivers draining sixteen watersheds in the northeastern US: Isotopic constraints[J]. Biogeochemistry, 57: 171−197.

McCarroll D, Loader N J. 2004. Stable isotopes in tree rings[J]. Quaternary Science Reviews, 23(7−8): 771−801.

McCorkle D C, Keigwin L D, Corliss B H, Emerson S R. 1990. The influence of microhabitats on the carbon isotopic composition of deep−sea benthic foraminifera[J]. Paleoceanography, 5(2): 161−185.

McLaughlin K, Kendall C, Silva S R, Young M, Paytan A. 2006. Phosphate oxygen isotope ratios as a tracer for sources and cycling of phosphate in North San Francisco Bay, California[J]. Journal of Geophysical Research: Biogeosciences, 111(G3): 03003.

Meijer H A J, Li W J. 1998. The use of electrolysis for accurate $\delta^{17}O$ and $\delta^{18}O$ isotope measurements in water[J]. Isotopes in Environmental and Health Studies, 34(4): 349−369.

Merlivat L, Coantic M. 1975. Study of mass transfer at the air−water interface by an isotopic method[J]. Journal of Geophysical Research, 80(24): 3455−3464.

Merlivat L, Jouzel J. 1979. Global climatic interpretation of the deuterium−oxygen 18 relationship for preci–pitation[J]. Journal of Geophysical Research: Oceans, 84(C8): 5029−5033.

Miall A D. 2013. Principles of Sedimentary Basin Analysis[M]. Springer Science & Business Media.

Miao Qing, Hou Xianhua, Yang Zhenjing. 2021. Application of several commonly used paleoclimate proxies in paleoenvironmental studies of salt lakes[J]. Scientific and Technological Innovation, (5): 31−32 (in Chinese).

Miao Tian, JinYaqi, Wang Lei, Wu Gaoyang, Chen Zhong. 2021. Research progress on the paleoclimate significance of loess carbonate[J]. Journal of Salt Lake Research, 29(4): 90−99 (in Chinese with English abstract).

Michalski G, Meixner T, Fenn M, Hernandez L, Sirulnik A, Allen E, Thiemens M. 2004. Tracing atmospheric nitrate deposition in a

complex semiarid ecosystem using $\Delta^{17}O$[J]. Environmental Science & Technology, 38(7): 2175−2181.

Michalski G, Scott Z, Kabiling M, Thiemens M H. 2003. First measurements and modeling of $\Delta^{17}O$ in atmospheric nitrate[J]. Geophysical Research Letters, 30(16): 1870.

Michalski G, Thiemens M. 2006. The use of multi–isotope ratio measurements as a new and unique technique to resolve NOx transformation, transport and nitrate deposition in the Lake Tahoe Basin[J]. California Air Resources Board, Sacramento,CA: 03−317.

Miller K G, Browning J V, Schmelz W J, Kopp R E, Mountain G S, Wright J D. 2020. Cenozoic sea–level and cryospheric evolution from deep–sea geochemical and continental margin records[J]. Science advances, 6(20): eaaz1346.

Miller K G, Wright J D, Browning J V, Kulpecz A, Kominz M, Naish T R, Cramer B S, Rosenthal Y, Peltier W R, Sosdian S. 2012. High tide of the warm Pliocene: Implications of global sea level for Antarctic deglaciation[J]. Geology, 40(5): 407−410.

Miller M F. 2002. Isotopic fractionation and the quantification of $^{17}O$ anomalies in the oxygen three–isotope system: An appraisal and geochemical significance[J]. Geochimica et Cosmochimica Acta, 66(11): 1881−1889.

Miller M F. 2018. Precipitation regime influence on oxygen triple–isotope distributions in Antarctic precipitation and ice cores[J]. Earth and Planetary Science Letters, 481: 316−327.

Mimmo T, Camin F, Bontempo L, Capici C, Tagliavini M, Cesco S, Scampicchio M. 2015. Traceability of different apple varieties by multivariate analysis of isotope ratio mass spectrometry data[J]. Rapid Communications in Mass Spectrometry, 29(21): 1984−1990.

Mix A C, Ruddiman W F. 1984. Oxygen–isotope analyses and Pleistocene ice volumes[J]. Quaternary Research, 21(1): 1−20.

Mosley–Thompson E, Thompson L G, Grootes P M, Gundestrup N. 1990. Little ice age (neoglacial) paleoenvironmental conditions at siple station, Antarctica[J]. Annals of Glaciology, 14: 199−204.

Moyé J, Picard–Lesteven T, Zouhri L, El Amari K, Hibti M, Benkaddour A. 2017. Groundwater assessment and environmental impact in the abandoned mine of Kettara (Morocco)[J]. Environmental Pollution, 231: 899−907.

Naylor H N, Defliese W F, Grossman E L, Maupin C R. 2020. Investigation of the thermal history of the Delaware Basin (West Texas, USA) using carbonate clumped isotope thermometry[J]. Basin Research, 32(5): 1140−1155.

Nestler A, Berglund M, Accoe F, Duta S, Xue D, Boeckx P, Taylor P. 2011. Isotopes for improved management of nitrate pollution in aqueous resources: review of surface water field studies[J]. Environmental Science and Pollution Research, 18: 519−533.

Newman C P, Poulson S R, Hanna B. 2020. Regional isotopic investigation of evaporation and water–rock interaction in mine pit lakes in Nevada, USA[J]. Journal of Geochemical Exploration, 210: 106445.

Newsome S D, Clementz M T, Koch P L. 2010. Using stable isotope biogeochemistry to study marine mammal ecology[J]. Marine Mammal Science, 26(3): 509−572.

Nishimoto N, Yamamoto Y, Yamagata S, Igarashi T, Tomiyama S. 2021. Acid mine drainage sources and impact on groundwater at the osarizawa mine, Japan[J]. Minerals, 11(9): 998.

O'driscoll M, DeWalle D, McGuire K, Gburek W. 2005. Seasonal $^{18}O$ variations and groundwater recharge for three landscape types in central Pennsylvania, USA[J]. Journal of Hydrology, 303(1/4): 108−124.

Oerter E J, Bowen G. 2017. In situ monitoring of H and O stable isotopes in soil water reveals ecohydrologic dynamics in managed soil systems[J]. Ecohydrology, 10(4): e1841.

Ogrinc N, Košir I J, Kocjančič M, Kidrič J. 2001. Determination of authenticy, regional origin, and vintage of Slovenian wines using a combination of IRMS and SNIF–NMR analyses[J]. Journal of Agricultural and Food Chemistry, 49(3): 1432−1440.

O'Neil J R, Clayton R N, Mayeda T K. 1969. Oxygen isotope fractionation in divalent metal carbonates[J]. The Journal of Chemical Physics, 51(12): 5547−5558.

Orellana S, Johansen A M, Gazis C. 2019. Geographic classification of US Washington State wines using elemental and water isotope composition[J]. Food Chemistry: X, 1: 100007.

Passey B H, Henkes G A. 2012. Carbonate clumped isotope bond reordering and geospeedometry[J]. Earth and Planetary Science Letters, 351: 223−236.

Passey B H, Ji H. 2019. Triple oxygen isotope signatures of evaporation in lake waters and carbonates: A case study from the western United States[J]. Earth and Planetary Science Letters, 518: 1−12.

Perini M, Thomas F, Ortiz A I C, Simoni M, Camin F. 2022. Stable isotope ratio analysis of lactose as a possible potential geographical tracer of milk[J]. Food Control, 139: 109051.

Peters M, Guo Q, Strauss H, Wei R, Li S, Yue F. 2019. Contamination patterns in river water from rural Beijing: A hydrochemical and multiple stable isotope study[J]. Science of the Total Environment, 654: 226−236.

Petit J–R, Jouzel J, Raynaud D, Barkov N I, Barnola J–M, Basile I, Bender M, Chappellaz J, Davis M, Delaygue G. 1999. Climate and atmospheric history of the past 420, 000 years from the Vostok ice core, Antarctica[J]. Nature, 399(6735): 429−436.

Pistocchi C, Mészáros É, Frossard E, Bünemann E K, Tamburini F. 2020. In or out of equilibrium? How microbial activity controls the oxygen isotopic composition of phosphate in forest organic horizons with low and high phosphorus availability[J]. Frontiers in Environmental Science, 8: 564778.

Porter T J, Pisaric M F, Field R D, Kokelj S V, Edwards T W,

deMontigny P, Healy R, LeGrande A N. 2014. Spring–summer temperatures since AD 1780 reconstructed from stable oxygen isotope ratios in white spruce tree–rings from the Mackenzie Delta, northwestern Canada[J]. Climate Dynamics, 42: 771−785.

Prell W L, Imbrie J, Martinson D G, Morley J J, Pisias N G, Shackleton N J, Streeter H F. 1986. Graphic correlation of oxygen isotope stratigraphy application to the Late Quaternary[J]. Paleoceanography, 1(2): 137−162.

Pritchard H D. 2019. Asia's shrinking glaciers protect large populations from drought stress[J]. Nature, 569(7758): 649−654.

Prud'Homme C, Lécuyer C, Antoine P, Moine O, Hatté C, Fourel F, Martineau F, Rousseau D–D. 2016. Palaeotemperature reconstruction during the Last Glacial from $\delta^{18}O$ of earthworm calcite granules from Nussloch loess sequence, Germany[J]. Earth and Planetary Science Letters, 442: 13−20.

Qiao Zhanfeng, Yu Zhou, She Min, Pan Liyin, Zhang Tianfu, Li Wenzheng, Shen Anjiang. 2023. Progresses on ancient ultra–deeply buried marine carbonate reservoir in China.[J]. Journal of Palaeogeography(Chinese Edition), 25(6): 1257−1276 (in Chinese with English abstract).

Qiu Nansheng, Liu Xin, Xiong Yujie, Liu Yuchen, Xu Qiuchen, Chang Qing. 2023. Progress in the study of carbonate clumped isotope in the thermal history of marine basins[J]. Petroleum Geology & Experiment, 45(5): 891−903 (in Chinese with English abstract).

Rao Z, Liu X, Hua H, Gao Y, Chen F. 2015. Evolving history of the East Asian summer monsoon intensity during the MIS5: Inconsistent records from Chinese stalagmites and loess deposits[J]. Environmental Earth Sciences, 73: 3937−3950.

Rasmussen S O, Abbott P M, Blunier T, Bourne A, Brook E, Buchardt S L, Buizert C, Chappellaz J, Clausen H, Cook E. 2013. A first chronology for the North Greenland Eemian Ice Drilling (NEEM) ice core[J]. Climate of the Past, 9(6): 2713−2730.

Rech J A, Currie B S, Jordan T E, Riquelme R, Lehmann S B, Kirk–Lawlor N E, Li S, Gooley J T. 2019. Massive Middle Miocene gypsic paleosols in the Atacamadesert and the formation of the Central Andean rain–shadow[J]. Earth and Planetary Science Letters, 506: 184−194.

Ren J, Xiao C, Hou S, Li Y, Sun B. 2009. New focuses of polar ice–core study: NEEM and Dome A[J]. Chinese Science Bulletin, 54(6): 1009−1011.

Ren K, Zeng J, Liang J, Yuan D, Jiao Y, Peng C, Pan 20X. 2021. Impacts of acid mine drainage on karst aquifers: Evidence from hydrogeochemistry, stable sulfur and oxygen isotopes[J]. Science of the Total Environment, 761: 143223.

Ren Kun, Pan Xiaodong, Lan Ganjiang, Peng Cong, Liang Jiapeng, Zeng Jie. 2021. Seasonal variation and sources identification of dissolved sulfate in a typical karst subterranean stream basin using sulfur and oxygen isotopes[J]. Environmental Science, 42(9): 4267−4274 (in Chinese with English abstract).

Ridley H E, Asmerom Y, Baldini J U, Breitenbach S F, Aquino V V, Prufer K M, Culleton B J, Polyak V, Lechleitner F A, Kennett D J. 2015. Aerosol forcing of the position of the intertropical convergence zone since AD 1550[J]. Nature Geoscience, 8(3): 195−200.

Roberts K, Defforey D, Turner B L, Condron L M, Peek S, Silva S, Kendall C, Paytan A. 2015. Oxygen isotopes of phosphate and soil phosphorus cycling across a 6500 year chronosequence under lowland temperate rainforest[J]. Geoderma, 257: 14−21.

Rockmann T, Brenninkmeijer C, Saueressig G, Bergamaschi P, Crowley J, Fischer H, Crutzen P. 1998. Mass–independent oxygen isotope fractionation in atmospheric CO as a result of the reaction CO+ OH[J]. Science, 281(5376): 544−546.

Roe L J, Thewissen J, Quade J, O'Neil J R, Bajpai S, Sahni A, Hussain S T. 1998. Isotopic approaches to understanding the terrestrial–to–marine transition of the earliest cetaceans[J]. The Emergence of Whales: Evolutionary Patterns in the Origin of Cetacea, 399–422.

Rohling E J, Grant K, Bolshaw M, Roberts A, Siddall M, Hemleben C, Kucera M. 2009. Antarctic temperature and global sea level closely coupled over the past five glacial cycles[J]. Nature Geoscience, 2(7): 500−504.

Rohling E J. 2013. Oxygen isotope composition of seawater[J]. The Encyclopedia of Quaternary Science. Amsterdam: Elsevier, 2: 915−922.

Rossmann A, Reniero F, Moussa I, Schmidt H L, Versini G, Merle M H. 1999. Stable oxygen isotope content of water of EU data–bank wines from Italy, France and Germany[J]. Zeitschrift Fur Lebensmittel–Untersuchung Und–Forschung a–Food Research and Technology, 208(5/6): 400−407.

Roy R, Wang Y, Jiang S. 2019. Growth pattern and oxygen isotopic systematics of modern freshwater mollusks along an elevation transect: Implications for paleoclimate reconstruction[J]. Palaeogeography, Palaeoclimatology, Palaeoecology, 532: 109243.

Ruhela M, Sharma K, Bhutiani R, Chandniha S K, Kumar V, Tyagi K, Ahamad F, Tyagi I. 2022. GIS–based impact assessment and spatial distribution of air and water pollutants in mining area[J]. Environmental Science and Pollution Research, 29(21): 31486−31500.

Ryu Y, Baldocchi D D, Kobayashi H, Van Ingen C, Li J, Black T A, Beringer J, Van Gorsel E, Knohl A, Law B E. 2011. Integration of MODIS land and atmosphere products with a coupled−process model to estimate gross primary productivity and evapotranspiration from 1 km to global scales[J]. Global Biogeochemical Cycles, 25: GB4017.

Sanci R, Panarello H O, Gozalvez M R. 2020. Environmental isotopes as tracers of mining activities and natural processes: A case study of

San Antonio de los Cobres River Basin, Puna Argentina[J]. Journal of Geochemical Exploration, 213: 106517.

Santesteban L, Miranda C, Barbarin I, Royo J. 2015. Application of the measurement of the natural abundance of stable isotopes in viticulture: A review[J]. Australian Journal of Grape and Wine Research, 21(2): 157−167.

Savarino J, Kaiser J, Morin S, Sigman D M, Thiemens M. 2007. Nitrogen and oxygen isotopic constraints on the origin of atmospheric nitrate in coastal Antarctica[J]. Atmospheric Chemistry and Physics, 7(8): 1925−1945.

Savarino J, Thiemens M H. 1999. Analytical procedure to determine both $\delta^{18}O$ and $\delta^{17}O$ of $H_2O_2$ in natural water and first measurements[J]. Atmospheric Environment, 33(22): 3683−3690.

Savin S M, Lee M. 1988. Isotopic studies of phyllosilicates[J]. Reviews in Mineralogy and Geochemistry, 19(1): 189−223.

Schauble E A, Ghosh P, Eiler J M. 2006. Preferential formation of $^{13}C$–$^{18}O$ bonds in carbonate minerals, estimated using first–principles lattice dynamics[J]. Geochimica et Cosmochimica Acta, 70(10): 2510−2529.

Schilt A, Baumgartner M, Blunier T, Schwander J, Spahni R, Fischer H, Stocker T F. 2010. Glacial–interglacial and millennial–scale variations in the atmospheric nitrous oxide concentration during the last 800,000 years[J]. Quaternary Science Reviews, 29(1/2): 182−192.

Schönbeck L C, Santiago L S. 2022. Time will tell: towards high–resolution temporal tree–ring isotope analyses[J]. Tree Physiology, 42(12): 2401−2403.

Schubert B A, Jahren A H. 2015. Seasonal temperature and precipitation recorded in the intra–annual oxygen isotope pattern of meteoric water and tree–ring cellulose[J]. Quaternary Science Reviews, 125: 1−14.

Shackleton N J, Opdyke N D. 1973. Oxygen isotope and palaeomagnetic stratigraphy of Equatorial Pacific core V28–238: Oxygen isotope temperatures and ice volumes on a 105 year and 106 year scale[J]. Quaternary Research, 3(1): 39−55.

Shackleton N J. 1967. Oxygen isotope analyses and Pleistocene temperatures re–assessed[J]. Nature, 215(5096): 15−17.

Shackleton N J. 1974. Attainment of isotopic equilibrium between ocean water and the benthonic foraminifera genus Uvigerina: isotopic changes in the ocean during the last glacial[J]. Colloques International du Centre National du Recherche Scientifique, 219: 203−210.

Shackleton N J. 1975. Paleotemperature history of the Cenozoic and the initiation of Antarctic glaciation: oxygen and carbon isotope analyses in DSDP Sites 277, 279, and 281[J]. Initial Reports Deep Sea Drilling Project, 29: 743−755.

Shao H M, Lu X, Gao B, Hong S X, Pan H F, Xu Z Y, Bai X J. 2019. Geochemical analyzing technique of the microzone's normal position and its application: A case study on the diagenetic evolution of the carbonate reservoir in Gucheng area[J]. Petroleum Geology & Oilfield Development in Daqing, 38(5): 160−168.

Sharp Z D, Wostbrock J A G, Pack A. 2018. Mass–dependent triple oxygen isotope variations in terrestrial materials[J]. Geochemical Perspectives Letters, 7: 27−31.

Shen C C, Kano A, Hori M, Lin K, Chiu T C, Burr G S. 2010. East Asian monsoon evolution and reconciliation of climate records from Japan and Greenland during the last deglaciation[J]. Quaternary Science Reviews, 29(23/24): 3327−3335.

Shen Zhaoli, Wang Yanxin, Guo Huaming. 2012. Opportunities and challenges of water–rock interaction studies[J]. Earth Science, 37(2): 207−219 (in Chinese with English abstract).

Sheng Xuefen, Chen Jun, Yang Jiedong, Ji Junfeng, Chen Yang. 2002. Carbon and oxygen isotopic composition of carbonate in different grain size fractions from loess–paleosol sequences, China[J]. Geochimica, 31(2): 105−112 (in Chinese with English abstract).

Shi X, Zhang F, Tian L, Joswiak D R, Zeng C, Qu D. 2014. Tracing contributions to hydro−isotopic differences between two adjacent lakes in the southern Tibetan Plateau[J]. Hydrological Processes, 28(22): 5503−5512.

Shi Y, Yu G, Liu X, Li B, Yao T. 2001. Reconstruction of the 30–40 ka BP enhanced Indian monsoon climate based on geological records from the Tibetan Plateau[J]. Palaeogeography, Palaeoclimatology, Palaeoecology, 169(1/2): 69–83.

Siddall M, Rohling E J, Almogi–Labin A, Hemleben C, Meischner D, Schmelzer I, Smeed D. 2003. Sea–level fluctuations during the last glacial cycle[J]. Nature, 423(6942): 853−858.

Siegenthaler M B, Tamburini F, Frossard E, Chadwick O, Vitousek P, Pistocchi C, Mészáros É, Helfenstein J. 2020. A dual isotopic ($^{32}P$ and $^{18}O$) incubation study to disentangle mechanisms controlling phosphorus cycling in soils from a climatic gradient (Kohala, Hawaii)[J]. Soil Biology and Biochemistry, 149: 107920.

Sierra C, Álvarez Saiz J R, Gallego J L R. 2013. Nanofiltration of acid mine drainage in an abandoned mercury mining area[J]. Water, Air, & Soil Pollution, 224: 1–12.

Siler N, Bailey A, Roe G H, Buizert C, Markle B, Noone D. 2021. The large–scale, long–term coupling of temperature, hydrology, and water isotopes[J]. Journal of Climate, 34(16): 6725−6742.

Sone T, Kano A, Okumura T, Kashiwagi K, Hori M, Jiang X, Shen C–C. 2013. Holocene stalagmite oxygen isotopic record from the Japan Sea side of the Japanese Islands, as a new proxy of the East Asian winter monsoon[J]. Quaternary Science Reviews, 75: 150−160.

Song K, Wang F, Peng Y, Liu J, Liu D. 2022. Construction of a hydrogeochemical conceptual model and identification of the groundwater pollution contribution rate in a pyrite mining area[J]. Environmental Pollution, 305: 119327.

Southon J. 2002. A first step to reconciling the GRIP and GISP2 ice–core chronologies, 0–14, 500 yr BP[J]. Quaternary Research, 57(1): 32−37.

Springer A E, Boldt E M, Junghans K M. 2017. Local vs. regional groundwater flow delineation from stable isotopes at western North America springs[J]. Groundwater, 55(1): 100−109.

Stevenson R, Desrochers S, Hélie J F. 2015. Stable and radiogenic isotopes as indicators of agri–food provenance: Insights from artisanal cheeses from Quebec, Canada[J]. International Dairy Journal, 49: 37−45.

Su Y Y, Gao J, Zhao Y F, Wen H S, Zhang J J, Zhang A, Yuan C L. 2020. Geographical origin classification of Chinese wines based on carbon and oxygen stable isotopes and elemental profiles[J]. Journal of Food Protection, 83(8): 1323−1334.

Suzuki Y, Nakashita R, Huque R, Khatun M A, Othman Z B, Salim N A B A, Thantar S, Pabroa P C, Kong P Y K, Waduge V A. 2022. Effects of processing on stable isotope compositions ($\delta^{13}$C, $\delta^{15}$N, and $\delta^{18}$O) of rice (Oryza sativa) and stable isotope analysis of asian rice samples for tracing their geographical origins[J]. Japan Agricultural Research Quarterly: JARQ, 56(1): 95−103.

Swart P K, Murray S T, Staudigel P T, Hodell D A. 2019. Oxygen isotopic exchange between $CO_2$ and phosphoric acid: Implications for the measurement of clumped isotopes in carbonates[J]. Geochemistry, Geophysics, Geosystems, 20(7): 3730–3750.

Syed T H, Famiglietti J S, Rodell M, Chen J, Wilson C R. 2008. Analysis of terrestrial water storage changes from GRACE and GLDAS[J]. Water Resources Research, 44(2): W02433.

Szymczak S, Joachimski M M, Bräuning A, Hetzer T, Kuhlemann J. 2012. Are pooled tree ring $\delta^{13}$C and $\delta^{18}$O series reliable climate archives?——A case study of Pinus nigra spp. laricio (Corsica/France)[J]. Chemical Geology, 308: 40−49.

Tachikawa K, Elderfield H. 2002. Microhabitat effects on Cd/Ca and $\delta^{13}$C of benthic foraminifera[J]. Earth and Planetary Science Letters, 202(3−4): 607−624.

Tan L, An Z, Huh C A, Cai Y, Shen C C, Shiau L J, Yan L, Cheng H, Edwards R L. 2014. Cyclic precipitation variation on the western Loess Plateau of China during the past four centuries[J]. Scientific Reports, 4(1): 6381.

Tan M. 2016. Circulation background of climate patterns in the past millennium: Uncertainty analysis and re–reconstruction of ENSO–like state[J]. Science China Earth Sciences, 59: 1225−1241.

Thiemens M H, Chakraborty S, Jackson T L. 2014. Decadal $\Delta^{17}$O record of tropospheric $CO_2$: Verification of a stratospheric component in the troposphere[J]. Journal of Geophysical Research: Atmospheres, 119(10): 6221−6229.

Thiemens M H, Heidenreich III J E. 1983. The mass–independent fractionation of oxygen: A novel isotope effect and its possible cosmochemical implications[J]. Science, 219(4588): 1073−1075.

Thiemens M H. 2006. History and applications of mass–independent isotope effects[J]. Annual Review of Earth and Planetary Sciences, 34: 217−262.

Thompson L G, Mosley–Thompson E, Dansgaard W, Grootes P M. 1986. The little ice age as recorded in the stratigraphy of the tropical Quelccaya ice cap[J]. Science, 234(4774): 361−364.

Thompson L o, Yao T, Davis M, Henderson K, Mosley Thompson E, Lin P N, Beer J, Synal H A, Cole Dai J, Bolzan J. 1997. Tropical climate instability: The last glacial cycle from a Qinghai–Tibetan ice core[J]. Science, 276(5320): 1821−1825.

Tian L, Guo Q, Yu G, Zhu Y, Lang Y, Wei R, Hu J, Yang X, Ge T. 2020. Phosphorus fractions and oxygen isotope composition of inorganic phosphate in typical agricultural soils[J]. Chemosphere, 239: 124622.

Tian L, Guo Q, Zhu Y, He H, Lang Y, Hu J, Zhang H, Wei R, Han X, Peters M. 2016. Research and application of method of oxygen isotope of inorganic phosphate in Beijing agricultural soils[J]. Environmental Science and Pollution Research, 23: 23406−23414.

Tian Lide, Yao Tandong. 2016. High–resolution climatic and environmental records from the Tibetan Plateau ice cores[J]. Chinese Science Bulletin, 61: 926−937 (in Chinese with English abstract).

Tichomirowa M, Heidel C, Junghans M, Haubrich F, Matschullat J. 2010. Sulfate and strontium water source identification by O, S and Sr isotopes and their temporal changes (1997–2008) in the region of Freiberg, central–eastern Germany[J]. Chemical Geology, 276 (1/2): 104−118.

Tomiyama S, Igarashi T, Tabelin C B, Tangviroon P, Ii H. 2019. Acid mine drainage sources and hydrogeochemistry at the Yatani mine, Yamagata, Japan: A geochemical and isotopic study[J]. Journal of Contaminant Hydrology, 225: 103502.

Touzeau A, Landais A, Stenni B, Uemura R, Fukui K, Fujita S, Guilbaud S, Ekaykin A, Casado M, Barkan E. 2016. Acquisition of isotopic composition for surface snow in East Antarctica and the links to climatic parameters[J]. The Cryosphere, 10(2): 837−852.

Treydte K S, Schleser G H, Helle G, Frank D C, Winiger M, Haug G H, Esper J. 2006. The twentieth century was the wettest period in northern Pakistan over the past millennium[J]. Nature, 440(7088): 1179−1182.

Trofimova T, Andersson C, Bonitz F G, Pedersen L E R, Schöne B R. 2021. Reconstructing early Holocene seasonal bottom–water temperatures in the northern North Sea using stable oxygen isotope records of Arctica islandica shells[J]. Palaeogeography, Palaeoclimatology, Palaeoecology, 567: 110242.

Trueman C N, Glew K S J. 2019. Isotopic Tracking of Marine Animal Movement[C]// Tracking Animal Migration with Stable Isotopes (137–172). Elsevier.

Trueman C N, MacKenzie K, Palmer M. 2012. Identifying migrations

in marine fishes through stable−isotope analysis[J]. Journal of Fish Biology, 81(2): 826−847.

Tuli S. 1985. Nuclear Wallet Cards. Natural Nuclear Data Center[M]. Brookhaven National Laboratory, 35pp.

Turpin M, Gressier V, Bahamonde J R, Immenhauser A. 2014. Component–specific petrographic and geochemical characterization of fine–grained carbonates along Carboniferous and Jurassic platform–to–basin transects[J]. Sedimentary Geology, 300: 62−85.

Vander Zanden H B, Soto D X, Bowen G J, Hobson K A. 2016. expanding The Isotopic Toolbox: Applications Of Hydrogen And Oxygen Stable Isotope Ratios To Food Web Studies[j]. frontiers In Ecology And Evolution, 4: 20.

Wang Chunlian, Liu Chenglin, Xu Haiming, Wang Licheng, Zhang Linbing. 2013. Carbon and oxygen isotopes characteristics of Palaeocene saline lake facies carbonates in Jiangling Depression and their environmental significance[J]. Acta Geoscientica Sinica, 34(5): 567−576 (in Chinese with English abstract).

Wang Jingzhong, Wu Jinglu, Zeng Haiao, Bai Ruidong. 2013. Characteristics of water isotope and hydrochemistry in Hetao Plain of Inner Mongolia[J]. Journal of Earth Sciences and Environment, 35(4): 104−112 (in Chinese with English abstract).

Wang Mili, Yang Zhichen, Liu Chenglin, XieZhichao, Jiao Pengcheng, Li Changhua. 1996. Potassium Deposits in Salt Lakes in the Northern Part of the Qaidam Basin and Their Development Prospects [M]. Beijing: Geological Publishing House, 33–51 (in Chinese with English abstract).

Wang W, Yu Z, Song X, Wu Z, Yuan Y, Zhou P, Cao X. 2017. Characteristics of the $\delta^{15}$ $N_{NO_3}$ distribution and its drivers in the Changjiang River estuary and adjacent waters[J]. Chinese Journal of Oceanology and Limnology, 35: 367−382.

Wang X T, Wang Y, Auderset A, Sigman D M, Ren H, Martínez–García A, Haug G H, Su Z, Zhang Y G, Rasmussen B. 2022a. Oceanic nutrient rise and the late Miocene inception of Pacific oxygen–deficient zones[J]. Proceedings of the National Academy of Sciences, 119(45): e2204986119.

Wang Y J, Cheng H, Edwards R L, An Z, Wu J, Shen C C, Dorale J A. 2001. A high–resolution absolute–dated Late Pleistocene monsoon record from Hulu Cave, China[J]. Science, 294(5550): 2345−2348.

Wang Y, Cheng H, Edwards R L, Kong X, Shao X, Chen S, Wu J, Jiang X, Wang X, An Z. 2008. Millennial–and orbital–scale changes in the East Asian monsoon over the past 224, 000 years[J]. Nature, 451(7182): 1090−1093.

Wang Yongjin, Liu Dianbing. 2016. Speleothem records of Asian paleomonsoon variability and mechanisms[J]. Chinese Science Bulletin, 61(9): 938−951 (in Chinese with English abstract).

Wang Z, Guo Q, Tian L. 2022b. Tracing phosphorus cycle in global watershed using phosphate oxygen isotopes[J]. Science of the Total Environment, 829: 154611.

Wang Z, Tian L, Zhao C, Du C, Zhang J, Sun F, Tekleab T Z, Wei R, Fu P, Gooddy D C. 2023. Source partitioning using phosphate oxygen isotopes and multiple models in a large catchment[J]. Water Research, 244: 120382.

Werner C, Meredith L K, Ladd S N, Ingrisch J, Kübert A, van Haren J, Bahn M, Bailey K, Bamberger I, Beyer M. 2021. Ecosystem fluxes during drought and recovery in an experimental forest[J]. Science, 374(6574): 1514−1518.

Wheatley P V, Peckham H, Newsome S D, Koch P L. 2012. Estimating marine resource use by the American crocodile Crocodylusacutus in southern Florida, USA[J]. Marine Ecology Progress Series, 447: 211−229.

Worden J, Noone D, Bowman K. 2007. Importance of rain evaporation and continental convection in the tropical water cycle[J]. Nature, 445(7127): 528−532.

Wu H, Tian L, Chen B, Jin B, Tian B, Xie L, Rogers K M, Lin G. 2019. Verification of imported red wine origin into China using multi isotope and elemental analyses[J]. Food Chemistry, 301: 125137.

Xia X, Li S, Wang F, Zhang S, Fang Y, Li J, Michalski G, Zhang L. 2019. Triple oxygen isotopic evidence for atmospheric nitrate and its application in source identification for river systems in the Qinghai–Tibetan Plateau[J]. Science of the Total Environment, 688: 270−280.

Xiong Zhifang, Hu Chaoyong, Huang Junhua, Xie Shucheng, Gan Yiqun. 2007. Mass–Independent oxygen isotope fractionation and its application to earth sciences[J]. Bulletin of Geological Science and Technology (2): 51–58 (in Chinese with English abstract).

Xu S, Kang P, Sun Y A. 2016. A stable isotope approach and its application for identifying nitrate source and transformation process in water[J]. Environmental Science and Pollution Research, 23: 1133−1148.

Yamaguchi K, Tomiyama S, Metugi H, Ii H, Ueda A. 2015. Flow and geochemical modeling of drainage from Tomitaka mine, Miyazaki, Japan[J]. Journal of Environmental Sciences, 36: 130−143.

Yancheva G, Nowaczyk N R, Mingram J, Dulski P, Schettler G, Negendank J F, Liu J, Sigman D M, Peterson L C, Haug G H. 2007. Influence of the intertropical convergence zone on the East Asian monsoon[J]. Nature, 445(7123): 74−77.

Yao T D, Qin D H, Wang N L, Liu Y Q, Xu B Q. 2020. Study on climatic and environmental changes recorded in ice cores: From science to policy[J]. Bulletin of Chinese Academy of Sciences(4): 466–474.

Yao T, Guo X, Thompson L, Duan K, Wang N, Pu J, Xu B, Yang X, Sun W. 2006. $\delta^{18}O$ record and temperature change over the past 100 years in ice cores on the Tibetan Plateau[J]. Science in China Series D, 49: 1−9.

Yao T. 1999. Abrupt climatic changes on the Tibetan Plateau during the Last Ice Age–Comparative study of the Guliya ice core with the

Greenland GRIP ice core[J]. Science in China (Ser.D), 42: 358−368.

Yao Tandong, Qin Dahe, Tian Lide, Jiao Keqin, Yang Zhihong, Xie Chao, L G Thompson. 1996. Temperature and precipitation changes on the Tibetan Plateau over a 2–ka period–Guria ice core record[J]. Scientia Sinica(Terrae) (4): 348–353 (in Chinese).

Ye F, Ni Z, Xie L, Wei G, Jia G. 2015. Isotopic evidence for the turnover of biological reactive nitrogen in the Pearl River Estuary, south China[J]. Journal of Geophysical Research: Biogeosciences, 120(4): 661−672.

Yiou F, Raisbeck G, Baumgartner S, Beer J, Hammer C, Johnsen S, Jouzel J, Kubik P, Lestringuez J, Stievenard M. 1997. Beryllium 10 in the Greenland ice core project ice core at summit, Greenland[J]. Journal of Geophysical Research: Oceans, 102(C12): 26783−26794.

Young E D, Galy A, Nagahara H. 2002. Kinetic and equilibrium mass–dependent isotope fractionation laws in nature and their geochemical and cosmochemical significance[J]. Geochimica et Cosmochimica Acta, 66(6): 1095−1104.

Yu Shengbo, Qu Junxia. 2021. Characteristics and significance of stable hydrogen and oxygen isotopes in groundwater of Sugan Lake basin[J]. Journal of Arid Land Resources and Environment, 35(1): 169−175 (in Chinese with English abstract).

Yu Z, Li B, Li H, Zhang J, Chen J. 2022. The influence of seasonal calcification depth change on the planktonic foraminiferal stable oxygen isotope signal[J]. Geochimica et Cosmochimica Acta, 327: 34−52.

Yuan D, Cheng H, Edwards R L, Dykoski C A, Kelly M J, Zhang M, Qing J, Lin Y, Wang Y, Wu J. 2004. Timing, duration, and transitions of the last interglacial Asian monsoon[J]. Science, 304(5670): 575−578.

Yuan H, Li Q, Kukkadapu R K, Liu E, Yu J, Fang H, Li H, Jaisi D P. 2019. Identifying sources and cycling of phosphorus in the sediment of a shallow freshwater lake in China using phosphate oxygen isotopes[J]. Science of the Total Environment, 676: 823−833.

Yuan H, Wang H, Dong A, Zhou Y, Huang R, Yin H, Zhang L, Liu E, Li Q, Jia B. 2022. Tracing the sources of phosphorus in lake at watershed scale using phosphate oxygen isotope ($\delta^{18}O_p$)[J]. Chemosphere, 305: 135382.

Yue F J, Li S L, Hu J. 2015. The contribution of nitrate sources in Liao Rivers, China, based on isotopic fractionation and Bayesian mixing model[J]. Procedia Earth and Planetary Science, 13: 16−20.

Yue F J, Li S L, Liu C Q, Zhao Z Q, Ding H. 2017. Tracing nitrate sources with dual isotopes and long term monitoring of nitrogen species in the Yellow River, China[J]. Scientific Reports, 7(1): 8537.

Yue F J, Liu C Q, Li S L, Zhao Z Q, Liu X L, Ding H, Liu B J, Zhong J. 2014. Analysis of $\delta^{15}N$ and $\delta^{18}O$ to identify nitrate sources and transformations in Songhua River, Northeast China[J]. Journal of Hydrology, 519: 329−339.

Yuntseover Y, Gat J R. 1981. Atmospheric Waters[M]. IAEA Technical Reports Series 210–Stable Isotope Hydrology (103–142).

Zachos J, Pagani M, Sloan L, Thomas E, Billups K. 2001. Trends, rhythms, and aberrations in global climate 65 Ma to present[J]. Science, 292(5517): 686−693.

Zahn R, Winn K, Sarnthein M. 1986. Benthic foraminiferal $\delta^{13}C$ and accumulation rates of organic carbon: Uvigerina peregrina group and Cibicidoideswuellerstorfi[J]. Paleoceanography, 1(1): 27−42.

Zeng Y, Zhu J, Wang Y, Hu W. 2018. Changes of water temperature and heat flux at water–sediment interface, East Lake Taihu[J]. Journal of Lake Sciences, 30(6): 1599−1609.

Zenteno L, Crespo E, Goodall N, Aguilar A, de Oliveira L, Drago M, Secchi E R, Garcia N, Cardona L. 2013. Stable isotopes of oxygen reveal dispersal patterns of the South American sea lion in the southwestern Atlantic Ocean[J]. Journal of Zoology, 291(2): 119−126.

Zhang Chi, Ji Hongbing, Chen Zhigang. 2018. The application of phosphate oxygen isotope in organophosphorus degradation[J]. Journal of Shandong Agricultural University, 49(6): 1008−1014 (in Chinese with English abstract).

Zhang Cuiyun, Zhong Zuo, Shen Zhaoli. 2003. The progress in the study of oxygen isotopes in groundwater nitrate[J]. Earth Science Frontiers, 10(2): 287−291 (in Chinese with English abstract).

Zhang Fangfang, Zheng Yonghong, Pan Guoyan, Yuan Shuai, Kong Fanxi, Qi Yongdong, Wang Dan. 2018. Climatic significance of tree–ring $\delta^{18}O$ in Shennongjia Mountain[J]. Progress in Geography, 37(7): 946−953 (in Chinese with English abstract).

Zhang J, Chen L, Hou X, Lin M, Ren X, Li J, Zhang M, Zheng X. 2021. Multi–isotopes and hydrochemistry combined to reveal the major factors affecting Carboniferous groundwater evolution in the Huaibei coalfield, North China[J]. Science of the Total Environment, 791: 148420.

Zhang Xin, Zhang Yan, Bi Zhilei, Shan Zexuan, Ren Lijiang, Li Qi. 2020. Distribution and source analysis of nitrate in surface waters of China[J]. Environmental Science, 41(4): 1594−1606 (in Chinese with English abstract).

Zhang Y, Shi P, Li F, Wei A, Song J, Ma J. 2018. Quantification of nitrate sources and fates in rivers in an irrigated agricultural area using environmental isotopes and a Bayesian isotope mixing model[J]. Chemosphere, 208: 493−501.

Zhang Yinghua, Wu Yanqing, Wen Xiaohu, SuJianping. 2006. Application of environmental isotopes in water cycle[J]. Advances in Water Science, 17(5): 738−747 (in Chinese with English abstract).

Zhang Ziyang, Yan Ming, Mulvaney Robert, Ji Junfeng, Xiao Cunde, Liu Leibao, An Chunlei. 2021. Preliminary study on air temperature

records from 1712 to 2001 revealed by LGB69 ice core in East Antarctica[J]. Advances in Earth Science, 36(2): 172−184 (in Chinese with English abstract).

Zhao Huabiao, Xu Baiqing, Wang Ninglian. 2014. Study on the water stable isotopes in Tibetan plateau ice cores as a proxy of temperature[J]. Quaternary Sciences, 34(6): 1215−1226 (in Chinese with English abstract).

Zhao Q, Xu C, An W, Liu Y, Xiao G, Huang C. 2023. Increasing tree growth in subalpine forests of central China due to earlier onset of the thermal growing season[J]. Agricultural and Forest Meteorology, 333: 109391.

Zhao Ruihan, Han Zhiwei, Fu Yong. 2022. A review of research progress of isotope technology in tracing pollution process in the mine environment[J]. Rock and Mineral Analysis, 41(6): 947−961 (in Chinese with English abstract).

Zhao Tiantian, Tian Kang, Hu Wenyou, Huang Biao, Zhao Yongcun. 2022. The application of phosphate oxygen isotopes in soil phosphorus cycling[J]. Acta Pedologica Sinica, 59(5): 1204−1214 (in Chinese with English abstract).

Zheng Mianping, Zhao Yuanyi, Liu Junying. 1998. Quaternary saline lake deposition and paleoclimate[J]. Quaternary Sciences, 18(4): 297−307 (in Chinese with English abstract).

Zheng Y F. 2016. Oxygen isotope fractionation in phosphates: The role of dissolved complex anions in isotope exchange[J]. Isotopes in Environmental and Health Studies, 52(1/2): 47−60.

Zheng Yongfei, Chen Jiangfeng. 2000. Stable Isotope Geochemistry[M]. Beijing: Science Press, 6–8, 143–195 (in Chinese).

Zhou J, Chafetz H S. 2009. The genesis of late Quaternary caliche nodules in Mission Bay, Texas: Stable isotopic compositions and palaeoenvironmental interpretation[J]. Sedimentology, 56(5): 1392−1410.

Zhu Dayun, Wang Jianli. 2013. Progress in palaeoclimate research on the Tibet Plateau based on ice core records[J]. Progress in Geography, 32(10): 1535−1544 (in Chinese with English abstract).

Zhu Hongyan, Ren Jia, Yang Qiang, Zhou Beibei, Jia Yanwu, LvJiaojiao, Zhou Xiaoping, Nie Weibo. 2021. Sources analysis of acid drainage from Lujiang alunite mine based on stable isotope composition of hydrogen and Oxygen[J]. Resources and Environment in the Yangtze Basin, (12): 2938–2948 (in Chinese with English abstract).

## 附中文参考文献

鲍睿, 盛雪芬, 陈骏. 2021. 陆生蜗牛壳体碳氧同位素组成与气候[J]. 第四纪研究, 41(4): 903–915.

曹超, 雷怀彦. 2012. 南海北部有孔虫碳氧同位素特征与晚第四纪水合物分解的响应关系[J]. 吉林大学学报 (地球科学版), 42(S1): 162–171.

曹佳璐, 牛振川, 梁单, 冯雪, 吕梦妮, 王国卫, 刘婉玉. 2023. 氧同位素非质量分馏在 $CO_2$ 相关研究中的进展[J]. 地球环境学报, 14(6): 714−724.

常凤琴, 张虎才, 雷国良, 蒲阳, 陈光杰, 张文翔, 杨伦庆. 2010. 湖相沉积物锶同位素和相关元素的地球化学行为及其在古气候重建中的应用——以柴达木盆地贝壳堤剖面为例[J]. 第四纪研究, 30(5): 962−971.

陈陆望, 桂和荣, 许光泉, 宋晓梅, 袁文华. 2003. 皖北矿区煤层底板岩溶水氢氧稳定同位素特征[J]. 合肥工业大学学报 (自然科学版), (3): 374–378.

陈瑶, 勾晓华, 刘文火, 陈巧湄, 苏佳佳, 林伟. 2017. 亚洲树轮稳定氧同位素研究进展[J]. 冰川冻土, 39(2): 308−316.

陈志刚, 黄奕普, 刘广山, 蔡毅华, 卢阳阳, 刘润. 2010. 磷酸盐氧同位素组成的测定方法及分馏机理研究进展[J]. 地球科学进展, 25(10): 1040−1050.

陈忠, 马海州, 曹广超, 周笃珺, 张西营, 谭红兵, 姚远. 2006. 黄土碳酸盐的研究[J]. 盐湖研究, (4): 66–72.

程海, 艾思本, 王先锋, 汪永进, 孔兴功, 袁道先, 张美良, 林玉石, 覃嘉铭, 冉景丞. 2005. 中国南方石笋氧同位素记录的重要意义[J]. 第四纪研究, (2): 157–163.

崔景伟, 黄俊华, 胡超涌. 2008. 石笋中的环境替代指标及其蕴含的古气候和古环境信息[J]. 地质科技情报, (1): 93–98.

崔蕊, 汪季, 张成福, 史小红, 韩知明. 2019. 吉兰泰盐湖氢氧同位素及湖水来源分析[J]. 内蒙古林业科技, 45(1): 17−21.

董庆民, 胡忠贵, 陈世悦, 李世临, 蔡家兰, 朱宜新, 张玉颖. 2021. 川东北地区长兴组–飞仙关组碳酸盐岩同位素地球化学响应及其地质意义[J]. 石油与天然气地质, 42(6): 1307−1320.

窦衍光, 李清, 吴永华, 赵京涛, 孙呈慧, 蔡峰, 陈晓辉, 张勇, 范佳慧, 石学法. 2022. 冲绳海槽 MIS6 期以来底栖有孔虫碳氧同位素特征及其古海洋指示意义[J]. 地学前缘, 29(4): 84−92.

樊娟, 南生辉, 刘英锋, 周天威, 张光明. 2021. 基于水化学和氢氧同位素特征的小屯煤矿充水条件研究[J]. 安全与环境工程, (4): 80–87.

付昌昌, 刘聪. 2022. 可可西里盐湖水化学特征及其形成机制[J]. 人民长江, 53(7): 36−41.

郭启梅, 李保华, 王晓燕, 俞宙菲, 徐烨, 张楷. 2020. 深海底栖有孔虫在古海洋学研究中的应用[J]. 古生物学报, 59(3): 365−379.

郭启梅, 刘静, 李保华. 2023. 沉积物单/多壳体底栖有孔虫稳定氧碳同位素组成、比较及其指示意义[J]. 微体古生物学报, 40(1): 53−65.

韩家懋, 姜文英, 刘东生, 吕厚远, 郭正堂, 吴乃琴. 1996. 黄土碳酸盐中古气候变化的同位素记录[J]. 中国科学 (D 辑: 地球科学), (5): 399–404.

韩家懋, 姜文英, 吕厚远, 吴乃琴, 郭正堂. 1995a. 黄土中钙结核的碳氧同位素研究 (二) 碳同位素及其古环境意义[J]. 第四纪研究, (4): 367–377.

韩家懋, 姜文英, 吴乃琴, 郭正堂. 1995b. 黄土中钙结核的碳氧同位素研究 (一) 氧同位素及其古环境意义[J]. 第四纪研究, (2): 130–138.

侯战方, 张军, 宋春晖, 李吉均, 刘佳, 刘善品, 惠争闯, 彭廷江. 2011. 青藏高原天水盆地中新世沉积物碳氧同位素对古气候演化的指示[J]. 海洋地质与第四纪地质, 31(3): 69−78.

胡泉旭, 王先彦, 孟先强, 刘全玉, 鹿化煜. 2018. 青藏高原东北部黄土次生碳酸盐氧同位素的古气候意义[J]. 地球科学, 43(11): 4128−4137.

黄思静, 石和, 毛晓冬, 张萌, 沈立成, 武文慧. 2003. 早古生代海相碳酸盐的成岩蚀变性及其对海水信息的保存性[J]. 成都理工大学学报 (自然科学版), (1): 9–18.

李建森, 蔡进福, 樊启顺, 山发寿, 凌智永, 韩元红, 张永兴. 2022. 柴达木盆地盐湖 K、B、Li 资源的成矿地球化学系统[J]. 盐湖研究, 30(3): 12−20.

李思远, 侯青叶, 杨忠芳, 余涛. 2024. 氮同位素分馏机制、分析测试与示踪技术及其在生态环境中的应用[J]. 中国地质, 51(5): 1617−1643.

李桐, 邱国玉. 2018. 基于稳定氢氧同位素的盐水与纯水蒸发差异分析[J]. 热带地理, 38(6): 857−865.

李小倩, 张彬, 周爱国, 刘运德. 2014. 酸性矿山废水对合山地下水污染的硫氧同位素示踪[J]. 水文地质工程地质, 41(6): 103−109.

李悦, 王汝建, 李文宝. 2016. 利用有孔虫氧同位素重建古海平面变化的研究进展[J]. 地球科学进展, 31(3): 310−319.

李智滔, 肖红伟, 伍作亭, 马艳, 肖扬宁, 陈振平, 陶继华. 2022. 基于水化学及氮氧同位素技术的硝酸盐来源解析——以鄱阳湖湿地为例[J]. 中国环境科学, 42(9): 4315−4322.

刘科, 侯书贵, 庞洪喜, 史贵涛, 耿雷, 胡焕婷, 宋靖, 张王滨, 邹翔, 安春雷, 于金海. 2022. 极地冰芯气候及环境记录指标研究现状与展望[J]. 极地研究, 34(4): 530−545.

吕凤琳, 刘成林, 焦鹏程, 张华, 孙小虹, 张永明. 2018. 罗布泊中更新世以来盐湖碳酸盐碳氧同位素组成及其古环境意义[J]. 地质学报, 92(8): 1589−1604.

马正明, 姜盼武, 李庆宽, 魏海成, 李永寿, 山发寿. 2021. 哈达贺休盐湖卤水氢氧同位素特征及成因分析[J]. 盐湖研究, 29(1): 80−87.

毛剑英, 朱建平, 肖建军. 2003. 近年来淮河干流氮污染状况与变化趋势[J]. 中国环境监测, (5): 41–43.

苗青, 侯献华, 杨振京. 2021. 几种常用古气候代用指标在盐湖古环境研究中的应用[J]. 科学技术创新, (5): 31–32.

苗甜, 金雅琪, 王磊, 吴高阳, 陈忠. 2021. 黄土碳酸盐古气候意义及其研究展望[J]. 盐湖研究, 29(4): 90−99.

乔占峰, 于洲, 佘敏, 潘立银, 张天付, 李文正, 沈安江. 2023. 中国古老超深层海相碳酸盐岩储集层成因研究新进展[J]. 古地理学报, 25(6): 1257−1276.

邱楠生, 刘鑫, 熊昱杰, 刘雨晨, 徐秋晨, 常青. 2023. 碳酸盐团簇同位素在海相盆地热史研究中的进展[J]. 石油实验地质, 45(5): 891−903.

任坤, 潘晓东, 兰干江, 彭聪, 梁嘉鹏, 曾洁. 2021. 硫氧同位素解析典型岩溶地下河流域硫酸盐季节变化特征和来源[J]. 环境科学, 42(9): 4267−4274.

沈照理, 王焰新, 郭华明. 2012. 水–岩相互作用研究的机遇与挑战[J]. 地球科学 (中国地质大学学报), 37(2): 207−219.

盛雪芬, 陈骏, 杨杰东, 季峻峰, 陈旸. 2002. 不同粒级黄土–古土壤中碳酸盐碳氧稳定同位素组成及其古环境意义[J]. 地球化学, (2): 105–112.

田立德, 姚檀栋. 2016. 青藏高原冰芯高分辨率气候环境记录研究进展[J]. 科学通报, 61(9): 926−937.

汪敬忠, 吴敬禄, 曾海鳌, 白瑞东. 2013. 内蒙古河套平原水体同位素及水化学特征[J]. 地球科学与环境学报, 35(4): 104−112.

汪永进, 刘殿兵. 2016. 亚洲古季风变率和机制的洞穴石笋档案[J]. 科学通报, 61(9): 938−951.

王春连, 刘成林, 徐海明, 王立成, 张林兵. 2013. 江陵凹陷古新世盐湖沉积碳酸盐碳氧同位素组成及其环境意义[J]. 地球学报, 34(5): 567−576.

王弭力, 杨智琛, 刘成林, 谢志超, 焦鹏程, 李长华. 1996. 柴达木盆地北部盐湖钾矿床及其开发前景[M]. 北京: 地质出版社, 33–51.

熊志方, 胡超涌, 黄俊华, 谢树成, 甘义群. 2007. 氧的非质量同位素分馏及其地学应用[J]. 地质科技情报, (2): 51–58.

姚檀栋, 秦大河, 田立德, 焦克勤, 杨志红, 谢超, L. G. Thompson. 1996. 青藏高原 2ka 来温度与降水变化–古里雅冰芯记录[J]. 中国科学 (D 辑: 地球科学), (4): 348–353.

喻生波, 屈君霞. 2021. 苏干湖盆地地下水氢氧稳定同位素特征及其意义[J]. 干旱区资源与环境, 35(1): 169−175.

张弛, 季宏兵, 陈志刚. 2018. 磷酸盐氧同位素在有机磷降解研究中的应用[J]. 山东农业大学学报 (自然科学版), 49(6): 1008−1014.

张翠云, 钟佐, 沈照理. 2003. 地下水硝酸盐中氧同位素研究进展[J]. 地学前缘, (2): 287–291.

张芳芳, 郑永宏, 潘国艳, 袁帅, 孔繁希, 起永东, 王丹. 2018. 神农架地区树轮 $\delta^{18}O$ 序列的气候指示意义[J]. 地理科学进展, 37(7): 946−953.

张鑫, 张妍, 毕直磊, 山泽萱, 任丽江, 李琦. 2020. 中国地表水硝酸盐分布及其来源分析[J]. 环境科学, 41(4): 1594−1606.

张应华, 仵彦卿, 温小虎, 苏建平. 2006. 环境同位素在水循环研究中的应用[J]. 水科学进展, (5): 738–747.

张子洋, 闫明, MULVANEY Robert, 季峻峰, 效存德, 刘雷保, 安春雷. 2021. 东南极 LGB69 冰芯 1712–2001 年气温变化记录的初步研究[J]. 地球科学进展, 36(2): 172−184.

赵华标, 徐柏青, 王宁练. 2014. 青藏高原冰芯稳定氧同位素记录的温度代用性研究[J]. 第四纪研究, 34(6): 1215−1226.

赵睿涵, 韩志伟, 付勇. 2022. 同位素技术应用于示踪矿山环境污染研究进展[J]. 岩矿测试, 41(6): 947−961.

赵甜甜, 田康, 胡文友, 黄标, 赵永存. 2022. 磷酸盐氧同位素技术在土壤磷循环中的应用[J]. 土壤学报, (5): 1204–1214.

郑绵平, 赵元艺, 刘俊英. 1998. 第四纪盐湖沉积与古气候[J]. 第四纪研究, (4): 297–307.

郑永飞, 陈江峰. 2000. 稳定同位素地球化学[M]. 北京: 科学出版社, 6–8, 143–195.

朱大运, 王建力. 2013. 青藏高原冰芯重建古气候研究进展分析[J]. 地理科学进展, 32(10): 1535−1544.

朱红艳, 任佳, 杨强, 周蓓蓓, 贾彦武, 吕佼佼, 周晓平, 聂卫波. 2021. 基于氢氧稳定同位素组成解析庐江矾矿酸性废水来源[J]. 长江流域资源与环境, (12): 2938–2948.